

AREAS OF CONTACT AND PRESSURE DISTRIBUTION
IN BOLTED JOINTS

H.H. Gould

B.B. Mikic

Final Technical Report

Prepared for

George C. Marshall Space Flight Center
Marshall Space Flight Center
Alabama 35812

under

Contract NAS 8-24867

June 1970

DSR Project 71821-68

Engineering Projects Laboratory
Department of Mechanical Engineering
Massachusetts Institute of Technology
Cambridge, Massachusetts 02139

ABSTRACT

When two plates are bolted (or riveted) together these will be in contact in the immediate vicinity of the bolt heads and separated beyond it. The pressure distribution and size of the contact zone is of considerable interest in the study of heat transfer across bolted joints.

The pressure distributions in the contact zones and the radii at which flat and smooth axisymmetric, linear elastic plates will separate were computed for several thicknesses as a function of the configuration of the bolt load by the finite element method. The radii of separation were also measured by two experimental methods. One method employed autoradiographic techniques. The other method measured the polished area around the bolt hole of the plates caused by sliding under load in the contact zone. The sliding was produced by rotating one plate of a mated pair relative to the other plate with the bolt force acting.

The computational and experimental results are in agreement and these yield smaller zones of contact than indicated by the literature. It is shown that the discrepancy is due to an assumption made in the previous analyses.

In addition to the above results this report contains the finite element and heat transfer computer programs used in this study. Instructions for the use of these programs are also included.

ACKNOWLEDGMENTS

This report was supported by the NASA Marshall Space Flight Center under contract NAS 8-24867 and sponsored by the Division of Sponsored Research at M.I.T.

TABLE OF CONTENTS

	<u>Page</u>
Title Page	1
Abstract	2
Acknowledgments	3
Table of Contents	4
List of Tables and Figures	6
Nomenclature	8
Chapter I: Introduction	10
Chapter II: Analysis	15
A. Problem Statement	15
B. Method of Analysis	18
Chapter III: Experimental Method	23
Chapter IV: Results	28
A. Pressure Distribution and Radii of Separation from Single Plate and Two Plate Finite Element Models	28
B. Radii of Separation from Experiment and Their Pre- dicted Values from the Two Plate Finite Element Computation	29
Chapter V: Application	32
Chapter VI: Conclusions	35
References	37
Appendices	
A. Finite Element Analysis of Axisymmetric Solids	39

	<u>Page</u>
B. Finite Element Program for the Analysis of Isotropic Elastic Axisymmetric Plates	44
C. Finite Element Program for the Analysis of Isotropic Elastic Axisymmetric Plates — Thermal Strains Included	68
D. Steady State Heat Transfer Program for Bolted Joint	94

LIST OF TABLES AND FIGURES

<u>Table</u>		<u>Page</u>
1	Separation Radius Comparison - Single and Two Plate Models	100
2	Test and Analytical Results for Radii of Separation of Bolted Plates	101
 <u>Figure</u>		
1	Bolted Joint	102
2	Roetscher's Rule of Thumb for Pressure Distribution in a Bolted Joint	102
3	Furnlund's Sequence of Superposition	103
4	Finite Element Idealization of Two Plates in Contact	107
5	Finite Element Models	108
6	Examples of Unacceptable Solutions	109
7	Plate Specimen, Bolt and Nuts, Fixture and Tools	110
8	Footprints on the Mating Surface of 1/16 - 1/16, 1/8 - 1/8, 3/16 - 3/16, 1/4 - 1/4, and 1/8 - 1/4 Pairs	111
9	Footprint of Nut on Plate	116
10	X-Ray Photographs of Contamination Transferred from Radioactive Plate to Mated Plate. 1/16, 1/4, 3/16, 1/4 Inch Pairs	117
11	Free Body Diagram for Two Plates in Contact	119
12	Single Plate Analysis-Midplane σ_z Stress Distribution	120
13	Single Plate Analysis-Midplane σ_z Stress Distribution	121
14	Single Plate Analysis-Midplane σ_z Stress Distribution	122

<u>Figure</u>		<u>Page</u>
15	Interface Pressure Distribution in a Bolted Joint	123
16	Interface Pressure Distribution in a Bolted Joint	124
17	Interface Pressure Distribution in a Bolted Joint	125
18	Finite Element Analysis Results for 1/4 Inch Plate Pair	126
19	Pressure in Joint, Triangular Loading	127
20	Variations of Loading and Boundary Conditions	128
21	Pressure in Joint, Uniform Displacement Under Nut	129
22	Deflection of Plate Under Nut	130
23	Finite Element Analysis Results for 3/16 Inch Plate Pair	131
24	Finite Element Analysis Results for 1/8 Inch Plate Pair	132
25	Gap Deformation for Free and Fixed Edges — Finite Element Analysis, 1/8 inch Plate Pair.	133
26	Finite Element Analysis Result for 1/16 Inch Plate Pair	134
27	Finite Element Analysis Results for 1/8 Inch Plate Mated With 1/4 Inch Plate	135
28	Comparison Between Tested and Measured Separation Radii	136
29	Location of Nodes — Steady State Heat Transfer Analysis	137

NOMENCLATURE

A, B, C	radii
D	thickness
E	modulus of elasticity
G	shear modulus
h_c, h_f	heat transfer coefficients
H	hardness
k, k_1, k_2	thermal conductivities
P, p	pressure
r	coordinate
R_o	radius of separation
u, w	displacement in r and z directions
x	coordinate
X_c	length of contact
y	coordinate
y'	slope
z	coordinate
δ	deflection
ϵ	dilation
$\epsilon_r, \epsilon_t, \epsilon_{rz}$	strains
$\sigma, \sigma_1, \sigma_2$	standard deviations
$\sigma_r, \sigma_t, \sigma_z$	stresses

λ, μ	Lame's constants
ν	Poisson's ratio
τ	shear stress
θ	angle

Subscripts

r	radial direction
t	tangential direction
z	z-direction

Chapter I

INTRODUCTION

When two plates are bolted (or riveted) together, these will be in contact in the immediate vicinity of the bolt heads and separated beyond it. The pressure distribution in the contact area and the separation of the plates is of considerable interest in the study of heat transfer across joints. Cooper, Mikic and Yovanovich [1] show that with assumed Gaussian distribution of surface heights, the microscopic contact conductance is related to the interface pressure, surface characteristics and the hardness of the softer material in

$$h_c = 1.45 \frac{\tan \theta}{\sigma} k \left(\frac{P}{H}\right)^{0.985} \quad (1.1)$$

where

$$k \equiv \frac{2k_1k_2}{k_1+k_2} \quad (1.2)$$

and k_1 and k_2 represent the thermal conductivities of two bodies in contact; σ is the combined standard deviation for the two surfaces which can be expressed as

$$\sigma = (\sigma_1^2 + \sigma_2^2)^{1/2} \quad (1.3)$$

where σ_1 and σ_2 are the individual standard deviation of height for the respective surfaces; $\tan \theta$ is the mean of the absolute value of slope for the combined profile and it is related, for normal distribution of slope, to the individual mean of absolute values of slopes as

$$\tan \theta = (\tan \theta_1^2 + \tan \theta_2^2)^{1/2} \quad (1.4)$$

where

$$\tan \theta_i = \lim_{L \rightarrow \infty} \frac{1}{L} \int_0^L |y'_i| dx; \quad i = 1, 2 \quad (1.5)$$

and y' is the slope of the respective surface profiles; P represents the local interface pressure; and H is the hardness of the softer material.

Relation (1.1), as written above, is applicable for contact in a vacuum. One can modify the expression by simply adding to it

$$h_f \equiv \frac{\text{conductivity of interstitial fluid}}{\text{average distance between the surfaces}} \quad (1.6)$$

in order to account approximately for the presence of the interstitial fluid.

All parameters in relation (1.1), except for the pressure, are functions of the material and geometry and can be easily obtained. The determination of the pressure distribution and the extent of the contact area between two plates present both mathematical and experimental

difficulties. From the mathematical point of view, the difficulty stems from the fact that the theory of elasticity will yield a three dimensional (axisymmetric) problem with mixed boundary conditions. Experimentally, the discrimination between contact and gaps of the order of millionths of an inch is required.

Roetscher [2] proposed in 1927, a rule of thumb that the pressure distribution of two bolted plates, Fig.1, is limited to the two frustums of the cones with a half cone angle of 45 degrees as shown in Fig. 2 and that at any level within the cone the pressure is constant. Also, for symmetric plates, according to Roetscher, separation will occur at the circle which is defined by the contact plane and the 45 degree truncated cone emanating from the outer radius of the bolt head.

Since 1961 Fernlund [3], Greenwood [4] and Lardner [5] among others reported solutions based upon the theory of elasticity. Although their solutions also yield separation radii at approximately 45 degrees as in Roetscher's rule, their solutions yield a much more reasonable pressure distribution as compared to Roetscher's constant pressure at each level of the frustrum. These investigators have made use of the Hankel transform method demonstrated by Sneddon [6] in his solution for the elastic stresses produced in a thick plate of infinite radius by the application of pressure to its free surfaces. The basic assumption in their approach is that two bolted plates can be represented by a single plate of the same thickness as the combined thickness of the two plates under the same external loading. It then follows that the z -stress distribution at the parting plane can be approximated by the z -stress distribution in the same plane of the single plate. It also follows that separation will occur at the smallest radius in that plane for which

the z -stress is tensile. In the case of two plates of equal thickness the σ_z stress at the midplane of the equivalent single plate is the stress of interest.

Fernlund [3], for example, used the method of superposition in the sequence shown in Figs. 3(a) to 3(c) to obtain annular loading. Then by superposition of shear and radial stresses at radius A , Figs. 3(d) and 3 (e), opposite in sign of those due to the annular loading at the free surfaces, Fernlund obtained the solution for a single plate with a hole under annular loading (Fig. 3(f)).

Experimental work in this area included Bradley's [7] measurements of the stress field by three dimensional photoelasticity techniques, and the use of introducing pressurized oil at various radii in the contact zone and measuring the pressure at which oil leaks out from the joint [3,8]. Both of these experimental methods have uncertainties as indicated by the authors.

Because of the cumbersomness of the Hankel transform solution and experimental difficulties, the body of work in this area has been very limited and definite verification of analytical results by experiment is not cited in the literature.

The research described in the succeeding chapters was undertaken with the following primary objectives:

- a) To provide a method of solution for the case of two bolted plates without the simplifying assumption of the single plate substitution.
- b) To devise a test to validate the two plate analysis.
- c) To test the validity of the single plate substitution.

A finite element computer program has been assembled for the analytical solution of two-plate problems. Experiments have been performed to verify the analytical results. Since in heat transfer calculations the extent of the radius of contact is of primary importance, and since by restricting the experimental effort to the verification of only this parameter, (rather than the verification of the entire pressure distribution,) many experimental uncertainties should be eliminated, the experiments were designed only for the determination of the contact area.

Agreement between analysis and experiment was obtained and the results show that the single plate substitution is not justified and the 45 degree rule is not valid for the flat and smooth surfaces studied.

Chapter II

ANALYSIS

A. Problem Statement

The objective of the analysis was to solve the linear elasticity problem of two plates in contact defined mathematically by the following equations for each plate:

The equations of equilibrium

$$\frac{\partial}{\partial r} (r \sigma_r) - \sigma_t + r \frac{\partial \tau}{\partial z} = 0 \tag{2.1}$$

$$\frac{\partial}{\partial r} (r \tau) + \frac{\partial}{\partial z} (r \sigma_z) = 0$$

where $\tau_{rz} = \tau_{zr} = \tau$ and $\tau_{rt} = \tau_{tr} = \tau_{zt} = \tau_{tz} = 0$.

The stress - strain relations, using standard notation for stress and strain,

$$\begin{aligned} \sigma_r &= \lambda \epsilon + 2 \mu \epsilon_r \\ \sigma_t &= \lambda \epsilon + 2 \mu \epsilon_t \\ \sigma_z &= \lambda \epsilon + 2 \mu \epsilon_z \\ \tau &= 2 \mu \epsilon_{rz} \end{aligned} \tag{2.2}$$

where λ and μ are Lamé's constants and

$$\lambda = \frac{2 G \nu}{1 - 2\nu} \quad (2.3)$$

$$\mu = G$$

if G is the modulus of elasticity in shear and ν is Poisson's ratio; and ϵ the volume expansion is defined by

$$\epsilon = \frac{\partial u}{\partial r} + \frac{u}{r} + \frac{\partial w}{\partial z} \quad (2.4)$$

where u is the displacement in the radial direction and w is the displacement in the axial direction.

The strain - displacement relations

$$\begin{aligned} \epsilon_r &= \frac{\partial u}{\partial r} \\ \epsilon_t &= \frac{u}{r} \\ \epsilon_z &= \frac{\partial w}{\partial z} \\ \epsilon_{rz} &= \frac{1}{2} \left(\frac{\partial u}{\partial z} + \frac{\partial w}{\partial r} \right) \end{aligned} \quad (2.5)$$

The above equations can be combined to yield the equilibrium equations in terms of displacements

$$\begin{aligned} \nabla^2 u - \frac{u}{r^2} + \frac{1}{1 - 2\nu} \frac{\partial \epsilon}{\partial r} &= 0 \\ \nabla^2 w + \frac{1}{1 - 2\nu} \frac{\partial \epsilon}{\partial z} &= 0 \end{aligned} \quad (2.6)$$

The applicable boundary conditions are (see Fig. 11)

$$\begin{aligned}
 \sigma_r^{(1)}(A,z) &= \sigma_r^{(2)}(A,z) = 0 \\
 \tau^{(1)}(A,z) &= \tau^{(2)}(A,z) = 0 \\
 \sigma_r^{(1)}(C,z) &= \sigma_r^{(2)}(C,z) = 0 \\
 \tau^{(1)}(C,z) &= \tau^{(2)}(C,z) = 0 \\
 \tau^{(1)}(r,D_1) &= \tau^{(2)}(r,-D_2) = 0, \\
 \tau^{(1)}(r,0) &= \tau^{(2)}(r,0), \quad A \leq r \leq R_0 \\
 \sigma_z^{(1)}(r,D_1) &= \sigma_z^{(2)}(r,-D_2) = 0, \quad B \leq r \leq C \\
 \tau^{(1)}(r,0) &= \tau^{(2)}(r,0) = 0, \quad R_0 \leq r \leq C \\
 \sigma_z^{(1)}(r,0) &= \sigma_z^{(2)}(r,0), \quad A \leq r \leq R_0 \\
 \sigma_z^{(1)}(r,0) &= \sigma_z^{(2)}(r,0) = 0, \quad R_0 \leq r \leq R \\
 \sigma_z^{(1)}(r,D_1) &= \sigma_z^{(2)}(r,-D_2) = P(r), \quad A \leq r \leq B \\
 w^{(1)}(r,0) &= w^{(2)}(r,0), \quad A \leq r \leq R_0
 \end{aligned} \tag{2.7}$$

$$2\pi \int_A^B Pr \, dr = 2\pi \int_A^{R_0} pr \, dr$$

Inspection of the above equations shows that the above constitutes a mixed boundary value problem and the most appropriate technique for solution is the finite element method.

B. Method of Analysis

A finite element computer program was assembled for the analytical solution of bolted plates. Descriptions of the finite element method are given in references [9,10], but for completeness, an outline of the mathematical formulation for this case is presented in Appendix A. A listing of the computer program and instructions for its use may be found in Appendix B. Appendix C contains user's instructions and a listing of the finite element program modified to include thermal strains.

As in the previous work axial symmetry and isotropic linear elastic material behavior were assumed. However, the computer programs accommodate plates with different material properties in a bolted pair.

The basic concept of the finite element method is that a body may be considered to be an assemblage of individual elements. The body then consists of a finite number of such elements interconnected at a finite number of nodal points or nodal circles. The finite character of the structural connectivity makes it possible to obtain a solution by means of simultaneous algebraic equations. When the problem, as is the case here, is expressed in a cylindrical coordinate system and in the presence of axial symmetry in geometry and load, tangential displacements do not exist, and the three-dimensional annular ring finite element is then reduced to the characteristics of a two-dimensional finite element.

The analysis consists of (a) structural idealization, (b) evaluation of the element properties, and (c) structural analysis of the assemblage of the elements. Items (b) and (c) are covered in the appendices and in the references quoted. The structural idealization and the criteria for acceptable solutions will be described in this chapter.

Fig. 4(a) shows two circular plates in contact under arbitrary axisymmetric loading. The plates are subdivided into a number of annular ring elements which are defined by the corner nodal circles (or node points when represented in a plane) as shown in Figs. 4(b) and 4(c). Unlike the cases described in Chapter I, which have been solved by the Hankel transform method, all plates solved by the finite element method have finite radii. The cross sections of each annular ring element is either a general quadrilateral or triangle. To improve accuracy smaller elements are used in zones where rapid variations in stress are anticipated than in zones of constant stress; thus the different size elements shown in Fig. 4(b). (However, the total number of elements allowable are subject to computer capacity.)

Figure 4(b) shows the two plates in contact for the radial distance X_c and separated beyond it. It is to be noted that the nodal points on the parting line and within the length of contact X_c are common to elements in both plates. The other elements adjacent to the parting line on each plate are separated from their corresponding elements in the mating plate and these elements have no common nodal points. Physically, it is equivalent to the welding together of the two plates in the contact zone. Mathematically, we are imposing the condition that

in the contact zone the displacements in the z and r directions be identical for both plates. In the case of bolted plates of equal thickness, i.e. in the presence of symmetry about the parting plane, these conditions apply exactly. Furthermore, because of this symmetry, one needs to analyze only one plate, as shown in Fig. 5(b), with the imposed boundary conditions on the contact zone of zero displacement in the z -direction and freedom to displace in the r -direction. It can also be observed that the solution of two plates with symmetry about the parting plane is equivalent to the solution of one of these plates under the same loading conditions, but resting on a frictionless infinitely rigid plane. Also, under the above conditions the shear stress in the contact zone is identically zero.

In the case of bolted plates of unequal thickness the model includes both plates as shown in Fig. 5(c). This model is an approximation because, in general, two plates of unequal thickness do not have the same displacement in the r -direction on the contact surface. The solution yields, therefore, a shearing stress distribution in the contact zone. The solution, however, should be exactly compatible with the physical model if the frictional forces in the joint prevent sliding.

The critical aspect of the approach used herein is the determination of the largest nodal circle on the parting plane which is common to an element on each plate. This nodal circle defines the contact zone and the radius, R_0 , at which separation occurs.

The output of the finite element computer program includes the displacement of each node in the r and z directions and the average

σ_z , σ_r , σ_t and τ_{rz} stresses for each element.

The computation is iterative and the objective is to achieve the lowest possible compressive σ_z stress in the outermost elements bordering the contact zone. Unacceptable solutions are shown in Fig. 6(a) and 6(b). If R_o for a given external load distribution is too small, then the solution will show that the two plates intersect (Fig. 6(a)). On the other hand, if R_o is assumed too large, the solution will show that the outer portion of the contact zone sustains a tensile σ_z stress (Fig. 6(b)). Neither of these two situations is physically feasible. In general, the procedure employed was to commence the iterations with a value for R_o which would yield a tensile σ_z stress in the outer elements adjacent to the contact zone and then move R_o inward. The iteration ended as soon as no tensile σ_z stress was present at the contact zone. For example, for the case shown in Fig. 5(b), if the σ_z stress for the element in the last row and to the left of the last roller is tensile, then the following iteration will proceed without the last roller. Thus, the resolution is one nodal interval. Finer resolution can be obtained by reducing the interval between nodal circles by introducing more elements or shifting the grid locally. The same criteria apply to the model shown in Fig. 5(c).

In the finite element analysis of the Fernlund (3) model, i.e. single plate with external loads at the faces $z = \pm D$ no iteration is required and the rollers shown in Fig. 5(c) would extend to the outer radius of the plate. (Although Fernlund's computations are based on infinite plates, computations show that there is no distinction between infinite plates and plates of radius greater than five times of the outer

radius, B , of the load. See Fig. 5(a).

Convergence was tested by subdividing elements further, with nodal points in the coarser grid remaining nodal points in the finer grid. Changing the mesh from 180 elements to 360 elements have shown no improvement in accuracy. Meshes from 180 to 300 elements were used in this analysis. Typical spacings between nodal points were 0.015 inch radially and 0.03 inch in the z -direction.

Chapter III

EXPERIMENTAL METHOD

The objective of the experiment was to determine the extent of contact between two plates when bolted together. Sixteen type 304 stainless steel plates, 4 inches in diameter, were machined to nominal thicknesses of 1/16, 1/8, 3/16 and 1/4 inch, 4 plates for each thickness. After rough machining these plates were stress relieved at 1875°F and ground flat to 0.0002 inch. One side of each plate was then lapped flat to better than one fringe of sodium light (11 micro-inches) in the case of the 1/8, 3/16 and 1/4 inch plates, and to better than two fringes in the case of the 1/16 inch plates. Disregarding scratches, the finish of the lapped surfaces was 5 micro-inches rms. Each plate had a central hole, 0.257 inch in diameter, for a 1/4 - 20 bolt, and two notches and two holes on the periphery (see Fig. 7). Two techniques were employed in determining the area of contact when two of these plates were bolted together. The first technique entailed the following procedure (see Fig. 7):

- (a) The plates were cleaned with alcohol and lens tissue.
- (b) One plate was placed on the base of the fixture shown in Fig. 7, lapped surface up and the two holes on the periphery of the plates engaged with two pins on the fixture. Spacers between the fixture base and plate prevented the pins from extending beyond the top surface of the plate.

- (c) A second plate was placed on top of the first plate, lapped surfaces mating. The notches on the two plates were lined up with each other and with notches in the base of the fixture. Thus, rotation of the plates was prevented.
- (d) A standard 1/4 - 20 hex-nut with its annular bearing surface (0.42 inch O.D.) lapped flat was engaged on a high strength 1/4 - 20 bolt. The nut was located about two threads away from the head of the bolt and served in lieu of the bolt head. The lapped surface of the nut faced away from the bolt head and since the nut was not sent home against the bolt head, the looseness of fit between nut and bolt offered a degree of self alignment.
- (e) The bolt and nut assembly described in (d) above was then inserted through the 1/4 inch central holes of the two plates and a second 1/4 - 20 lapped nut was engaged on the bolt. Thus the two plates were captured by the two 1/4 -20 nuts with the lapped surfaces of the nuts bearing against the plates.
- (f) With the torque wrench shown on the right in Fig. 7, the nuts were torqued down to 70 pound-inches of torque to yield a 1100 pound force in the bolt [11].
- (g) The position of the keys was changed to engage with only the lower plate and the fixture and a special spanner wrench, as shown in Fig. 7, was engaged with the top plate. The spanner wrench was restrained to move in the horizontal plane and it was set into motion by the screw pressing against the wrench handle.

- (h) With the aid of the spanner wrench the upper plate was rotated relative to the lower plate several times approximately + 5 degrees.

Thus, the above procedure allowed for the rubbing of one plate relative to its mate while under a bolt force of approximately 1100 lbs. The remaining steps were the disassembly and the measurement of the extent of the contact zone which was defined by the shine due to the rubbing in the contact zone. It is to be noted that the boundaries of the contact zone as measured by the naked eye and by searching for marks of "polished" or "damaged" surface under a 10.5 power magnification are essentially the same.

The above test was performed on 5 pairs of specimen. These were

1. One 0.07 in. plate mated to a 0.65 in. plate
2. One 0.126 in. plate mated to a 0.126 in. plate
3. One 0.191 in. plate mated to a 0.192 in. plate
4. One 0.253 in. plate mated to a 0.256 in. plate
5. One 0.124 in. plate mated to a 0.257 in. plate

The identical tests were repeated for

1. One 0.124 in. plate mated to a 0.126 in. plate; and
2. One 0.191 in. plate mated to a 0.192 in. plate,

but in lieu of the 1/4 - 20 nuts in direct contact with the plates special washers, 1.000 in. O.D., 0.257 in. I.D. and 0.620 in. high, were interposed between the bolt head and nut.

The diameters of the contact zones were measured with a machinist ruler with 100 divisions to the inch and with a Jones and Lamston Vertac 14 Optical Comparator.

The second technique used the same parts and fixture, but it involved autoradiographic measurements.

Four plates, 1/4, 3/16, 1/8 and 1/16 inch thick were sent to Tracerlab, Inc., Waltham, Mass., for electrolytic plating with radioactive silver $\text{Ag } 110^{\text{M}}$ (half life of 8 months). Each plate was masked except for an area on the lapped face one inch in radius. The plates then received a plating of copper about 5 microinches thick and then approximately a 5 microinch plating of silver containing the radioactive isotope. The resultant activity on each plate was about 2 millicuries.

These plates were then mated to plates of equal thickness (not plated) and assembled in a shielded hood as indicated in steps (a) to (h) above except that in the case of the pair of 1/4 inch plates care was taken not to rotate the plates during and after assembly and in the remaining cases the rotation specified in step (h) was done only once in one direction.

The plates were then disassembled and the radioactive contamination on the plates which were in contact with the radioactive plates measured. The transferred activity was:

1/4 in. plate	approximately	0.05 microcuries
3/16 in. plate	approximately	3. microcuries
1/8 in. plate	approximately	0.1 microcuries
1/16 in. plate	approximately	0.4 microcuries

It was also observed in handling that the adhesion of the silver on the 3/16 in. plate was poor.

Kodak type R single coated industrial x-ray film was then placed on the contaminated plates under darkroom conditions. The sensitive side of the film was pressed against the radioactive sides of the plates with a uniform load of about five pounds and left for exposure for three days. After three days, the film was removed and developed. The results are shown in Fig. 10.

Chapter IV

RESULTS

A. Pressure Distribution and Radii of Separation from Single Plate and Two Plate Finite Element Models.

Using the finite element procedure described in Chapter II, the midplane stress distribution of single circular plates of thickness $2D$, outer radii of 1.54 in., inner radii of 0.1 in., Poisson ratio of 0.3, and loaded by a constant pressure between radii A and B , Fig. 3(f), was computed. Computations were performed for D values of 0.1, 0.1333 and 0.2 in. For each value of D the radius B , which defines the region of the symmetric external load, assumed the values of 0.31, 0.22, 0.16 and 0.13 in. The σ_z stress distribution at the midplane, from the inner radius to the radius at which the above stress is no longer compressive, is shown in Figs. 12, 13 and 14 as a function of radius.

The identical cases were then recomputed, using again the finite element method, in accordance with the two plate model shown in Figs. 4(b) and 5(b). These results are given in Figs. 15, 16 and 17.

Inspection of the above figures show that the two plate model yields a somewhat different stress distribution in the contact zone than the stress distribution approximated from the single plate model, and more significantly, from the heat transfer point of view, the two plate model yields a lower value for the radius of separation, R_o , which

results in a reduction in area for heat transfer. Table 1 gives a comparison of the values for R_o obtained from the two models.

It may be observed that the single plate result of Fernlund (Ref. 3, pp. 56, 124) is in fair agreement with the finite element results obtained for the single plate model.

B. Radii of Separation from Experiment and Their Predicted Values from the Two Plate Finite Element Computation.

As described in Chapter III, stainless steel circular plate specimen (Fig. 7) were bolted together, rotated relative to each other with the bolt force acting, and after disassembly the contact area of the joint was determined by measuring the footprints (the shiny, polished areas) on each plate due to the plates rubbing against each other. Photographs of these footprints are shown in Fig. 8. Fig. 9 also shows a typical footprint of the annular bearing surface of the 1/4 - 20 nut against a plate. All plates tested were of 304 stainless steel, 4 inch O.D., .257 I.D., and the nominal thicknesses of the plates were 1/16, 1/8, 3/16 and 1/4 inch. In addition to the plates fastened with standard nuts which gave a loading circle of radius B (Fig. 5) of 0.211 inch, plates fastened by the special nuts described in Chapter III for which B was 0.5 inch were also tested.

Figure 10 shows the results of the autoradiographic tests described in Chapter III. For all plate pairs tested, i.e. 1/16, 1/8, 3/16 and 1/4 inch nominal, the value of B was 0.211 inch.

The pressure distributions and radii of separation for all the

above test cases were computed independently by the two plate model finite element analysis. Table 2 gives the test and analytical results for all test cases. The test results are an average of all measurements (minimum of six readings). A description of the analyses follows.

Figure 18 shows the results of a two plate and a single plate model analysis for the 0.253 inch bolted test specimen. For Figure 19 the external pressure distribution between radii A and B is triangular. (The total force, however, is equal to the force exerted in the case of uniform pressure.) In one case, the peak external pressure is at A, Fig. 20(a), and in the other case at B, Fig. 20(b). Results of another computation which assumed a uniform displacement of 50 microinches under each nut is shown in Fig. 21. It is interesting to note that the point of separation obtained by using the two plate model for all variations of loading given above occurs in the range of r/A values of 2.73 to 2.93 while the two plate model yields separation at a value for r/A of 3.5. The computed deflections under the nuts are given in Fig. 22.

The finite element analysis results for the 0.191 in. plate pair specimen are given in Fig. 23. Figures 24 and 25 show the computed pressure distribution and deflection patterns in the joint, respectively, for the 1/8 in. plate pair. In order to investigate the possible influence misalignments of the spanner wrench, i.e. vertical forces or restraints exerted at edge of plate, may have on the results of the experiment, the extreme case of fixing the outer edges of the plate as shown in Fig. 20(c) was considered. As Fig. 24 shows, within the

resolution of the finite element grid size, the effect is negligible. This model, Fig. 20(c), and result also indicate that the influence of additional fasteners 2 inches away would not have an influence on the contact zone for the geometry considered. (However, if the distance between bolts is considerably reduced, then the contact area should increase.) The computed results for the 1/16 inch plate pair is given in Fig. 26.

Figure 27 gives the finite element analysis results for the asymmetric case of a 1/8 in. plate bolted to a 1/4 in. plate. The model shown in Fig. 5(c) was used and as discussed in Chapter II, this model is strictly valid only if the friction in the joint prevents sliding between the plates. Nevertheless, the percent discrepancy between the computed value and tested value (see Table 2) falls within the range of the symmetric cases analyzed and tested.

In summary, the results obtained from the two plate finite element model and from experiment are in good agreement (Fig. 28).

Chapter V

APPLICATION

An application of the above results for the evaluation of the thermal contact conductance, h_c , and the determination of the heat transferred in a specific, but typical, lap joint section is illustrated in this chapter.

An aluminum lap joint in a vacuum environment, the relevant section and boundary conditions as shown in Fig. 29, was analyzed by means of a nodal analysis. The plate thickness was 0.1 in. and the hole diameter, 2A, was 0.2 in. The bearing surface of the bolt, 2B, was 0.26 in. in diameter. Because of the high conductivity and small thickness of the plates, no z dependence (see Fig. 29) was assumed for the temperature in the main body of the plate. However, heat flow in the z -direction in the nodes above and below the contact zone is considered. Qualitatively, the heat flow in the joint proceeds in the x - y plane from the left end (Fig. 29) toward the 0.2 in. diameter hole. In the vicinity of the hole, a macroscopic constriction for heat flow is encountered because the flow is being channeled toward the small contact zone. The flow of heat then encounters the microscopic constrictions at the contacting asperities (which determine h_c) in the contact zone; spreads out in the x - y directions in the second plate; and continues to the right edge of the lap joint.

The material properties assumed were (refer to equation 1.1):

$$\begin{aligned}
 H &= 150,000 \text{ psi} \\
 k &= 100 \text{ Btu/hr-}^\circ\text{F-ft} \quad (k_1 = k_2 = 100) \\
 \sigma &= 5.9 \times 10^{-6} \text{ ft.} \quad (\sigma_1 = \sigma_2 = 50 \times 10^{-6} \text{ in.}) \\
 \tan \theta &= 0.1
 \end{aligned}$$

Assuming further, a uniform load of 46,500 psi on the loading surface (#10 screw; 1000 lb. bolt force) and referring to Fig. 15, curve $\frac{B}{A} = 1.3$, the following interface stresses, σ_z , contact heat transfer coefficient, h_c , and conductance, (area) $\cdot(h_c)$, were obtained as a function of inner and outer radii. (These radii define increments of area, the sum of which define one quarter of the contact zone.):

$\underline{r_{\text{outer}}}$ inch	$\underline{r_{\text{inner}}}$ inch	$\underline{\sigma_z}$ psi	$\underline{h_c}$ Btu/hr- $^\circ$ F-ft ²	Area x h_c Btu/hr- $^\circ$ F-ft ²
.13	.1	27,900	446,000	16.6
.16	.13	14,000	223,000	10.6
.175	.16	3,950	63,100	1.7

The conductance between nodal points were then computed and with the aid of the steady state heat transfer program listed in Appendix D, the nodal temperatures for the conditions given in Fig. 29 were computed. The heat transferred from the edge maintained at 20 $^\circ$ F to the edge at 0 $^\circ$ F (Fig. 29) for this case was 2.88 Btu/hour. The same computation was repeated for the case of a bearing surface between the plate

and the bolt (2B) of 0.44 in. in diameter, but the bolt force was left unchanged. The heat transferred from the 20°F edge to the 0°F edge in this case was 3.15 Btu/hour. In the absence of the joint the heat transfer along an equivalent 7 inch length of solid aluminum would have been 3.58 Btu/hour. This data shows that the thermal resistance of the contact zone (not entire 7 inch lap joint) was decreased from 1.52 to 0.92 °F-hr/Btu by the increase of the effective bolt head diameter from .26 to .44 in. It should be observed that the change in thermal resistance of the joint is primarily due to the increase in contact area and the resulting decrease in macroscopic constriction resistance at the hole. Also, the heat flux in this example is mainly controlled by the 7 inch length and 0.1 inch thickness rather than the joint resistance. This emphasizes the importance of a balanced thermal design.

For large heat fluxes where thermal strains may have an influence on the radii of separation, the finite element program given in Appendix C may be used. Also, in a non-vacuum environment the effect of the interstitial fluid is added in two ways. Firstly, equation (1.6) is applied to account for the presence of interstitial fluid in the contact zone, and secondly, conduction across the gaps between the plates and convection from the plates is considered. (Radiation heat transfer, if applicable, should also be included.)

Chapter VI

CONCLUSIONS

The finite element technique used in this work for the analysis of the pressure distribution and deformation of smooth and flat bolted plates under conditions of axial symmetry predicts contact areas in joints considerably lower than reported previously in the literature. These results were verified experimentally. The discrepancy between the previously reported results and the results reported here is due to the simplifying assumption made by earlier researchers that a joint can be modeled as a single plate.

The computer programs listed in the appendices will also accommodate joints made up of plates of dissimilar materials and the presence of thermal gradients.

Of the eleven tests performed, only one (case 3, autoradiographic) yielded inconsistent results. (This data point could probably be ignored because of the poor adhesion of the plating material which manifested itself by the high radioactive contamination count during test.)

The finite element analysis performed for the test specimen show that the gap between the $1/4$ inch bolted steel specimen is 98.6 microinches at the outer radius of the plate of 2 inches, and $1/32$ of an inch away from the radius of separation (0.35 in.), the gap is

only 3 microinches for the test load. This data indicates the difficulties previous workers have encountered in their experiments. (This also explains the oval shape of several of the footprints.) Furthermore, this data shows that the effects of surface roughness and the lack of flatness could have a significant effect on the size of contour area.

An application of the above work to a heat transfer problem is illustrated in Chapter V.

REFERENCES

1. Cooper, M.G., Mikic, B.B., and Yovanovich, M.M., "Thermal Contact Conductance," International Journal of Heat and Mass Transfer, Vol. 12, No. 3 (March 1969), 279-300.
2. Roetscher, F., Die Maschinenelemente, Erster Band. Berlin: Julius Springer, 1927.
3. Fernlund, I., "A Method to Calculate the Pressure Between Bolted or Riveted Plates," Transactions of Chalmers, University of Technology. Gothenburg, Sweden, No. 245, 1961.
4. Greenwood, J.A., "The Elastic Stresses Produced in the Mid-Plane of a Slab by Pressure Applied Symmetrically at its Surface," Proc. Camb. Phil. Soc. Cambridge, England, Vol. 60, 1964, 159-169.
5. Lardner, T.J., "Stresses in a Thick Plate with Axially Symmetric Loading," J. of Applied Mechanics, Trans. ASME, Series E, Vol. 32, June 1965 (458-459).
6. Sneddon, I.N., "The Elastic Stresses Produced in a Thick Plate by the Application of Pressure to its Free Surfaces," Proc. Camb. Phil. Soc. Cambridge, England, Vol. 42, 1946 (260-271).
7. Bradley, T.L., "Stress Analysis for Thermal Contact Resistance Across Bolted Joints," M.S. Thesis, Massachusetts Institute of Technology, Mechanical Engineering Department, Cambridge, Mass. August 1968.
8. Louisiana State University, Division of Engineering Research, The Thermal Conductance of Bolted Joints. NASA Grant No. 19-001-035, C.A. Whitehurst, Dir. Baton Rouge: LSU Div. of Eng. Res., May 1968.
9. Zienkiewicz, O.C., The Finite Element Method in Structural and Continuum Mechanics. London: McGraw-Hill Publishing Co., Ltd., 1967.
10. Przemieniecki, J.S., Theory of Matrix Structural Analysis. New York: McGraw-Hill Book Co., 1968.
11. Cobb, B.J., "Preloading of Bolts," Product Engineering, August 19, 1963 (62-66).
12. Wilson, E.L., "Structural Analysis of Axisymmetric Solids," AIAA Journal, Vol. 3, No. 12, (Dec. 1965), 2269-2274.

13. Jones, R.M. and Crose, J.G., SAAS II Finite Element Stress Analysis of Axisymmetric Solids. United States Air Force Report No. SAMS0-TR-68-455 (Sept. 1968).
14. Christian, J.T. and others, FEAST-1 and FEAST-3 Programs. Cambridge: Computer Program Library, M.I.T. Department of Civil Engineering, Soil Mechanics Division, 1969.
15. Clough, R.W., "The Finite Element Method in Structural Mechanics," Ch. 7, Stress Analysis, Zienkiewicz, O.C. and Holister, G.S., editors. London: John Wiley and Sons, Ltd., 1965.

APPENDIX A

FINITE ELEMENT ANALYSIS OF AXISYMMETRIC SOLIDS

The finite element method and the equations which govern the stresses and displacements in axisymmetric solids is given in the literature [9,10,12,13,15] and the procedure will be briefly summarized in this appendix.

The procedure for the standard stiffness analysis method is as follows [15]:

- (a) The internal displacements, v , are expressed as

$$\{v(r,z)\} = [M(r,z)] \{\alpha\} \quad (A.1)$$

where M is a displacement function and α are the generalized coordinates representing the amplitudes of the displacement functions.

- (b) The nodal displacements v_i are expressed in terms of the generalized coordinates

$$\{v_i\} = [A] \{\alpha\} \quad (A.2)$$

where A is obtained by substituting the coordinates of the nodal points into M .

- (c) The generalized coordinates are expressed in terms of the nodal displacements

$$\{\alpha\} = [A]^{-1} \{v_i\} \quad (A.3)$$

(d) The element strains, ϵ , are evaluated

$$\{\epsilon\} = [B(r,z)] \{\alpha\} \quad (\text{A.4})$$

where B is obtained from the appropriate differentiation of M .

(e) The element stresses are expressed in terms of the stress-strain relation D

$$\{\sigma(r,z)\} = [D] \{\epsilon\} = [D] [B] \{\alpha\} \quad (\text{A.5})$$

(f) Assuming a virtual strain $\bar{\epsilon}$ and a generalized virtual coordinate displacement $\bar{\alpha}$ the internal virtual work, W_i , in the differential volume, dV , is given by

$$dW_i = \{\epsilon\}^T \{\sigma\} dV = \{\alpha\}^T [B]^T [D] [B] \{\alpha\} dV \quad (\text{A.6})$$

and the total internal virtual work is

$$W_i = \{\bar{\alpha}\}^T \left[\int_{\text{Vol}} [B]^T [D] [B] dV \right] \alpha \quad (\text{A.7})$$

(g) The external work, W_e , associated with the generalized displacement $\bar{\alpha}$ is

$$W_e = \{\bar{\alpha}\}^T \{\beta\} \quad (\text{A.8})$$

where β are generalized forces corresponding with the displacements α .

(h) After equating W_i and W_e and setting the $\bar{\alpha}$ displacement to unity

$$\{\beta\} = \left[\int_{Vol} [B]^T [D] [B] \right] \alpha = [\bar{k}] \{\alpha\} \quad (A.9)$$

where $[\bar{k}] = \int_{Vol} [B]^T [D] [B] dV$ (A.10)

and which transforms to the nodal point surfaces

$$k = [A^{-1}] [\bar{k}] [A^{-1}] \quad (A.11)$$

(i) The stiffness matrix for the complete system is then

$$[K] = \sum_{m=1}^n [k]_m \quad (A.12)$$

where n equals the number of elements and the equilibrium relationship becomes

$$\{Q\} = [K] \{v_i\} \quad (A.13)$$

where

$$\{Q\} = \sum_{m=1}^n \{R\}_m \quad (A.14)$$

$$\{R\} = \int_{Area} [A^{-1}]^T [M]^T \{P\}_m dA \quad (A.15)$$

and P are the surface forces.

The above procedure applies with minor modification to problems with thermal and body force loading.

The expression

$$\{Q\} = [K] \{v_i\} \quad (A.16)$$

represents the relationship between all nodal point forces and all nodal point displacements. Mixed boundary conditions are considered by rewriting this equation in the partitioned form

$$\begin{Bmatrix} Q_a \\ Q_b \end{Bmatrix} = \begin{bmatrix} K_{aa} & K_{ab} \\ K_{ba} & K_{bb} \end{bmatrix} \begin{Bmatrix} u_a \\ u_b \end{Bmatrix} \quad (A.17)$$

where $v_i = u$.

The first part of the partitioned equation can be written as

$$\{Q_a\} = [K_{aa}] \{u_a\} + [K_{ab}] \{u_b\} \quad (A.18)$$

and then expressed in the reduced form

$$\{Q^*\} = [K_{aa}] \{u_a\} \quad (A.19)$$

where

$$\{Q^*\} = \{Q_a\} - [K_{ab}] \{u_b\} \quad (A.20)$$

The matrix equation (A.19) is solved for the nodal point displacements by standard techniques. Once the displacement are known the strains are evaluated from the strain displacement relationship and the stresses in turn are evaluated from the stress strain relations.

Both triangular and quadrilateral elements are used. The displacements in the $r-z$ plane in the element are assumed to be of the form

$$v_r = \alpha_1 + \alpha_2 r + \alpha_3 z \tag{A.21}$$

$$v_z = \alpha_4 + \alpha_5 r + \alpha_6 z$$

This linear displacement field assures continuity between elements since lines which are initially straight remain straight in their displaced position. Six equilibrium equations are developed for each triangular element.

A quadrilateral element is composed of four triangular elements and ten equilibrium equations correspond to each element.

APPENDIX B

FINITE ELEMENT PROGRAM FOR THE ANALYSIS OF ISOTROPIC
ELASTIC AXISYMMETRIC PLATES (ref. 13,14)

Input Instructions:

<u>Card Sequence</u>	<u>Item</u>	<u>Format</u>	<u>Columns</u>
1	Title	18A4	1-72
2	Total number of nodal points	I5	1-5
	Total number of elements	I5	6-10
	Total number of materials	I5	11-15
	Normalizing stress (NORM)	I5	16-20
	Number of pressure cards	I5	21-25

(If NORM = 0, put in value of E in material card;
if NORM = 1, put in value $E/\sigma_{\text{vertical}}$;
if NORM = -1, put in value $E/\sigma_{\text{octahedral}}$;

NOTE: Use NORM = 0 for this application.)

3	(Material property cards - one set of (a) and (b) for each material)		
	(a) 1st card		
	Material No.	I5	1-5
	Initial σ_z stress	F10.0	6-15
	Initial σ_r stress	F10.0	16-25
	(b) Second Card		
	E	F10.0	1-10
	ν	F10.0	11-20

<u>Card Sequence</u>	<u>Item</u>	<u>Format</u>	<u>Column</u>
4	Nodal point information (One for each node)	2I5,4F10.0	
	Node number		1-5
	CODE		6-10
	r-coordinate		11-20
	z-coordinate		21-30
	XR		31-40
	XZ		41-50

If the number in column 10 is

		<u>Condition</u>
0	XR is the specified R-load and XZ is the specified Z-load	free
1	XR is the specified R-displacement and XZ is the specified Z-load	
2	XR is the specified R-load and XZ is the specified Z-displacement.	
3	XR is the specified R-displacement and XZ is the specified Z-displacement.	fixed

Remarks

The following restrictions are placed on the size of problems which can be handled by the program.

<u>Item</u>	<u>Maximum Number</u>
Nodal Points	450
Elements	450
Materials	25
Boundary Pressure Cards	200

All loads are considered to be total forces acting on a one radian segment. Nodal point cards must be in numerical sequence. If cards are omitted, the omitted nodal points are generated at equal intervals along a straight line between the defined nodal points. The boundary code (column 10), XR and XZ are set equal to zero.

If the number in columns 6-10 of the nodal point cards is other than 0, 1, 2 or 3, it is interpreted as the magnitude of an angle in degrees. The terms in columns 31-50 of the nodal point card are then interpreted as follows:

XR is the specified load in the s-direction

XZ is the specified displacement in the n-direction

The angle must always be input as a negative angle and may range from -.001 to -180 degrees. Hence, +1.0 degree is the same as -179.0 degrees. The displacements of these nodal points which are printed by the program are

u_r = the displacement in the s-direction

u_z = the displacement in the n-direction

Element cards must be in element number sequence. If element cards are omitted, the program automatically generates the omitted information by incrementing by one the preceding I, J, K and L. The material identification code for the generated cards is set equal to the value given on the last card. The last element card must always be supplied.

Triangular elements are also permissible; they are identified by repeating the last nodal point number (i.e. I, J, K, K).

One card for each boundary element which is subjected to a normal pressure is required. The boundary element must be on the left as one

progresses from I to J. Surface tensile force is input as a negative pressure.

Printed output includes:

1. Reprint of input data.
2. Nodal point displacement
3. Stresses at the center of each element.

Nodal point numbers must be entered counterclockwise around the element when coding element data.

The maximum difference between the nodal point numbers on an element must be less than 25. However, on a nodal diagram elements and nodes need not be numbered sequentially.

Listing:

```

C *****
C FINITE ELEMENT PROGRAM FOR THE ANALYSIS OF ISOTROPIC ELASTIC
C AXYSYMMETRIC PLATES REF FEAST 1,3 SAAS 2
C *****
C
C      IMPLICIT REAL*8 (A-H,O-Z)
C      IMPLICIT INTEGER*2(I-N)
C      COMMON      STTOP,HED(18),SIGIR(25),SIGI7(25),GAMMA(25),ZKNOT(25),
C 1 DEPTH(25),E(10,25),SIG(7),R(450),Z(450),UR(450),
C 2 UZ(450),SICOTAL(450,4),KSW
C      COMMON /INTEGR/ NUMNP,NUMEL,NUMMAT,NDEPTH,NORM,MTYPE,ICODE(450)
C      COMMON /ARG/ RRR(5),ZZZ(5),S(10,10),P(10),LM(4),DD(3,3),
C 1 HH(6,10),RR(4),ZZ(4),C(4,4),H(6,10),D(6,6),F(6,10),TP(6),XI(6),
C 2 FE(10),IX(450,5)
C      COMMON /BANARG/ B(900),A(900,54),MBAND
C      COMMON/PRESS/ IBC(200),JBC(200),PR(200),NUMPC
C      DATA STRS / ***** /
C *****
C READ AND PRINT CONTROL INFORMATION
C *****
C 50 READ (5,1000,END=950) HED
C      WRITE (6,2000) HED
C
C      READ(5,1001) NUMNP,NUMEL,NUMMAT,NORM,NUMPC
C      WRITE (6,2006) NUMNP,NUMEL
C      IF (NORM) 65,65,66
C 66 WRITE (6,2041)
C *****
C READ AND PRINT MATERIAL PROPERTIES
C *****
C 65 CONTINUE
C
C      DO 80 M=1,NUMMAT
C      READ (5,1002) MTYPE,
C      WRITE (6,2007) MTYPE,SIGIZ(MTYPE),SIGIR(MTYPE)
C      READ (5,1003) (E(J,MTYPE),J=1,2)

```

```

FENT0001
FENT0002
FENT0003
FENT0004
FENT0005
FENT0006
FENT0007
FENT0008
FENT0009
FENT0010
FENT0011
FENT0012
FENT0013
FENT0014
FENT0015
FENT0016
FENT0017
FENT0018
FENT0019
FENT0020
FENT0021
FENT0022
FENT0023
FENT0024
FENT0025
FENT0026
FENT0027
FENT0028
FENT0029
FENT0030
FENT0031
FENT0032
FENT0033
FENT0034
FENT0035
FENT0036

```


	IX(N,4)=IX(N-1,4)+1	FENT0073
	IX(N,5)=IX(N-1,5)	FENT0074
170	WRITE (6,2017) N,(IX(N,I),I=1,5)	FENT0075
	IF (M-N) 180,180,140	FENT0076
180	IF (NUMEL-N) 300,300,130	FENT0077
C	*****	FENT0078
C	READ AND PRINT THE PRESSURE CARDS	FENT0079
C	*****	FENT0080
300	IF(NUMPC) 290,210,290	FENT0081
290	WRITE(6,9000)	FENT0082
	DO 200 L=1,NUMPC	FENT0083
	READ(5,9001) IRC(L),JBC(L),PR(L)	FENT0084
200	WRITE(6,9002) IRC(L),JBC(L),PR(L)	FENT0085
210	CONTINUE	FENT0086
C	*****	FENT0087
C	DETERMINE PAND WIDTH	FENT0088
C	*****	FENT0089
	J=0	FENT0090
	DO 340 N=1,NUMEL	FENT0091
	DO 340 I=1,4	FENT0092
	DO 325 L=1,4	FENT0093
	KK=IX(N,I)-IX(N,L)	FENT0094
	IF (KK.LT.0) KK=-KK	FENT0095
	IF (KK.GT.J) J=KK	FENT0096
325	CONTINUE	FENT0097
340	CONTINUE	FENT0098
	MRAND=2*J+2	FENT0099
C	*****	FENT0100
C	SOLVE FOR DISPLACEMENTS AND STRESSES	FENT0101
C	*****	FENT0102
	KSW=0	FENT0103
	CALL STIFF	FENT0104
	IF (KSW.NE.0) GO TO 900	FENT0105
C		FENT0106
	CALL BANSCL	FENT0107
	WRITE(6,2052)	FENT0108

```

WRITE (6,2025) (N,B      (2*N-1),B      (2*N),N=1,NUMNP)
C
C 450 CALL STRESS(SPLOT)
C *****
C PROCESS ALL DECKS EVEN IF ERROR
C *****
GO TO 910
900 WRITE (6,4000)
910 WRITE (6,4001) HED
C
920 READ (5,1000) CHK
IF (CHK.NE.STRS) GO TO 920
GO TO 50
950 CONTINUE
WRITE (6,4002)
CALL EXIT
C *****
C *****
1000 FORMAT (18A4)
1001 FORMAT (12I5)
1002 FORMAT ( 15,2F10.0)
1003 FORMAT(2F10.0)
1004 FORMAT (2F10.0)
1005 FORMAT (3F10.0)
1006 FORMAT (2I5,4F10.0)
1007 FORMAT (6I5)
C *****
2000 FORMAT (1H1,20A4)
2006 FORMAT (28HONUMBER OF NODAL POINTS----- I3/
1 28H NUMBER OF ELEMENTS----- I3)
2007 FORMAT (20HOMATERIAL NUMBER----- I3/
1 25H INITIAL VERTICAL STRESS= F10.3 ,5X,
2 26HINITIAL HORIZONTAL STRESS= F10.3)
2013 FORMAT (12H1NODAL POINT ,4X, 4HTYPE ,4X, 10HR-ORDINATE ,4X,
1 10HZ-ORDINATE ,10X, 6HR-LOAD ,10X, 6HZ-LOAD )
2014 FORMAT (I12,I8,2F14.3,2E16.5)

```

```

FENTO109
FENTO110
FENTO111
FENTO112
FENTO113
FENTO114
FENTO115
FENTO116
FENTO117
FENTO118
FENTO119
FENTO120
FENTO121
FENTO122
FENTO123
FENTO124
FENTO125
FENTO126
FENTO127
FENTO128
FENTO129
FENTO130
FENTO131
FENTO132
FENTO133
FENTO134
FENTO135
FENTO136
FENTO137
FENTO138
FENTO139
FENTO140
FENTO141
FENTO142
FENTO143
FENTO144

```

2015	FORMAT (26HONODAL POINT CARD ERROR N= I5)	FENT0145
2016	FORMAT (49H1ELEMENT NO. I J K L MATERIAL)	FENT0146
2017	FORMAT (1I13,4I6,1I12)	FENT0147
2025	FORMAT (12HONODAL POINT ,6X, 14HR-DISPLACEMENT ,6X, 14HZ-DISPLACEMENT / (I12,1P2D20.7))	FENT0148
2041	FORMAT (76HOMODULUS AND YIELD STRESS NORMALIZED WITH RESPECT TO INITIAL VERTICAL STRESS)	FENT0149
2051	FORMAT(1H0,10X,'E',8X,'NU',/,3X,F11.1,F10.4/)	FENT0150
2052	FORMAT(1H1)	FENT0151
C	*****	FENT0152
3003	FORMAT (16I5)	FENT0153
C	*****	FENT0154
4000	FORMAT (//// ' ABNORMAL TERMINATION')	FENT0155
4001	FORMAT (//// ' END OF PROBLEM ' 20A4)	FENT0156
4002	FORMAT (////' END OF JOB')	FENT0157
C	*****	FENT0158
9000	FORMAT(29H0PRESSURE BOUNDARY CONDITIONS/ 24H I J PRESSURE)	FENT0159
9001	FORMAT(2I5,F10.0)	FENT0160
9002	FORMAT(2I6,F12.3)	FENT0161
	END	FENT0162
	SUBROUTINE STIFF	FENT0163
C		FENT0164
	IMPLICIT REAL*8 (A-H,O-Z)	FENT0165
	IMPLICIT INTEGER*2(I-N)	FENT0166
	COMMON STTCP,HED(18),SIGIR(25),SIGIZ(25),GAMMA(25),ZKNOT(25),	FENT0167
	1 DEPTH(25),E(10,25),SIG(7),R(450),Z(450),UR(450),	FENT0168
	2 UZ(450),STOTAL(450,4),KSW	FENT0169
	COMMON /INTEGR/ NUMNP,NUMEL,NUMMAT,NDEPTH,NORM,MTYPE,ICODE(450)	FENT0170
	COMMON /ARG/ RRR(5),ZZZ(5),S(10,10),P(10),LM(4),DD(3,3),	FENT0171
	1 HH(6,10),RR(4),ZZ(4),C(4,4),H(6,10),D(6,6),F(6,10),TP(6),XI(6),	FENT0172
	2 EE(10),IX(450,5)	FENT0173
	COMMON /BANARG/ B(900),A(900,54),MBAND	FENT0174
	COMMON/PRFSS/ IBC(200),JBC(200),PR(200),NUMPC	FENT0175
	DIMENSION CODE(450)	FENT0176
C	*****	FENT0177
		FENT0178
		FENT0179
		FENT0180

FENT0181
 FENT0182
 FENT0183
 FENT0184
 FENT0185
 FENT0186
 FENT0187
 FENT0188
 FENT0189
 FENT0190
 FENT0191
 FENT0192
 FENT0193
 FENT0194
 FENT0195
 FENT0196
 FENT0197
 FENT0198
 FENT0199
 FENT0200
 FENT0201
 FENT0202
 FENT0203
 FENT0204
 FENT0205
 FENT0206
 FENT0207
 FENT0208
 FENT0209
 FENT0210
 FENT0211
 FENT0212
 FENT0213
 FENT0214
 FENT0215
 FENT0216

```

C      INITIALIZATION
C      *****
NB=27
ND=2*NB
ND2=2*NUMNP
DO 50 N=1,ND2
  B(N)=0.0
  DO 50 M=1,ND
    A(N,M)=0.0
  *****
  C      FORM STIFFNESS MATRIX
  C      *****
  DO 210 N=1,NUMEL
    *****
    90 CALL QUAD(N,VOL)
    IF (VOL) 142,142,144
    142 WRITE (6,2003) N
    KSW=1
    GO TO 210
  *****
  C      144 IF (IX(N,3)-IX(N,4)) 145,165,145
  C      145 DO 150 II=1,9
  C      CC=S(II,10)/S(10,10)
  C      DO 150 JJ=1,9
  C      150 S(II,JJ)=S(II,JJ)-CC*S(10,JJ)
  C      *****
  C      DO 160 II=1,8
  C      CC=S(II,9)/S(9,9)
  C      DO 160 JJ=1,8
  C      160 S(II,JJ)=S(II,JJ)-CC*S(9,JJ)
  C      *****
  C      ADD ELEMENT STIFFNESS TO TOTAL STIFFNESS
  C      *****
  C      165 DO 166 I=1,4
  C      166 LM(I)=2*IX(N,I)-2
  *****

```

FENT0217
 FENT0218
 FENT0219
 FENT0220
 FENT0221
 FENT0222
 FENT0223
 FENT0224
 FENT0225
 FENT0226
 FENT0227
 FENT0228
 FENT0229
 FENT0230
 FENT0231
 FENT0232
 FENT0233
 FENT0234
 FENT0235
 FENT0236
 FENT0237
 FENT0238
 FENT0239
 FENT0240
 FENT0241
 FENT0242
 FENT0243
 FENT0244
 FENT0245
 FENT0246
 FENT0247
 FENT0248
 FENT0249
 FENT0250
 FENT0251
 FENT0252

C

```

DO 200 I=1,4
DO 200 K=1,2
II=LM(I)+K
KK=2*I-2+K
DO 200 J=1,4
DO 200 L=1,2
JJ=LM(J)+L-II+1
LL=2*J-2+L
IF (JJ) 200,200,175
175 IF (ND-JJ) 180,195,195
180 WRITE (6,2004) N
    KSW=1
    GO TO 210
195 A(II,JJ)=A(II,JJ)+S(KK,LL)
200 CONTINUE
210 CONTINUE
IF(KSW.EQ.1) GO TO 500

C
C
C
    ADD CONCENTRATED FORCES

DO 250 N=1,NUMNP
K=2*N
B(K)=B(K)+U7(N)
R(K-1)=B(K-1)+UR(N)
250 CONTINUE

C
C
C
    PRESSURE BOUNDARY CONDITIONS

IF(NUMPC) 260,310,260
260 DO 300 L=1,NUMPC
    I=IRC(L)
    J=JRC(L)
    CCDF(I)=ICCODE(I)
    CCDF(J)=ICCODE(J)

```

C

C

FENT0253
FENT0254
FENT0255
FENT0256
FENT0257
FENT0258
FENT0259
FENT0260
FENT0261
FENT0262
FENT0263
FENT0264
FENT0265
FENT0266
FENT0267
FENT0268
FENT0269
FENT0270
FENT0271
FENT0272
FENT0273
FENT0274
FENT0275
FENT0276
FENT0277
FENT0278
FENT0279
FENT0280
FENT0281
FENT0282
FENT0283
FENT0284
FENT0285
FENT0286
FENT0287
FENT0288

```
PP=PR(L)/6.  
DZ=(Z(I)-Z(J))*PP  
DR=(R(J)-R(I))*PP  
RX=2.0*R(I)+R(J)  
ZX=R(I)+2.0*R(J)  
264 II=2*I  
JJ=2*J  
270 SINA=C.0  
COSA=1.0  
IF(CODE(I)) 271,272,272  
271 SINA=DSIN(CODE(I))  
COSA=DCCS(CODE(I))  
272 B(II-1)=B(II-1)+RX*(COSA*DZ+SINA*DR)  
B(II)=B(II)-RX*(SINA*DZ-COSA*DR)  
290 SINA=C.0  
COSA=1.0  
IF(CODE(J)) 291,292,292  
291 SINA=DSIN(CODE(I))  
COSA=DCOS(CODE(I))  
292 B(JJ-1)=B(JJ-1)+ZX*(COSA*DZ+SINA*DR)  
B(JJ)=B(JJ)-ZX*(SINA*DZ-COSA*DR)  
300 CONTINUE  
310 CONTINUE  
DISPLACEMENT B.C.  
C  
C  
DO 400 M=1,NUMNP  
U=UR(M)  
N=2*M-1  
KX=ICODE(M)+1  
GO TO (400,370,390,380),KX  
370 CALL MODIFY(N,U,ND2)  
GO TO 400  
380 CALL MODIFY(N,U,ND2)  
390 U=UZ(M)  
N=N+1  
CALL MODIFY(N,U,ND2)
```

```

400 CONTINUE
C
500 RETURN
C *****
2003 FORMAT (26HNEGATIVE AREA ELEMENT NO. I4)
2004 FORMAT (29HOBAND WIDTH EXCEEDS ALLOWABLE I4)
C *****
      FND
      SUBROUTINE QUAD(N,VOL)
C
      IMPLICIT REAL*8 (A-H,O-Z)
      IMPLICIT INTEGER*2(I-N)
      COMMON      STTOP,HED(18),SIGIR(25),SIGIZ(25),GAMMA(25),ZKNOT(25),
1 DEPTH(25),E(10,25),SIG(7),R(450),Z(450),UR(450),
2 UZ(450),STOTAL(450,4),KSW
      COMMON /INTEGR/ NUMNP,NUMEL,NUMMAT,NDEPTH,NORM,MTYPE,ICODE(450)
      COMMON /ARG/ RRR(5),ZZZ(5),S(10,10),P(10),LM(4),DD(3,3),
1 HH(6,10),RR(4),ZZ(4),C(4,4),H(6,10),D(6,6),F(6,10),TP(6),XI(6),
2 FE(10),IX(450,5)
      COMMON /BANARG/ B(900),A(900,54),MBAND
C *****
      I=IX(N,1)
      J=IX(N,2)
      K=IX(N,3)
      L=IX(N,4)
C
      I1=1
      I2=2
      I3=3
      I4=4
      I5=5
C *****
C DETERMINE ELASTIC CONSTANTS AND STRESS-STRAIN RELATIONSHIP
C *****
C CALL MPROP(N)

```

```

FENT0289
FENT0290
FENT0291
FENT0292
FENT0293
FENT0294
FENT0295
FENT0296
FENT0297
FENT0298
FENT0299
FENT0300
FENT0301
FENT0302
FENT0303
FENT0304
FENT0305
FENT0306
FENT0307
FENT0308
FENT0309
FENT0310
FENT0311
FENT0312
FENT0313
FENT0314
FENT0315
FENT0316
FENT0317
FENT0318
FENT0319
FENT0320
FENT0321
FENT0322
FENT0323
FENT0324

```


FENT0361
 FENT0362
 FENT0363
 FENT0364
 FENT0365
 FENT0366
 FENT0367
 FENT0368
 FENT0369
 FENT0370
 FENT0371
 FENT0372
 FENT0373
 FENT0374
 FENT0375
 FENT0376
 FENT0377
 FENT0378
 FENT0379
 FENT0380
 FENT0381
 FENT0382
 FENT0383
 FENT0384
 FENT0385
 FENT0386
 FENT0387
 FENT0388
 FENT0389
 FENT0390
 FENT0391
 FENT0392
 FENT0393
 FENT0394
 FENT0395
 FENT0396

```

C      DO 140 II=1,6
      DO 140 JJ=1,10
140  HH(II,JJ)=HH(II,JJ)/4.0
C
C      160 RETURN
      ***
C      2000 FORMAT (' ZERO AREA ELEMENT',I5)
      END
      SURROUTINE TRISTF(II,JJ,KK)
      IMPLICIT REAL*8 (A-H,C-Z)
      IMPLICIT INTEGER*2(I-N)
      COMMON STTOP,HED(18),SIGIR(25),SIGIZ(25),GAMMA(25),ZKNOT(25),
1 DEPTH(25),E(10,25),SIG(7),R(450),Z(450),UR(450),
2 UZ(450),STOTAL(450,4),KSW
      COMMON /INTEGR/ NUMNP,NUMEL,NUMMAT,NDEPTH,NORM,MTYPE,ICODE(450)
      COMMON /ARG/ RRR(5),ZZZ(5),S(10,10),P(10),LM(4),DD(3,3),
1 HH(6,10),RR(4),ZZ(4),C(4,4),H(6,10),D(6,6),F(6,10),TP(6),XI(6),
2 EE(10),IX(450,5)
      COMMON /BANARG/ R(900),A(900,54),M BRAND
      *****
C      INITIALIZATION
C
      LM(1)=II
      LM(2)=JJ
      LM(3)=KK
C
      RR(1)=RRR(II)
      RR(2)=RRR(JJ)
      RR(3)=RRR(KK)
      RR(4)=RRR(II)
      ZZ(1)=ZZZ(II)
      ZZ(2)=ZZZ(JJ)
      ZZ(3)=ZZZ(KK)
      ZZ(4)=ZZZ(II)

```

FENT0397
 FENT0398
 FENT0399
 FENT0400
 FENT0401
 FENT0402
 FENT0403
 FENT0404
 FENT0405
 FENT0406
 FENT0407
 FENT0408
 FENT0409
 FENT0410
 FENT0411
 FENT0412
 FENT0413
 FENT0414
 FENT0415
 FENT0416
 FENT0417
 FENT0418
 FENT0419
 FENT0420
 FENT0421
 FENT0422
 FENT0423
 FENT0424
 FENT0425
 FENT0426
 FENT0427
 FENT0428
 FENT0429
 FENT0430
 FENT0431
 FENT0432

```

C      85 DO 100 I=1,6
      DC 90 J=1,10
      F(I,J)=0.0
      90 H(I,J)=0.0
      DO 100 J=1,6
      100 D(I,J)=0.0
C
C      FORM INTEGRAL (G)T*(C)*(G)
      CALL INTER(XI,RR,ZZ)
C
      D(2,6)=XI(1)*(C(1,2)+C(2,3))
      D(3,5)=XI(1)*C(4,4)
      D(5,5)=D(3,5)
      D(6,6)=XI(1)*C(2,2)
      D(1,1)=XI(3)*C(3,3)
      D(1,2)=XI(2)*(C(1,3)+C(3,3))
      D(1,3)=XI(5)*C(3,3)
      D(1,6)=XI(2)*C(2,3)
      D(2,2)=XI(1)*(C(1,1)+2.0*C(1,3)+C(3,3))
      D(2,3)=XI(4)*C(1,3)+C(3,3)
      D(3,3)=XI(6)*C(3,3)+XI(1)*C(4,4)
      D(3,6)=XI(4)*C(2,3)
      DO 110 I=1,6
      DO 110 J=1,6
      110 D(J,I)=D(I,J)
C
C      FORM COEFFICIENT-DISPLACEMENT MATRIX
      COMM=RR(2)*(ZZ(3)-ZZ(1))+RR(1)*(ZZ(2)-ZZ(3))+RR(3)*(ZZ(1)-ZZ(2))
      DD(1,1)=(RR(2)*ZZ(3)-RR(3)*ZZ(2))/COMM
      DD(1,2)=(RR(3)*ZZ(1)-RR(1)*ZZ(3))/COMM
      DD(1,3)=(RR(1)*ZZ(2)-RR(2)*ZZ(1))/COMM
      DD(2,1)=(ZZ(2)-ZZ(3))/COMM
      DD(2,2)=(ZZ(3)-ZZ(1))/COMM

```

FENT0433
 FENT0434
 FENT0435
 FENT0436
 FENT0437
 FENT0438
 FENT0439
 FENT0440
 FENT0441
 FENT0442
 FENT0443
 FENT0444
 FENT0445
 FENT0446
 FENT0447
 FENT0448
 FENT0449
 FENT0450
 FENT0451
 FENT0452
 FENT0453
 FENT0454
 FENT0455
 FENT0456
 FENT0457
 FENT0458
 FENT0459
 FENT0460
 FENT0461
 FENT0462
 FENT0463
 FENT0464
 FENT0465
 FENT0466
 FENT0467
 FENT0468

```
DD(2,3)=(ZZ(1)-ZZ(2))/COMM
DD(3,1)=(RR(3)-RR(2))/COMM
DD(3,2)=(RR(1)-RR(3))/COMM
DD(3,3)=(RR(2)-RR(1))/COMM
```

C

```
DO 120 I=1,3
J=2*LM(I)-1
H(1,J)=DD(1,I)
H(2,J)=DD(2,I)
H(3,J)=DD(3,I)
H(4,J+1)=DD(1,I)
H(5,J+1)=DD(2,I)
120 H(6,J+1)=DD(3,I)
```

C

```
FORM STIFFNESS MATRIX (H)T*(D)*(H)
```

C

C

```
DO 130 J=1,10
DO 130 K=1,6
IF (H(K,J)) 128,130,128
128 DO 129 I=1,6
129 F(I,J)=F(I,J)+D(I,K)*H(K,J)
130 CONTINUE
```

C

```
DO 140 I=1,10
DO 140 K=1,6
IF (H(K,I)) 138,140,138
138 DO 139 J=1,10
139 S(I,J)=S(I,J)+H(K,I)*F(K,J)
140 CONTINUE
```

C

C

C

```
FORM STRAIN TRANSFORMATION MATRIX
```

```
DO 410 I=1,6
DO 410 J=1,10
410 HH(I,J)=HH(I,J)+H(I,J)
```

C

FENT0469
 FENT0470
 FENT0471
 FENT0472
 FENT0473
 FENT0474
 FENT0475
 FENT0476
 FENT0477
 FENT0478
 FENT0479
 FENT0480
 FENT0481
 FENT0482
 FENT0483
 FENT0484
 FENT0485
 FENT0486
 FENT0487
 FENT0488
 FENT0489
 FENT0490
 FENT0491
 FENT0492
 FENT0493
 FENT0494
 FENT0495
 FENT0496
 FENT0497
 FENT0498
 FENT0499
 FENT0500
 FENT0501
 FENT0502
 FENT0503
 FENT0504

```

C      500 RETURN
      FND
      SUBROUTINE MPRCP(N)
      IMPLICIT REAL*8 (A-H,O-Z)
      IMPLICIT INTEGER*2(I-N)
      COMMON      STTOP,HED(18),SIGIR(25),SIGIZ(25),GAMMA(25),ZKNOT(25),
1 DEPTH(25),E(10,25),SIG(7),R(450),Z(450),UR(450),
2 UZ(450),STOTAL(450,4),KSW
      COMMON /INTEGR/ NUMNP,NUMEL,NUMMAT,NDEPTH,NORM,MTYPE,ICODE(450)
      COMMON /ARG/ RRR(5),ZZZ(5),S(10,10),P(10),LM(4),DD(3,3),
1 HH(6,10),RR(4),ZZ(4),C(4,4),H(6,10),L(6,6),F(6,10),IP(6),XI(6),
2 EE(10),IX(450,5)
      COMMON /BANARG/ B(900),A(900,54),MBAND
      *****
      I=IX(N,1)
      J=IX(N,2)
      K=IX(N,3)
      L=IX(N,4)
      MTYPE=IX(N,5)

      DO 5 II=1,4
      DO 5 JJ=1,4
5 C(II,JJ)=0.0
      *****
      DETERMINE ELASTIC CONSTANTS
      *****
      DO 55 KK=1,2
      55 EF(KK)=E(KK,MTYPE)
      60 IF (NORM) 65,75,65
      65 FF(1)=EE(1)*SIGIZ(MTYPE)
      *****
      FORM STRESS STRAIN RELATIONSHIP
      *****
      75 COFF=EE(1)/(1.-EE(2)-2.*EE(2))*EE(2)
  
```

```

C(1,1)=COEF*(1.-EE(2))
C(1,2)=COEF*EE(2)
C(1,3)=EE(2)*COEF
C(2,1)=C(1,2)
C(2,2)=C(1,1)
C(2,3)=C(1,2)
C(3,1)=C(1,3)
C(3,2)=C(1,2)
C(3,3)=C(1,1)
C(4,4)=COEF*(0.5-EE(2))
RETURN
END

```

C

```

SUBROUTINE MODIFY(N,U,ND2)

```

```

IMPLICIT REAL*8 (A-H,O-Z)
IMPLICIT INTEGER*2(I-N)
COMMON /BANARG/ R(900),A(900,54),MBAND
DD 250 M=2,MBAND
K=N-M+1
IF (K) 235,235,230
230 R(K)=R(K)-A(K,M)*U
A(K,M)=0.0
235 K=N+M-1
IF (ND2-K) 250,240,240
240 R(K)=R(K)-A(N,M)*U
A(N,M)=0.0
250 CONTINUE
A(N,1)=1.0
R(N)=U
RETURN
END

```

C

```

SUBROUTINE BANSOL

```

```

IMPLICIT REAL*8 (A-H,O-Z)
IMPLICIT INTEGER*2(I-N)
COMMON STOP,HED(18),SIGIR(25),SIGIZ(25),GAMMA(25),ZKNOT(25),

```

FENT0505
FENT0506
FENT0507
FENT0508
FENT0509
FENT0510
FENT0511
FENT0512
FENT0513
FENT0514
FENT0515
FENT0516
FENT0517
FENT0518
FENT0519
FENT0520
FENT0521
FENT0522
FENT0523
FENT0524
FENT0525
FENT0526
FENT0527
FENT0528
FENT0529
FENT0530
FENT0531
FENT0532
FENT0533
FENT0534
FENT0535
FENT0536
FENT0537
FENT0538
FENT0539
FENT0540

FENT0541
 FENT0542
 FENT0543
 FENT0544
 FENT0545
 FENT0546
 FENT0547
 FENT0548
 FENT0549
 FENT0550
 FENT0551
 FENT0552
 FENT0553
 FENT0554
 FENT0555
 FENT0556
 FENT0557
 FENT0558
 FENT0559
 FENT0560
 FENT0561
 FENT0562
 FENT0563
 FENT0564
 FENT0565
 FENT0566
 FENT0567
 FENT0568
 FENT0569
 FENT0570
 FENT0571
 FENT0572
 FENT0573
 FENT0574
 FENT0575
 FENT0576

```

1 DEPTH(25),E(10,25),SIG(7),R(450),7(450),UR(450),
2 UZ(450),STOTAL(450,4),KSW
COMMON /INTEGR/ NUMNP,NUMEL,NUMMAT,NDEPTH,NURM,MTYPE,ICODE(450)
COMMON /BANARG/ B(900),A(900,54),MBAND
ND2=2*NUMNP
C
DO 280 N=1,ND2
DO 260 L=2,MBAND
C=A(N,L)/A(N,1)
I=N+L-1
C
IF (ND2.LT.I) GO TO 260
C
J=0
DO 250 K=L,MBAND
J=J+1
250 A(I,J)=A(I,J)-C*A(N,K)
R(I)=B(I)-C*B(N)
260 A(N,L)=C
280 B(N)=B(N)/A(N,1)
C
BACKSUBSTITUTION
C
N=ND2
300 N=N-1
C
IF (N.LE.0) GO TO 500
DO 400 K=2,MRAND
L=N+K-1
IF (ND2.LT.L) GO TO 400
B(N)=B(N)-A(N,K)*B(L)
400 CONTINUE
C
GO TO 300
C
500 RETURN

```


FENT0613
FENT0614
FENT0615
FENT0616
FENT0617
FENT0618
FENT0619
FENT0620
FENT0621
FENT0622
FENT0623
FENT0624
FENT0625
FENT0626
FENT0627
FENT0628
FENT0629
FENT0630
FENT0631
FENT0632
FENT0633
FENT0634
FENT0635
FENT0636
FENT0637
FENT0638
FENT0639
FENT0640
FENT0641
FENT0642
FENT0643
FENT0644
FENT0645
FENT0646
FENT0647
FENT0648

```
JJ=2*IX(N,I)
P(I I-1)=B(JJ-1)
120 P(I I)=B(JJ)
C
P(9)=0.0
P(10)=0.0
130 DO 150 I=1,2
RR(I)=P(I+8)
DO 150 K=1,8
150 RR(I)=RR(I)-S(I+8,K)*P(K)
C
COMM=S(9,9)*S(10,10)-S(9,10)*S(10,9)
IF (COMM) 155,160,155
155 P(9)=(S(10,10)*RR(1)-S(9,10)*RR(2))/COMM
P(10)=(-S(10,9)*RR(1)+S(9,9)*RR(2))/COMM
C
160 DO 170 I=1,6
TP(I)=0.0
DO 170 K=1,10
170 TP(I)=TP(I)+HH(I,K)*P(K)
C
RR(1)=TP(2)
RR(2)=TP(6)
RR(3)=(TP(1)+TP(2)*RRR(5)+TP(3)*ZZZ(5))/RRR(5)
RR(4)=TP(3)+TP(5)
C
C COMPUTE STRESSES
C
DO 180 I=1,4
SIG(I)=0.0
DO 180 K=1,4
180 SIG(I)=SIG(I)+C(I,K)*RR(K)
C
C COMPUTE PRINCIPLE STRESSES
C
CC=(SIG(1)+SIG(2))/2.0
```

FENT0649
 FENT0650
 FENT0651
 FENT0652
 FENT0653
 FENT0654
 FENT0655
 FENT0656
 FENT0657
 FENT0658
 FENT0659
 FENT0660
 FENT0661
 FENT0662
 FENT0663
 FENT0664
 FENT0665
 FENT0666
 FENT0667
 FENT0668
 FENT0669
 FENT0670
 FENT0671
 FENT0672
 FENT0673
 FENT0674
 FENT0675
 FENT0676
 FENT0677
 FENT0678
 FENT0679
 FENT0680
 FENT0681
 FENT0682
 FENT0683
 FENT0684

```

BB=(SIG(1)-SIG(2))/2.0
CR=DSQRT(BB**2+SIG(3)**2)
SIG(5)=CC+CR
SIG(6)=CC-CR
**
C CALCULATE ROTATION OF PRINCIPLE PLANES
**
500 IF(DABS(SIG(4)).LT.1.0E-09) SIG(4)=0.0
IF(DABS(BB).GT.1.0E-09) GO TO 510
BB=0.0
510 IF ((SIG(4).NE.0.).OR.(BB.NE.0.)) GO TO 520
ANG=0.0
GO TO 530
520 ANG=DATAN2(SIG(4),BB)/2.0
530 SIG(8)=57.396*ANG
SIG(7)=(SIG(5)-SIG(6))/2.0
**
C OUTPUT STRESSES
**
IF(NE.1) GO TO 615
WRITE (6,2000)
615 WRITE (6,2001) N,RRR(5),ZZZ(5),(SIG(I),I=1,4)
300 CONTINUE
2000 FORMAT (8H1ELEMENT,8X,'R',8X,'Z',6X,'SIG(R)',6X,'SIG(Z)',5X,'SIG(T
1)',4X,'TAU(RZ)')
2001 FORMAT (I8,2F9.3, 1P7D12.3, 0P1F10.2)
RETURN
END
SUBROUTINE INTER(XI,RR,ZZ)
IMPLICIT REAL*8 (A-H,C-Z)
IMPLICIT INTEGER*2(I-N)
DIMENSION RR(1),ZZ(1),XI(1)
DIMENSION XM(7),R(7),Z(7),XX(9)
XX(1)=.1259391805448
XX(2)=XX(1)

```

FENT0685
 FENT0686
 FENT0687
 FENT0688
 FENT0689
 FENT0690
 FENT0691
 FENT0692
 FENT0693
 FENT0694
 FENT0695
 FENT0696
 FENT0697
 FENT0698
 FENT0699
 FENT0700
 FENT0701
 FENT0702
 FENT0703
 FENT0704
 FENT0705
 FENT0706
 FENT0707
 FENT0708
 FENT0709
 FENT0710
 FENT0711
 FENT0712
 FENT0713
 FENT0714
 FENT0715
 FENT0716
 FENT0717
 FENT0718
 FENT0719
 FENT0720

```

XX(3)=XX(1)
XX(4)=.1323941527884
XX(5)=XX(4)
XX(6)=XX(4)
XX(7)=.225
XX(8)=.696140478028
XX(9)=.410426152314
R(7)=(RR(1)+RR(2)+RR(3))/3.
Z(7)=(ZZ(1)+ZZ(2)+ZZ(3))/3.
C
DO 100 I=1,3
J=I+3
R(I)=XX(8)*RR(I)+(1.-XX(8))*R(7)
R(J)=XX(9)*RR(I)+(1.-XX(9))*R(7)
Z(I)=XX(8)*Z(I)+(1.-XX(8))*Z(7)
100 Z(J)=XX(9)*Z(I)+(1.-XX(9))*Z(7)
C
DO 200 I=1,7
XM(I)=XX(I)*R(I)
200
C
DO 300 I=1,6
XI(I)=0.
300
C
AREA=.5*(RR(1)*(ZZ(2)-ZZ(3))+RR(2)*(ZZ(3)-ZZ(1))+RR(3)*(ZZ(1)-ZZ(2)
1))
C
DO 400 I=1,7
XI(1)=XI(1)+XM(I)
XI(2)=XI(2)+XM(I)/R(I)
XI(3)=XI(3)+XM(I)/(R(I)**2)
XI(4)=XI(4)+XM(I)*Z(I)/R(I)
XI(5)=XI(5)+XM(I)*Z(I)/(R(I)**2)
400 XI(6)=XI(6)+XM(I)*(Z(I)**2)/(R(I)**2)
C
DO 500 I=1,6
XI(I)=XI(I)*AREA
500

```

FENT0721
FENT0722
FENT0723

C
RETURN
END

APPENDIX C

FINITE ELEMENT PROGRAM FOR THE ANALYSIS OF ISOTROPIC
ELASTIC AXISYMMETRIC PLATES - THERMAL STRAINS INCLUDED (Ref. 13, 14)

Program Capabilities:

The following restrictions are placed on the size of problems which can be handled by the program.

<u>Item</u>	<u>Maximum Number</u>
Nodal Points	450
Elements	450
Materials	25
Boundary Pressure Cards	200

Printed output includes:

1. Reprint of Input Data
2. Nodal Point Displacements
3. Stresses at the center of each element.

Input Data Format:

- A. Identification card - (18A4)

Columns 1 to 72 of this card contain information to be printed with results.

- B. Control card - (5I5,F10.0)

Columns 1 - 5 Number of nodal points
 6 - 10 Number of elements
 11 - 15 Number of different materials

- 16 - 20 Normalizing stress (see NORM, Appendix B)
- 21 - 25 Number of boundary pressure cards
- 26 - 35 Reference temperature (stress free temperature)

C. Material Property information

The following group of cards must be supplied for each different material:

First Card - (2I5, 2F10.0)

- Columns 1 - 5 Materials identification - any number from 1 to 12.
- 6 - 10 Number of different temperatures for which properties are given = 8 maximum.
- 11 - 20 Initial Z stress.
- 21 - 30 Initial R stress.

Following Cards - (4F10.0) One card for each temperature

- Columns 1 - 10 Temperature
- 11 - 20 Modulus of elasticity - E
- 21 - 30 Poisson's ratio - ν
- 31 - 40 Coefficient of thermal expansion

D. Nodal Point Cards - (2I5, 5F10.0)

One card for each nodal point with the following information:

- Columns 1 - 5 Nodal point number
- 10 Number which indicates if displacements or forces are to be specified.
- 11 - 20 R - ordinate
- 21 - 30 Z - ordinate
- 31 - 40 XR
- 41 - 50 XZ
- 51 - 60 Temperature

If the number in column 10 is

		<u>Condition</u>
0	XR is the specified R-load and XZ is the specified Z - load	free
1	XR is the specified R-displacement and XZ is the specified Z-load.	
2.	XR is the specified R-load and XZ is the specified Z-displacement.	
3	XR is the specified R-displacement and XZ is the specified Z- displacement.	fixed

All loads are considered to be total forces acting on a one radian segment. Nodal point cards must be in numerical sequence. If cards are omitted, the omitted nodal points are generated at equal intervals along a straight line between the defined nodal points. The necessary temperatures are determined by linear interpolation. The boundary code (column 10), XR and XZ are set equal to zero.

Skew Boundaries:

If the number in columns 5-10 of the nodal point cards is other than 0, 1, 2 or 3, it is interpreted as the magnitude of an angle in degrees. The terms in columns 31-50 of the nodal point card are then interpreted as follows:

XR is the specified load in the s-direction

XZ is the specified displacement in the n-direction

The angle must always be input as a negative angle and may range from -.001 to -180 degrees. Hence, +1.0 degree is the same as -179.0 degrees.

The displacements of these nodal points which are printed by the program are

u_r = the displacement in the s-direction

u_z = the displacement in the n-direction

E. Element Cards - (6I5)

One card for each element

Columns	1 - 5	Element number	1. Order nodal points counter-clockwise around element.
	6 - 10	Nodal Point I	
	11 - 15	Nodal Point J	
	16 - 20	Nodal Point K	2. Maximum difference between nodal point I.D. must be less than 25.
	21 - 25	Nodal Point L	
	26 - 30	Material Identification	

Element cards must be in element number sequence. If element cards are omitted, the program automatically generates the omitted information by incrementing by one the preceding I, J, K and L. The material identification code for the generated cards is set equal to the value given on the last card. The last element card must always be supplied.

Triangular elements are also permissible; they are identified by repeating the last nodal point number (i.e., I, J, K, K).

F. Pressure Cards - (2I5, 1F10.0)

One card for each boundary element which is subjected to a normal pressure.

Columns	1 - 5	Nodal Point I
	6 - 10	Nodal Point J
	11 - 20	Normal Pressure

The boundary element must be on the left as one progresses from I to J. Surface tensile force is input as a negative pressure.

Listing:

```
C      *****
C      FINITE ELEMENT PROGRAM FOR THE ANALYSIS OF ISOTROPIC ELASTIC
C      AXYSYMMETRIC PLATES REF FEAST 1,3 SAAS 2
C      *****
C
C      IMPLICIT REAL*8 (A-H,O-Z)
C      IMPLICIT INTEGER*2(I-N)
C      COMMON      STTOP,HED(18),SIGIR(25),SIGIZ(25),GAMMA(25),ZKNOT(25),
1 DEPTH(25),F(8,4,25),SIG(7),R(450),Z(450),UR(450),TT(3),
2 U7(450),STOTAL(450,4),
3 T(450),TFMP,Q,KSW
C      COMMON /INTEGR/ NUMNP,NUMEL,NUMMAT,NDEPTH,NORM,MTYPE,ICODE(450)
C      COMMON /ARG/ RRR(5),ZZZ(5),S(10,10),P(10),LM(4),DD(3,3),
1 HH(6,10),RR(4),ZZ(4),C(4,4),H(6,10),D(6,6),F(6,10),TP(6),XI(6),
2 EE(10),IX(450,5)
C      COMMON /BANARG/ R(900),A(900,54),MBAND
C      COMMON/PRESS/ IBC(200),JBC(200),PR(200),NUMPC
C      DATA STRS /'*****'/
C      *****
C      READ AND PRINT CONTROL INFORMATION
C      *****
50 READ (5,1000,END=950) HED
   WRITE (6,2000) HED
C
   READ(5,1001) NUMNP,NUMEL,NUMMAT,NORM,NUMPC,Q
   WRITE(6,2006) NUMNP,NUMEL,NUMMAT,NUMPC,Q
   IF (NORM) 65,65,66
66 WRITE (6,2041)
C      *****
C      READ AND PRINT MATERIAL PROPERTIES
C      *****
65 CONTINUE
C
   DO 80 M=1,NUMMAT
   READ(5,1012) MTYPE,NUMTC,SIGIZ(MTYPE),SIGIR(MTYPE)
   WRITE(6,2011) MTYPE,NUMTC,SIGIZ(MTYPE),SIGIR(MTYPE)
```

```
FEWT0001
FEWT0002
FEWT0003
FEWT0004
FEWT0005
FEWT0006
FEWT0007
FEWT0008
FEWT0009
FEWT0010
FEWT0011
FEWT0012
FEWT0013
FEWT0014
FEWT0015
FEWT0016
FEWT0017
FEWT0018
FEWT0019
FEWT0020
FEWT0021
FEWT0022
FEWT0023
FEWT0024
FEWT0025
FEWT0026
FEWT0027
FEWT0028
FEWT0029
FEWT0030
FEWT0031
FEWT0032
FEWT0033
FEWT0034
FEWT0035
FEWT0036
```

```

      READ(5,1011) ((E(I,J,MTYPE),J=1,4),I=1,NUMTC)
      WRITE(6,2010) ((E(I,J,MTYPE),J=1,4),I=1,NUMTC)
D0 81 I=NUMTC,8
D0 81 J=1,4
81 E(I,J,MTYPE)=E(NUMTC,J,MTYPE)
80 CONTINUE
C *****
C READ AND PRINT NODAL POINT DATA
C *****
100 WRITE (6,2013)
    L=0
105 READ(5,1006) N,ICODE(N),R(N),Z(N),UR(N),UZ(N),T(N)
106 NL=L+1
    IF (L,FO,0) GO TO 110
    ZX=N-L
    DR=(R(N)-R(L))/ZX
    DZ=(Z(N)-Z(L))/ZX
    DT=(T(N)-T(L))/ZX
110 L=L+1
    IF (N-L) 113,112,111
111 ICODE(L)=0
    R(L)=R(L-1)+DR
    Z(L)=Z(L-1)+DZ
    T(L)=T(L-1)+DT
    UR(L)=0.0
    UZ(L)=0.0
    GO TO 110
112 WRITE(6,2014) (K,ICODE(K),R(K),Z(K),UR(K),UZ(K),T(K),K=NL,N)
113 WRITE (6,2015) N
    GO TO 900
C *****
C READ AND PRINT ELEMENT PROPERTIES
C *****
120 WRITE (6,2016)
    N=0
FEWT0037
FEWT0038
FEWT0039
FEWT0040
FEWT0041
FEWT0042
FEWT0043
FEWT0044
FEWT0045
FEWT0046
FEWT0047
FEWT0048
FEWT0049
FEWT0050
FEWT0051
FEWT0052
FEWT0053
FEWT0054
FEWT0055
FEWT0056
FEWT0057
FEWT0058
FEWT0059
FEWT0060
FEWT0061
FEWT0062
FEWT0063
FEWT0064
FEWT0065
FEWT0066
FEWT0067
FEWT0068
FEWT0069
FEWT0070
FEWT0071
FEWT0072

```

130	READ (5,1007) M,(IX(M,I),I=1,5)	FEWT0073
140	N=N+1	FEWT0074
	IF (M-N) 170,170,150	FEWT0075
150	IX(N,1)=IX(N-1,1)+1	FEWT0076
	IX(N,2)=IX(N-1,2)+1	FEWT0077
	IX(N,3)=IX(N-1,3)+1	FEWT0078
	IX(N,4)=IX(N-1,4)+1	FEWT0079
	IX(N,5)=IX(N-1,5)	FEWT0080
170	WRITE (6,2017) N,(IX(N,I),I=1,5)	FEWT0081
	IF (M-N) 180,180,140	FEWT0082
180	IF (NUMEL-N) 300,300,130	FEWT0083
C	*****	FEWT0084
C	READ AND PRINT THE PRESSURE CARDS	FEWT0085
C	*****	FEWT0086
300	IF(NUMPC) 290,210,290	FEWT0087
290	WRITE(6,9000)	FEWT0088
	DO 200 L=1,NUMPC	FEWT0089
	READ(5,9001) IBC(L),JBC(L),PR(L)	FEWT0090
200	WRITE(6,9002) IBC(L),JBC(L),PR(L)	FEWT0091
210	CONTINUE	FEWT0092
C	*****	FEWT0093
C	DETERMINE BAND WIDTH	FEWT0094
C	*****	FEWT0095
	J=0	FEWT0096
	DO 340 N=1,NUMEL	FEWT0097
	DO 340 I=1,4	FEWT0098
	DO 325 L=1,4	FEWT0099
	KK=IX(N,I)-IX(N,L)	FEWT0100
	IF (KK.LT.0) KK=-KK	FEWT0101
	IF (KK.GT.J) J=KK	FEWT0102
325	CONTINUE	FEWT0103
340	CONTINUE	FEWT0104
	MBAND=2*J+2	FEWT0105
C	*****	FEWT0106
C	SOLVE FOR DISPLACEMENTS AND STRESSES	FEWT0107
C	*****	FEWT0108

	KSW=0		FEWT0109
	CALL STIFF		FEWT0110
	IF (KSW.NE.0) GO TO 900		FEWT0111
C			FEWT0112
	CALL BANSOL		FEWT0113
	WRITE(6,2052)		FEWT0114
	WRITE (6,2025) (N,B (2*N-1),B (2*N),N=1,NUMNP)		FEWT0115
C			FEWT0116
	450 CALL STRESS(SPLOT)		FEWT0117
C	*****		FEWT0118
C	PROCCSS ALL DECKS EVEN IF ERROR		FEWT0119
C	*****		FEWT0120
	GO TO 910		FEWT0121
	900 WRITE (6,4000)		FEWT0122
	910 WRITE (6,4001) HED		FEWT0123
C			FEWT0124
	920 READ (5,1000) CHK		FEWT0125
	IF (CHK.NE.STRS) GO TO 920		FEWT0126
	GO TO 50		FEWT0127
	950 CONTINUE		FEWT0128
	WRITE (6,4002)		FEWT0129
	CALL EXIT		FEWT0130
C	*****		FEWT0131
C	*****		FEWT0132
	1000 FORMAT (18A4)		FEWT0133
	1001 FORMAT(5I5,F10.0)		FEWT0134
	1002 FORMAT (I5,2F10.0)		FEWT0135
	1003 FORMAT(2F10.0)		FEWT0136
	1004 FORMAT (2F10.0)		FEWT0137
	1005 FORMAT (3F10.0)		FEWT0138
	1006 FORMAT(2I5,5F10.0)		FEWT0139
	1007 FORMAT (6I5)		FEWT0140
	1011 FORMAT(4F10.0)		FEWT0141
	1012 FORMAT(2I5,2F10.0)		FEWT0142
C	*****		FEWT0143
	2000 FORMAT (1H1,20A4)		FEWT0144

```

2006 FORMAT (//,
  1 30HO NUMBER OF NODAL POINTS----- I3 /
  2 30HO NUMBER OF ELEMENTS----- I3 /
  3 30HO NUMBR OF DIFF. MATERIALS--- I3 /
  4 30HO NUMBR OF PRESSURE CARDS---- I3 /
  5 30HO REFERENCE TEMPERATURE----- F12.4)
2010 FORMAT (15HO TEMPERATURE 15X 5HE      15X 6HNU      15X 6HALPHA      9X
  1/4F20.8)
2011 FORMAT (17HOMATERIAL NUMBER= I3, 30H, NUMBER OF TEMPERATURE CARDS=
  1 I3,25H INITIAL VERTICAL STRESS= F10.3,5X,
  2 27H INITIAL HCRIZONTAL STRESS= F10.3)
2013 FORMAT (12H1NODAL POINT ,4X, 4HTYPE ,4X, 10HR-ORDINATE ,4X,
  1 10HZ-ORDINATE ,10X,6HR-LOAD ,10X, 6HZ-LOAD,10X,4HTEMP )
2014 FORMAT(I12,I8,2F14.3,2F16.5,F14.3)
2015 FORMAT (26HONODAL POINT CARD ERROR N= I5)
2016 FORMAT (49H1ELEMENT NO.      I      J      K      L      MATERIAL )
2017 FORMAT (1I13,4I6,1I12)
2025 FORMAT (12HONODAL POINT ,6X, 14HR-DISPLACEMENT ,6X, 14HZ-DISPLACEM
  IENT / (I12,1P2D20.7))
2041 FORMAT (76HOMODULUS AND YIELD STRESS NORMALIZED WITH RESPECT TO IN
  IITIAL VERTICAL STRESS )
2051 FORMAT(1HO,10X,'E',8X,'NU',/,3X,F11.1,F10.4/)
2052 FORMAT(1H1)
C *****
3003 FORMAT (16I5)
C *****
4000 FORMAT (//// ' ABNORMAL TERMINATION')
4001 FORMAT (//// ' END OF PROBLEM ' 20A4)
4002 FORMAT (////' END OF JOB')
C *****
9000 FORMAT(29HOPRESSURE BOUNDARY CONDITIONS/ 24H      I      J      PRESSU
  IRE )
9001 FORMAT(2I5,F10.0)
9002 FORMAT(2I6,F12.3)
      END
      SUBROUTINE STIFF

```

```

FEWT0145
FEWT0146
FEWT0147
FEWT0148
FEWT0149
FEWT0150
FEWT0151
FEWT0152
FEWT0153
FEWT0154
FEWT0155
FEWT0156
FEWT0157
FEWT0158
FEWT0159
FEWT0160
FEWT0161
FEWT0162
FEWT0163
FEWT0164
FEWT0165
FEWT0166
FEWT0167
FEWT0168
FEWT0169
FEWT0170
FEWT0171
FEWT0172
FEWT0173
FEWT0174
FEWT0175
FEWT0176
FEWT0177
FEWT0178
FEWT0179
FEWT0180

```


FEWT0217
 FEWT0218
 FEWT0219
 FEWT0220
 FEWT0221
 FEWT0222
 FEWT0223
 FEWT0224
 FEWT0225
 FEWT0226
 FEWT0227
 FEWT0228
 FEWT0229
 FEWT0230
 FEWT0231
 FEWT0232
 FEWT0233
 FEWT0234
 FEWT0235
 FEWT0236
 FEWT0237
 FEWT0238
 FEWT0239
 FEWT0240
 FEWT0241
 FEWT0242
 FEWT0243
 FEWT0244
 FEWT0245
 FEWT0246
 FEWT0247
 FEWT0248
 FEWT0249
 FEWT0250
 FEWT0251
 FEWT0252

```

144 IF (IX(N,3)-IX(N,4)) 145,165,145
145 DO 150 II=1,9
    CC=S(II,10)/S(10,10)
    P(II)=P(II)-CC*P(10)
    DO 150 JJ=1,9
150 S(II, JJ)=S(II, JJ)-CC*S(10, JJ)
C
    DO 160 II=1,8
    CC=S(II,9)/S(9,9)
    P(II)=P(II)-CC*P(9)
    DO 160 JJ=1,8
160 S(II, JJ)=S(II, JJ)-CC*S(9, JJ)
C
C      ADD ELEMENT STIFFNESS TO TOTAL STIFFNESS
C
165 DO 166 I=1,4
166 LM(I)=2*IX(N, I)-2
C
    DO 200 I=1,4
    DO 200 K=1,2
    II=LM(I)+K
    KK=2*I-2+K
    B(II)=R(II)+P(KK)
    DO 200 J=1,4
    DO 200 L=1,2
    JJ=LM(J)+L-II+1
    LL=2*J-2+L
    IF (JJ) 200,200,175
175 IF (ND-JJ) 180,195,195
180 WRITE (6,2004) N
    KSW=1
    GO TO 210
195 A(II, JJ)=A(II, JJ)+S(KK, LL)
200 CONTINUE
210 CONTINUE
    IF (KSW.EQ.1) GO TO 500

```


	COSA=DCOS(CODE(I))	FEWT0289
292	B(JJ-1)=B(JJ-1)+ZX*(COSA*DZ+SINA*DR)	FEWT0290
	B(JJ)=B(JJ)-ZX*(SINA*DZ-COSA*DR)	FEWT0291
300	CONTINUE	FEWT0292
310	CONTINUE	FEWT0293
C	DISPLACEMENT B.C.	FEWT0294
C	DO 400 M=1,NUMNP	FEWT0295
	U=UR(M)	FEWT0296
	N=2*M-1	FEWT0297
	KX=ICODE(M)+1	FEWT0298
	GO TO (400,370,390,380),KX	FEWT0299
370	CALL MODIFY(N,U,ND2)	FEWT0300
	GO TO 400	FEWT0301
380	CALL MODIFY(N,U,ND2)	FEWT0302
390	U=UZ(M)	FEWT0303
	N=N+1	FEWT0304
	CALL MODIFY(N,U,ND2)	FEWT0305
400	CONTINUE	FEWT0306
C	500 RETURN	FEWT0307
C	*****	FEWT0308
2003	FORMAT (26HNEGATIVE AREA ELEMENT NO. I4)	FEWT0309
2004	FORMAT (29HBAND WIDTH EXCEEDS ALLOWABLE I4)	FEWT0310
C	*****	FEWT0311
	END	FEWT0312
	SUBROUTINE QUAC(N,VOL)	FEWT0313
C	IMPLICIT REAL*8 (A-H,O-Z)	FEWT0314
	IMPLICIT INTEGER*2(I-N)	FEWT0315
	COMMON STTOP,HED(18),SIGIR(25),SIGIZ(25),GAMMA(25),ZKNOT(25),	FEWT0316
	1DEPTH(25),E(8,4,25),SIG(7),R(450),Z(450),UR(450),TT(3),	FEWT0317
	2 UZ(450),STOTAL(450,4).	FEWT0318
	3 T(450),TEMP,Q,KSW	FEWT0319
	COMMON /INTEGR/ NUMNP,NUMEL,NUMMAT,NDEPTH,NORM,MTYPE,ICODE(450)	FEWT0320
	COMMON /ARG/ RRR(5),ZZZ(5),S(10,10),P(10),LM(4),DD(3,3),	FEWT0321
		FEWT0322
		FEWT0323
		FEWT0324

	1 HH(6,10),RR(4),ZZ(4),C(4,4),H(6,10),D(6,6),F(6,10),TP(6),XI(6),	FEWT0325
	2 EE(10),IX(450,5)	FEWT0326
	COMMON /BANARG/ B(900),A(900,54),MBAND	FEWT0327
C	*****	FEWT0328
	I=IX(N,1)	FEWT0329
	J=IX(N,2)	FEWT0330
	K=IX(N,3)	FEWT0331
	L=IX(N,4)	FEWT0332
C		FEWT0333
	I1=1	FEWT0334
	I2=2	FEWT0335
	I3=3	FEWT0336
	I4=4	FEWT0337
	I5=5	FEWT0338
C	THERMAL STRESSES	FEWT0339
	TEMP=(T(I)+T(J)+T(K)+T(L))/4.0	FEWT0340
	DO 103 M=2,8	FEWT0341
	IF(E(M,1,MTYPE)-TEMP) 103,104,104	FEWT0342
103	CONTINUE	FEWT0343
104	RATIO=0.0	FEWT0344
	DEN=E(M,1,MTYPE)-E(M-1,1,MTYPE)	FEWT0345
	IF(DEN) 70,71,70	FEWT0346
70	RATIO=(TEMP-E(M-1,1,MTYPE))/DEN	FEWT0347
71	DO 105 KK=1,3	FEWT0348
105	FE(KK)=E(M-1,KK+1,MTYPE)+RATIO*(E(M,KK+1,MTYPE)-E(M-1,KK+1,MTYPE))	FEWT0349
	TEMP=TEMP-Q	FEWT0350
C	*****	FEWT0351
C	DETERMINE ELASTIC CONSTANTS AND STRESS-STRAIN RELATIONSHIP	FEWT0352
C	*****	FEWT0353
C		FEWT0354
	CALL MPROP(N)	FEWT0355
C		FEWT0356
88	DO 110 M=1,3	FEWT0357
110	TT(M)=(C(M,1)+C(M,2)+C(M,3))*EE(3)*TEMP	FEWT0358
C	*****	FEWT0359
C	FORM QUADRILATERAL STIFFNESS MATRIX	FEWT0360

FEWT0361

FEWT0362

FEWT0363

FEWT0364

FEWT0365

FEWT0366

FEWT0367

FEWT0368

FEWT0369

FEWT0370

FEWT0371

FEWT0372

FEWT0373

FEWT0374

FEWT0375

FEWT0376

FEWT0377

FEWT0378

FEWT0379

FEWT0380

FEWT0381

FEWT0382

FEWT0383

FEWT0384

FEWT0385

FEWT0386

FEWT0387

FEWT0388

FEWT0389

FEWT0390

FEWT0391

FEWT0392

FEWT0393

FEWT0394

FEWT0395

FEWT0396

C

210 RRR(5)=(R(I)+R(J)+R(K)+R(L))/4.0

ZZZ(5)=(Z(I)+Z(J)+Z(K)+Z(L))/4.0

DO 94 M=1,4

MM=IX(N,M)

IF(R(MM).EQ.0..AND.ICODE(MM).EQ.0) ICODE(MM)=1

93 RRR(M)=R(MM)

94 ZZZ(M)=Z(MM)

C

DO 100 II=1,10

P(II)=0.0

DO 95 JJ=1,6

95 HH(JJ,II)=0.0

DO 100 JJ=1,10

100 S(II,JJ)=0.0

IF (K-L) 125,120,125

120 CALL TRISTF(I1,I2,I3)

RRR(5)=(RRR(1)+RRR(2)+RRR(3))/3.0

ZZZ(5)=(ZZZ(1)+ZZZ(2)+ZZZ(3))/3.0

VOL=XI(1)

GO TO 160

125 VOL=0.0

CALL TRISTF(I4,I1,I5)

IF(XI(1).EQ.0.) WRITE(6,2000) N

VOL=VOL+XI(1)

CALL TRISTF(I1,I2,I5)

IF(XI(1).EQ.0) WRITE(6,2000) N

VOL=VOL+XI(1)

CALL TRISTF(I3,I4,I5)

IF(XI(1).EQ.0) WRITE(6,2000) N

VOL=VOL+XI(1)

CALL TRISTF(I2,I3,I5)

IF(XI(1).EQ.0) WRITE(6,2000) N

VOL=VOL+XI(1)

C

DO 140 II=1,6

FEW10397
FEW10398
FEW10399
FEW10400
FEW10401
FEW10402
FEW10403
FEW10404
FEW10405
FEW10406
FEW10407
FEW10408
FEW10409
FEW10410
FEW10411
FEW10412
FEW10413
FEW10414
FEW10415
FEW10416
FEW10417
FEW10418
FEW10419
FEW10420
FEW10421
FEW10422
FEW10423
FEW10424
FEW10425
FEW10426
FEW10427
FEW10428
FEW10429
FEW10430
FEW10431
FEW10432

```

DO 140 JJ=1,10
140 HH(II,JJ)=HH(II,JJ)/4.0
C
C
160 RETURN
***
2000 FORMAT (' ZERO AREA ELEMENT',I5)
END
SUBROUTINE TRISTF(II,JJ,KK)
IMPLICIT REAL*8 (A-H,O-Z)
IMPLICIT INTEGER*2(I-N)
COMMON STTOP,HED(18),SIGIR(25),SIGIZ(25),GAMMA(25),ZKNCT(25),
1DEPTH(25),E(8,4,25),SIG(7),R(450),Z(450),UR(450),TT(3),
2UZ(450),STOTAL(450,4),
3T(450),TEMP,Q,KSW
COMMON /INTEGR/ NUMNP,NUMEL,NUMMAT,NDEPTH,NORM,MIYPE,ICODE(450)
COMMON /ARG/ RRR(5),ZZZ(5),S(10,10),P(10),LM(4),DD(3,3),
1HH(6,10),RR(4),ZZ(4),C(4,4),H(6,10),D(6,6),F(6,10),TP(6),XI(6),
2EE(10),IX(450,5)
COMMON /BANARG/ B(900),A(900,54),MBAND
*****
INITIALIZATION
LM(1)=II
LM(2)=JJ
LM(3)=KK
C
C
RR(1)=RRR(II)
RR(2)=RRR(JJ)
RR(3)=RRR(KK)
RR(4)=RRR(II)
ZZ(1)=ZZZ(II)
ZZ(2)=ZZZ(JJ)
ZZ(3)=ZZZ(KK)
ZZ(4)=ZZZ(II)
C

```

FEWT0433
 FEWT0434
 FEWT0435
 FEWT0436
 FEWT0437
 FEWT0438
 FEWT0439
 FEWT0440
 FEWT0441
 FEWT0442
 FEWT0443
 FEWT0444
 FEWT0445
 FEWT0446
 FEWT0447
 FEWT0448
 FEWT0449
 FEWT0450
 FEWT0451
 FEWT0452
 FEWT0453
 FEWT0454
 FEWT0455
 FEWT0456
 FEWT0457
 FEWT0458
 FEWT0459
 FEWT0460
 FEWT0461
 FEWT0462
 FEWT0463
 FEWT0464
 FEWT0465
 FEWT0466
 FEWT0467
 FEWT0468

```

85 DO 100 I=1,6
   DO 90 J=1,10
     F(I,J)=0.0
   90 H(I,J)=0.0
   DO 100 J=1,6
     100 D(I,J)=0.0

```

```

C
C   FORM INTEGRAL (G)T*(C)*(G)
C   CALL INTER(XI,RR,ZZ)
C

```

```

D(2,6)=XI(1)*(C(1,2)+C(2,3))
D(3,5)=XI(1)*C(4,4)
D(5,5)=D(3,5)
D(6,6)=XI(1)*C(2,2)
D(1,1)=XI(3)*C(3,3)
D(1,2)=XI(2)*(C(1,3)+C(3,3))
D(1,3)=XI(5)*C(3,3)
D(1,6)=XI(2)*C(2,3)
D(2,2)=XI(1)*(C(1,1)+2.0*C(1,3)+C(3,3))
D(2,3)=XI(4)*C(1,3)+C(3,3)
D(3,3)=XI(6)*C(3,3)+XI(1)*C(4,4)
D(3,6)=XI(4)*C(2,3)

```

```

DO 110 I=1,6
   DO 110 J=1,6
     110 D(J,I)=D(I,J)

```

FORM COEFFICIENT-DISPLACEMENT MATRIX

```

COMM=RR(2)*(ZZ(3)-ZZ(1))+RR(1)*(ZZ(2)-ZZ(3))+RR(3)*(ZZ(1)-ZZ(2))
DD(1,1)=(RR(2)*ZZ(3)-RR(3)*ZZ(2))/COMM
DD(1,2)=(RR(3)*ZZ(1)-RR(1)*ZZ(3))/COMM
DD(1,3)=(RR(1)*ZZ(2)-RR(2)*ZZ(1))/COMM
DD(2,1)=(ZZ(2)-ZZ(3))/COMM
DD(2,2)=(ZZ(3)-ZZ(1))/COMM
DD(2,3)=(ZZ(1)-ZZ(2))/COMM

```

C
 C
 C
 C

FEWT0469
FEWT047C
FEWT0471
FEWT0472
FEWT0473
FEWT0474
FEWT0475
FEWT0476
FEWT0477
FEWT0478
FEWT0479
FEWT0480
FEWT0481
FEWT0482
FEWT0483
FEWT0484
FEWT0485
FEWT0486
FEWT0487
FEWT0488
FEWT0489
FEWT0490
FEWT0491
FEWT0492
FEWT0493
FEWT0494
FEWT0495
FEWT0496
FEWT0497
FEWT0498
FEWT0499
FEWT0500
FEWT0501
FEWT0502
FEWT0503
FEWT0504

DD(3,1)=(RR(3)-RR(2))/COMM
DD(3,2)=(RR(1)-RR(3))/COMM
DD(3,3)=(RR(2)-RR(1))/COMM

C

DO 120 I=1,3
J=2*LM(I)-1
H(1,J)=DD(1,I)
H(2,J)=DD(2,I)
H(3,J)=DD(3,I)
H(4,J+1)=DD(1,I)
H(5,J+1)=DD(2,I)
H(6,J+1)=DD(3,I)

120

FORM STIFFNESS MATRIX (H)T*(D)*(H)

C

C

C

DO 130 J=1,10
DO 130 K=1,6
IF (H(K,J)) 128,130,128
128 DO 129 I=1,6
129 F(I,J)=F(I,J)+D(I,K)*H(K,J)
130 CONTINUE

C

DO 140 I=1,10
DO 140 K=1,6
IF (H(K,I)) 138,140,138
138 DO 139 J=1,10
139 S(I,J)=S(I,J)+H(K,I)*F(K,J)
140 CONTINUE

TP(1)=XI(2)*TT(3)
TP(2)=XI(1)*TT(1)+TT(3)
TP(3)=XI(4)*TT(3)
TP(4)=0.0
TP(5)=0.0
TP(6)=XI(1)*TT(2)
DO 160 I=1,10
DO 160 K=1,6

```

160 P(I)=P(I)+H(K,I)*TP(K)
C
C      FORM STRAIN TRANSFORMATION MATRIX
C
      DO 410 I=1,6
      DO 410 J=1,10
410  HH(I,J)=HF(I,J)+H(I,J)
C
C      500 RETURN
      END
      SUBROUTINE MPROP(N)
      IMPLICIT REAL*8 (A-H,C-Z)
      IMPLICIT INTEGER*2(I-N)
      COMMON  STTOP,HED(18),SIGIR(25),SIGIZ(25),GAMMA(25),ZKNOT(25),
1 DEPTH(25),E(8,4,25),SIG(7),R(450),Z(450),UR(450),TT(3),
2 UZ(450),STDIAL(450,4),
3 T(450),TEMP,Q,KSW
      COMMON /INTEGR/ NUMNP,NUMEL,NUMMAT,NDEPTH,NORM,MTYPE,ICODE(450)
      COMMON /ARG/ RRR(5),ZZZ(5),S(10,10),P(10),LM(4),DD(3,3),
1 HH(6,10),RR(4),ZZ(4),C(4,4),H(6,10),D(6,6),F(6,10),TP(6),XI(6),
2 EE(10),IX(450,5)
      COMMON /BANARG/ B(900),A(900,54),MBAND
C      *****
      I=IX(N,1)
      J=IX(N,2)
      K=IX(N,3)
      L=IX(N,4)
      MTYPE=IX(N,5)
C
      DO 5 II=1,4
      DO 5 JJ=1,4
5  C(II,JJ)=0.0
      *****
C      DETERMINE ELASTIC CONSTANTS
      *****
C
C
C

```

```

FEWT0505
FEWT0506
FEWT0507
FEWT0508
FEWT0509
FEWT0510
FEWT0511
FEWT0512
FEWT0513
FEWT0514
FEWT0515
FEWT0516
FEWT0517
FEWT0518
FEWT0519
FEWT0520
FEWT0521
FEWT0522
FEWT0523
FEWT0524
FEWT0525
FEWT0526
FEWT0527
FEWT0528
FEWT0529
FEWT0530
FEWT0531
FEWT0532
FEWT0533
FEWT0534
FEWT0535
FEWT0536
FEWT0537
FEWT0538
FEWT0539
FEWT0540

```

FEWT0541
FEWT0542
FEWT0543
FEWT0544
FEWT0545
FEWT0546
FEWT0547
FEWT0548
FEWT0549
FEWT0550
FEWT0551
FEWT0552
FEWT0553
FEWT0554
FEWT0555
FEWT0556
FEWT0557
FEWT0558
FEWT0559
FEWT0560
FEWT0561
FEWT0562
FEWT0563
FEWT0564
FEWT0565
FEWT0566
FEWT0567
FEWT0568
FEWT0569
FEWT0570
FEWT0571
FEWT0572
FEWT0573
FEWT0574
FEWT0575
FEWT0576

```

C      60 IF (NORM) 65,75,65
C      65 FE(1)=EE(1)*SIGIZ(MTYPE)
C      ***
C      FORM STRESS STRAIN RELATIONSHIP
C      ***
C      75 COEF=EE(1)/(1.-EE(2))-2.*EE(2)*EE(2)
C      C(1,1)=COEF*(1.-EE(2))
C      C(1,2)=COEF*EE(2)
C      C(1,3)=EE(2)*COEF
C      C(2,1)=C(1,2)
C      C(2,2)=C(1,1)
C      C(2,3)=C(1,2)
C      C(3,1)=C(1,3)
C      C(3,2)=C(1,2)
C      C(3,3)=C(1,1)
C      C(4,4)=COEF*(0.5-EE(2))
C      RETURN
C      END
C      SUBROUTINE MODIFY(N,U,ND2)
C      IMPLICIT REAL*8 (A-H,O-Z)
C      IMPLICIT INTEGER*2(I-N)
C      COMMON /BANARG/ R(900),A(900,54),MBAND
C      DO 250 M=2,MBAND
C      K=N-M+1
C      IF (K) 235,235,230
C      230 R(K)=R(K)-A(K,M)*U
C      A(K,M)=0.0
C      235 K=N+M-1
C      IF (NC2-K) 250,240,240
C      240 B(K)=R(K)-A(N,M)*U
C      A(N,M)=0.0
C      250 CONTINUE
C      A(N,1)=1.0
C      R(N)=U

```

FEWT0577
FEWT0578
FEWT0579
FEWT0580
FEWT0581
FEWT0582
FEWT0583
FEWT0584
FEWT0585
FEWT0586
FEWT0587
FEWT0588
FEWT0589
FEWT0590
FEWT0591
FEWT0592
FEWT0593
FEWT0594
FEWT0595
FEWT0596
FEWT0597
FEWT0598
FEWT0599
FEWT0600
FEWT0601
FEWT0602
FEWT0603
FEWT0604
FEWT0605
FEWT0606
FEWT0607
FEWT0608
FEWT0609
FEWT0610
FEWT0611
FEWT0612

```

RETURN
END
SURROUTINE BANSOL
C
  IMPLICIT REAL*8 (A-H,O-Z)
  IMPLICIT INTEGER*2 (I-N)
  COMMON STTOP, HED(18), SIGIR(25), SIGIZ(25), GAMMA(25), ZKNCT(25),
1 DEPTH(25), E(8,4,25), SIG(7), R(450), Z(450), UR(450), TT(3),
2 UZ(450), STOTAL(450,4),
3 T(450), TEMP,Q,KSW
  COMMON /INTEGR/ NUMNP, NUMEL, NUMMAT, NDEPTH, NORM, MTYPE, ICODE(450)
  COMMON /BANARG/ B(900), A(900,54), MBAND
  ND2=2*NUMNP
C
  DO 280 N=1,ND2
  DO 260 L=2,MBAND
  C=A(N,L)/A(N,1)
  I=N+L-1
C
  IF (ND2.LT.1) GO TO 260
C
  J=0
  DO 250 K=L,MBAND
  J=J+1
  250 A(I,J)=A(I,J)-C*A(N,K)
  B(I)=B(I)-C*B(N)
  260 A(N,L)=C
  280 B(N)=B(N)/A(N,1)
C
  BACKSUBSTITUTION
C
  N=ND2
  300 N=N-1
C
  IF (N.LE.0) GO TO 500
  DO 400 K=2,MBAND

```

```

FEWT0613
FEWT0614
FEWT0615
FEWT0616
FEWT0617
FEWT0618
FEWT0619
FEWT0620
FEWT0621
FEWT0622
FEWT0623
FEWT0624
FEWT0625
FEWT0626
FEWT0627
FEWT0628
FEWT0629
FEWT0630
FEWT0631
FEWT0632
FEWT0633
FEWT0634
FEWT0635
FEWT0636
FEWT0637
FEWT0638
FEWT0639
FEWT0640
FEWT0641
FEWT0642
FEWT0643
FEWT0644
FEWT0645
FEWT0646
FEWT0647
FEWT0648

```

```

L=N+K-1
IF (ND2.LT.L) GO TO 400
B(N)=B(N)-A(N,K)*B(L)
400 CONTINUE
C
GO TO 300
C
500 RETURN
END
SUBROUTINE STRESS(SPLOTT)
IMPLICIT REAL*8 (A-H,O-Z)
IMPLICIT INTEGER*2(I-N)
COMMON STTOP, HED(18), SIGIR(25), SIGIZ(25), GAMMA(25), ZKNOD(25),
1DEPTH(25), E(8,4,25), SIG(7), R(450), Z(450), UR(450), TT(3),
2 UZ(450), STOTAL(450,4),
3 T(450), TEMP, Q, KSW
COMMON /INTEGR/ NUMNP, NUMEL, NUMMAT, NDEPTH, NORM, MTYPE, ICODE(450)
COMMON /ARG/ RRR(5), ZZZ(5), S(10,10), P(10), LM(4), DD(3,3),
1 HH(6,10), RR(4), ZZ(4), C(4,4), H(6,10), D(6,6), F(6,10), TP(6), XI(6),
2 EE(10), IX(450,5)
COMMON /BANARG/ R(900), A(900,54), MBAND
*****
C COMPUTE ELEMENT STRESSES AND STRAINS
*****
DO 300 N=1,NUMEL
CALL QUAD(N,VOL)
C
C FIND ELEMENT COORDINATES
C
I1=IX(N,1)
J1=IX(N,2)
K1=IX(N,3)
L1=IX(N,4)
C
IF (K1-L1.EQ.0) GO TO 50
RPR(5)=(R(I1)+R(J1)+R(K1)+R(L1))/4.0

```

```
FEWT0649
FEWT0650
FEWT0651
FEWT0652
FEWT0653
FEWT0654
FEWT0655
FEWT0656
FEWT0657
FEWT0658
FEWT0659
FEWT0660
FEWT0661
FEWT0662
FEWT0663
FEWT0664
FEWT0665
FEWT0666
FEWT0667
FEWT0668
FEWT0669
FEWT0670
FEWT0671
FEWT0672
FEWT0673
FEWT0674
FEWT0675
FEWT0676
FEWT0677
FEWT0678
FEWT0679
FEWT0680
FEWT0681
FEWT0682
FEWT0683
FEWT0684

ZZZ(5)=(Z(I1)+Z(J1)+Z(K1)+Z(L1))/4.0
GO TO 100
50 RRR(5)=(R(I1)+R(J1)+R(K1))/3.0
ZZZ(5)=(Z(I1)+Z(J1)+Z(K1))/3.0
C
C COMPUTE STRAINS
C
100 DO 120 I=1,4
II=2*I
JJ=2*IX(N,I)
P(II-1)=B(JJ-1)
120 P(II)=R(JJ)
C
C P(9)=0.0
P(10)=0.0
130 DO 150 I=1,2
RR(I)=P(I+8)
DO 150 K=1,8
150 RR(I)=RR(I)-S(I+8,K)*P(K)
C
C COMM=S(9,9)*S(10,10)-S(9,10)*S(10,9)
IF (COMM) 155,160,155
155 P(9)=(S(10,10)*RR(1)-S(9,10)*RR(2))/COMM
P(10)=(-S(10,9)*RR(1)+S(9,9)*RR(2))/COMM
C
160 DO 170 I=1,6
TP(I)=0.0
DO 170 K=1,10
170 TP(I)=TP(I)+HH(I,K)*P(K)
C
C RR(1)=TP(2)
RR(2)=TP(6)
RR(3)=(TP(1)+TP(2)*RRR(5)+TP(3)*ZZZ(5))/RRR(5)
RR(4)=TP(3)+TP(5)
C
C COMPUTE STRESSES
```

```

C
DO 180 I=1,4
SIG(I)=0.0
DN 180 K=1,4
180 SIG(I)=SIG(I)+C(I,K)*RR(K)

C
COMPUTE PRINCIPLE STRESSES

C
CC=(SIG(1)+SIG(2))/2.0
R8=(SIG(1)-SIG(2))/2.0
CR=DSQRT(BR**2+SIG(3)**2)
SIG(5)=CC+CR
SIG(6)=CC-CR
*****

C
CALCULATE ROTATION OF PRINCIPLE PLANES
*****

C
500 IF(DABS(SIG(4)).LT.1.0E-09) SIG(4)=0.0
IF(DABS(BB).GT.1.0E-09) GO TO 510
BR=0.0

510 IF ((SIG(4).NE.0.)OR.(BB.NE.0.)) GO TO 520
ANG=0.0
GO TO 530

520 ANG=DATAN2(SIG(4),BB)/2.0
530 SIG(8)=57.396*ANG
SIG(7)=(SIG(5)-SIG(6))/2.0
*****

C
OUTPUT STRESSFS
*****

C
IF(N.NE.1) GO TO 615
WRITE (6,2000)
615 WRITE (6,2001) N,RRR(5),ZZZ(5),(SIG(I),I=1,4)
300 CONTINUE
2000 FORMAT (8H1ELEMENT,8X,'R',8X,'Z',6X,'SIG(R)',6X,'SIG(Z)',5X,'SIG(T
1)',4X,'TAU(RZ)')
2001 FORMAT (I8,2F9.3, 1P7D12.3, CP1F10.2)
RETURN

```

```

FEWT0685
FEWT0686
FEWT0687
FEWT0688
FEWT0689
FEWT0690
FEWT0691
FEWT0692
FEWT0693
FEWT0694
FEWT0695
FEWT0696
FEWT0697
FEWT0698
FEWT0699
FEWT0700
FEWT0701
FEWT0702
FEWT0703
FEWT0704
FEWT0705
FEWT0706
FEWT0707
FEWT0708
FEWT0709
FEWT0710
FEWT0711
FEWT0712
FEWT0713
FEWT0714
FEWT0715
FEWT0716
FEWT0717
FEWT0718
FEWT0719
FEWT0720

```

FEWT0721
 FEWT0722
 FEWT0723
 FEWT0724
 FEWT0725
 FEWT0726
 FEWT0727
 FEWT0728
 FEWT0729
 FEWT0730
 FEWT0731
 FEWT0732
 FEWT0733
 FEWT0734
 FEWT0735
 FEWT0736
 FEWT0737
 FEWT0738
 FEWT0739
 FEWT0740
 FEWT0741
 FEWT0742
 FEWT0743
 FEWT0744
 FEWT0745
 FEWT0746
 FEWT0747
 FEWT0748
 FEWT0749
 FEWT0750
 FEWT0751
 FEWT0752
 FEWT0753
 FEWT0754
 FEWT0755
 FEWT0756

```

END
SUBROUTINE INTER(XI,RR,ZZ)
IMPLICIT REAL*8 (A-H,C-Z)
IMPLICIT INTEGER*2(I-N)
DIMENSION RR(1),ZZ(1),XI(1)
DIMENSION XM(7),R(7),Z(7),XX(9)

C
XX(1)=.1259391805448
XX(2)=XX(1)
XX(3)=XX(1)
XX(4)=.1323941527884
XX(5)=XX(4)
XX(6)=XX(4)
XX(7)=.225
XX(8)=.696140478028
XX(9)=.410426192314
R(7)=(RR(1)+RR(2)+RR(3))/3.
Z(7)=(ZZ(1)+ZZ(2)+ZZ(3))/3.

C
DO 100 I=1,3
J=I+3
R(I)=XX(8)*RR(I)+(1.-XX(8))*R(7)
R(J)=XX(9)*RR(I)+(1.-XX(9))*R(7)
Z(I)=XX(8)*ZZ(I)+(1.-XX(8))*Z(7)
100 Z(J)=XX(9)*Z(I)+(1.-XX(9))*Z(7)

C
DO 200 I=1,7
200 XM(I)=XX(I)*R(I)

C
DO 300 I=1,6
300 XI(I)=0.

C
AREA=.5*(RR(1)*(ZZ(2)-ZZ(3))+RR(2)*(ZZ(3)-ZZ(1))+RR(3)*(ZZ(1)-ZZ(2)
1))

C
DO 400 I=1,7

```

```

      XI(1)=XI(1)+XM(I)
      XI(2)=XI(2)+XM(I)/R(I)
      XI(3)=XI(3)+XM(I)/(R(I)**2)
      XI(4)=XI(4)+XM(I)*Z(I)/R(I)
      XI(5)=XI(5)+XM(I)*Z(I)/(R(I)**2)
      XI(6)=XI(6)+XM(I)*(Z(I)**2)/(R(I)**2)
400
C
      DO 500 I=1,6
      500 XI(I)=XI(I)*AREA
C
      RETURN
      END

```

```

FEMT0757
FEMT0758
FEMT0759
FEMT0760
FEMT0761
FEMT0762
FEMT0763
FEMT0764
FEMT0765
FEMT0766
FEMT0767
FEMT0768

```

APPENDIX D

STEADY STATE HEAT TRANSFER PROGRAM FOR BOLTED JOINT

Program Capacity: 50 nodal points

Output Data:

- (a) Input data
- (b) Inverse of matrix
- (c) Nodal temperature
- (d) Given and calculated augmenting vector and residual error

Input Data Sequence:

- A. Case identification (12A4) followed by two blank cards
- B. Card (11) with a 1
- C. Card (17) with dimension of matrix
- D. Card (11) with a 1
- E. Cards (11, 3(2I3, E15.8)) with node indices started in the first I3 field followed by conductance between these nodes. Only input from lower node number to higher node number required (since the conductance from node i to j equals the conductance from j to i.) Each card has three groups of z node numbers followed by a conductance value except the last card. Last card could have 1, 2 or 3 groups and has a 1 in column 1.
- F. Cards (11, 3(I6, E15.8)) with number of node followed by conductance from the node to ground node which is at specified temperature. Each card has 3 groups of node number followed by conductance. The 11 field is skipped except for the last card for ground conductances which can have 1, 2 or 3 fields and the first column has a 1. A

node can be connected to only one ground node.

- G. Same as F above, but code temperature specified for ground node instead of the conductance value.
- H. Same as F above, but code internal power dissipation for the particular node instead of the conductance value.

Listing:

```

C      STFADY STATE HEAT TRANSFER PROGRAM      BOLTED JOINT
      DIMENSION IDENT(12),A(050,050),AA(050,050),B( 50),BI( 50 ),
      IBC( 50),RES( 50),ACON( 50),TACCN( 50),Q( 50)
101 WRITE(6,23)
      41 READ(5,51) K,IDENT
      51 FORMAT(11,12A4)
      WRITE(6,111) IDENT
111 FORMAT(12A6)
      IF(K .NE. 1) GO TO 41
      READ(5,55) N,K
      55 FORMAT(I7/I1)
      M = N+1
      DO 3 I = 1,N
      DO 3 J = 1,N
      AA(I,J) = 0.0
      ACON(I)=0.
      Q(I) = 0.
      TACCN(I) = 0.
      3 CONTINUE
C      READ IN COEFF. MATRIX ELEMENTS
      42 READ(5,52) K,(I,J,AA(I,J),JM=1,3)
      52 FORMAT(11,3(2I3,E15.8))
      IF(K .NE. 1) GO TO 42
      43 READ(5,53) K,(I,ACON(I),JM=1,3)
      IF(K .NE. 1) GO TO 43
      44 READ(5,53) K,(I,TACON(I),JM=1,3)
      IF(K .NE. 1) GO TO 44
      45 READ(5,53) K,(I,Q(I),JM=1,3)
      IF(K .NE. 1) GO TO 45
      53 FORMAT(11,3(I6,E15.8))
      DO 500 I=1,N
      500 B(I) = -(Q(I) + ACON(I) * TACCN(I))
      DO 1000 I=1,N
      DO 1000 J=1,N
      1000 AA(J,I) = AA(I,J)
      DO 3000 I=1,N

```

```

SSHT0001
SSHT0002
SSHT0003
SSHT0004
SSHT0005
SSHT0006
SSHT0007
SSHT0008
SSHT0009
SSHT0010
SSHT0011
SSHT0012
SSHT0013
SSHT0014
SSHT0015
SSHT0016
SSHT0017
SSHT0018
SSHT0019
SSHT0020
SSHT0021
SSHT0022
SSHT0023
SSHT0024
SSHT0025
SSHT0026
SSHT0027
SSHT0028
SSHT0029
SSHT0030
SSHT0031
SSHT0032
SSHT0033
SSHT0034
SSHT0035
SSHT0036

```

```

SSHT0037
SSHT0038
SSHT0039
SSHT0040
SSHT0041
SSHT0042
SSHT0043
SSHT0044
SSHT0045
SSHT0046
SSHT0047
SSHT0048
SSHT0049
SSHT0050
SSHT0051
SSHT0052
SSHT0053
SSHT0054
SSHT0055
SSHT0056
SSHT0057
SSHT0058
SSHT0059
SSHT0060
SSHT0061
SSHT0062
SSHT0063
SSHT0064
SSHT0065
SSHT0066
SSHT0067
SSHT0068
SSHT0069
SSHT0070
SSHT0071
SSHT0072

IN=I
AA(I,I) = 0.
DO 2001 J=1,N
JN=J
IF (JN.EQ. IN) GO TO 2001
2000 AA(I,I) = AA(I,I) + AA(I,J)
2001 CONTINUE
3000 AA(I,I) =(AA(I,I)+ACGN(I)) * (-1.)
WRITE(6,26)
26 FORMAT(1H1,27X,1H1,12X,1HQ,15X,1CHGRD. CCND.,10X,1CHGRD. TEMP.//)
WRITE(6,25)(I,Q(I),ACGN(I),TACGN(I),I=1,N)
25 FORMAT(1H ,26X,I3,7X,F10.5,10X,F10.5,10X,F10.5,10X)
MM = 1
DO 4 I=1,N
DO 4 J = 1,N
A(I,J) = AA(I,J)
4 CONTINUE
WRITE(6,5)
5 FCRMAT( 1H1,39X17HA = COEFF. MATRIX //
1 40X21HB = AUGMENTING VECTOR //
2 40X19HT = SOLUTION VECTOR //
3 40X16HAI= INVERSE OF A //
4 40X33HRC = AUGMENTING VECTOR CALCULATED //
5 40X21H( A ) * ( T ) = ( R ) /// )
DO 7 I = 1,N
7 WRITE(5,6)( I,J,A(I,J), J = 1,N )
6 FORMAT(1H / (4( 5H A(I3,1H,I3,2H)=F10.5,5X)))
DO 8 I = 1,N
BI(I) = B(I)
8 CONTINUE
CALL MAT(N,M,A,B )
WRITE(6,22)
22 FORMAT(1H1 )
WRITE INVERSE MATRIX
DO 9 I = 1,N
9 WRITE(6,10)( I,J,A(I,J), J = 1,N )

```

SSHTC0073
 SSHT0074
 SSHT0075
 SSHT0076
 SSHT0077
 SSHT0078
 SSHT0079
 SSHT0080
 SSHT0081
 SSHT0082
 SSHT0083
 SSHT0084
 SSHT0085
 SSHT0086
 SSHT0087
 SSHT0088
 SSHT0089
 SSHT0090
 SSHT0091
 SSHT0092
 SSHT0093
 SSHT0094
 SSHT0095
 SSHT0096
 SSHT0097
 SSHT0098
 SSHT0099
 SSHT0100
 SSHT0101
 SSHT0102
 SSHT0103
 SSHT0104
 SSHT0105
 SSHT0106
 SSHT0107
 SSHT0108

```

10 FCFORMAT(1H / (4( 5H AI(I3,1H,I3,2H)=E15.8)))
   WRITE(6,23)
23 FCFORMAT(1H1)
   WRITE SOLUTION VECTOR
12 WRITE(6,11)( J, B(J) , J = 1,N )
11 FCFORMAT(1H / 4(5H T(I3,2H)=F10.5,9X))
   DO 13 I = 1,N
     BC(I) =0.0
     DO 13 J = 1,N
       BC(I) = BC(I) + (AA(I,J) * B(J))
13 CCNTINUE
   DO 15 J = 1,N
     RES(J) = ABS(BI(J)) - ABS( BC(J))
15 CCNTINUE
   WRITE(6,16)
16 FFORMAT(1H1,30X76H AUGMENTING VECTOR      CALCU.AUGMENTING VECTOR
1  RESIDUAL ERROR // )
17 WRITE (6,18) (J,I,BI(J),J,I,BC(J),RES(J),J=1,N)
18 FFORMAT(25X4H B(I3,1H, I3,2H)=E15.8,2X4H BC(I3,1H,I3,2H)=E15.8,
1  6XE15.8 /)
   GO TO 101
END
SUBROUTINE MAT (N,M,A,B)
  M = N + 1
  N = SIZE OF MATRIX TO BE INVERTED
  TO SOLVE AX = B, WHERE INPUT A = A, INPUT B = B
  OUTPUT B= X, OUTPUTA = A INVERSE
  DIMENSION A(50,50),B(50)
  N1 = N - 1
  TEMP 15 = A(1,1)
  A(M,N) = 1.0 / TEMP 15
  B(M) = A(1,2) / TEMP 15
  DO 1 I=2,N1
    A(M,I-1)= A(1,I+1) / TEMP 15
  1 CCNTINUE
  A(M,N1) = B(1) / TEMP 15

```

```
SSHT0109
SSHT0110
SSHT0111
SSHT0112
SSHT0113
SSHT0114
SSHT0115
SSHT0116
SSHT0117
SSHT0118
SSHT0119
SSHT0120
SSHT0121
SSHT0122
SSHT0123
SSHT0124
SSHT0125
SSHT0126
SSHT0127
SSHT0128
SSHT0129
SSHT0130
SSHT0131
SSHT0132
SSHT0133
SSHT0134
SSHT0135
SSHT0136
SSHT0137
SSHT0138
SSHT0139
SSHT0140
SSHT0141
SSHT0142
SSHT0143
SSHT0144

DO 10 I=1,N1
TEMP 6 = A(I+1,1)
B(I) = A(I+1,2) - TEMP 6 * B(M)
DO 5 J=2,N1
A(I,J-1) = A(I+1,J+1) - TEMP 6 * A(M,J-1)
5 CCNTINUE
A(I,N1) = B(I+1) - TEMP 6 * A(M,N1)
A(I,N) = -TEMP6 / TEMP 15
10 CONTINUE
B(N) = B(M)
DO 15 I=1,N
A(N,I) = A(M,I)
15 CONTINUE
REPEATS N - 1 TIMES
DO 100 K=1,N1
TEMP 15 = B(1)
A(M,N) = 1.0 / TEMP 15
B(M) = A(1,1) / TEMP 15
DO 51 I=2,N
A(M,I-1) = A(1,I) / TEMP 15
51 CONTINUE
DO 60 I =1,N1
TEMP 6 = B(I+1)
B(I) = A(I+1,1) - TEMP 6 * B(M)
DO 55 J=2,N
A(I,J-1) = A(I+1,J) - TEMP 6* A(M,J-1)
55 CCNTINUE
A(I,N) = -TEMP 6 / TEMP 15
60 CONTINUE
B(N) = B(M)
DC 65 I=1,N
A(N,I) = A(M,I)
65 CONTINUE
100 CONTINUE
RETURN
END
```

TABLE 1

Separation Radius Comparison - Single and Two Plate Models

(see Figs. 12 - 17)

$\frac{A}{B}$	$\frac{B}{A}$	R_o/A		Percent Discrepancy Between Models
		Single Plate Model	Two Plate Model	
1	3.1	4.2	3.7	13.5
	2.2	3.3	2.7	22.2
	1.6	2.7	2.1	28.6
	1.3	2.4	1.7	41.7
.75	3.1	4.5	3.8	18.5
	2.2	3.6	2.8	28.9
	1.6	3.0	2.2	36.4
	1.3	2.7	2.0	35.0
.5	3.1	5.1	4.1	24.4
	2.2	4.2	3.2	31.3
	1.6	3.6	2.8	28.6
	1.3	3.3	2.5	32.0

TABLE 2

Test and Analytical Results for Radii of Separation of Bolted Plates (see Fig. 5)

Case	D in.	2B in.	Separation Diameters, $2 R_o$ - in.					% Discrepancy Between Computed Values and Tested Values	
			"Rubbing Test"		Autoradiographic Test		Computed	Rub. Test	Autorad. Test
			Range	Average	Range	Average			
1	.065	.422	.42-.48	.45	.41-.46	.44	.488	7.8	9.8
2	.124	.422	.50-.53	.51	.4 - .6	.55	.554	7.9	.7
3	.191	.422	.58-.64	.62	.76-.81	.78*	.620	0	25.8
4	.253	.422	.70-.76	.72	.68-.73	.7**	.700	2.9	0
5.	Unmatch- ed Pair .124/ .257	.422	.54-.58	.56	—	—	.588	4.8	—
6.	.124	1.0	1.06-1.10	1.09	—	—	1.104	1.3	—
7.	.191	1.0	1.11-1.17	1.16	—	—	1.210	4.1	—

* Original x-ray film shows hole in plate and 0.6 inch diameter zone more distinctly than remainder of area sensitized by the radioactive contamination. Loose radiographic contamination observed during test.

** Assembled and disassembled radioactive and non-radioactive plates without rotating plates relative to each other.

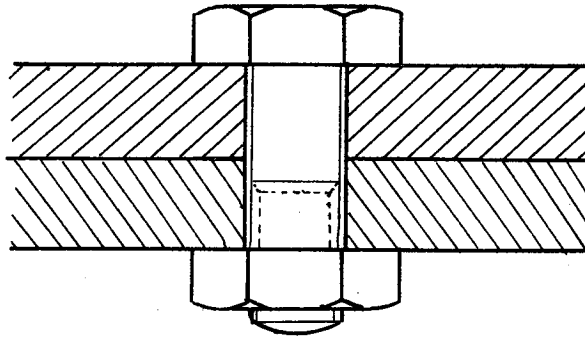


FIG. 1. BOLTED JOINT

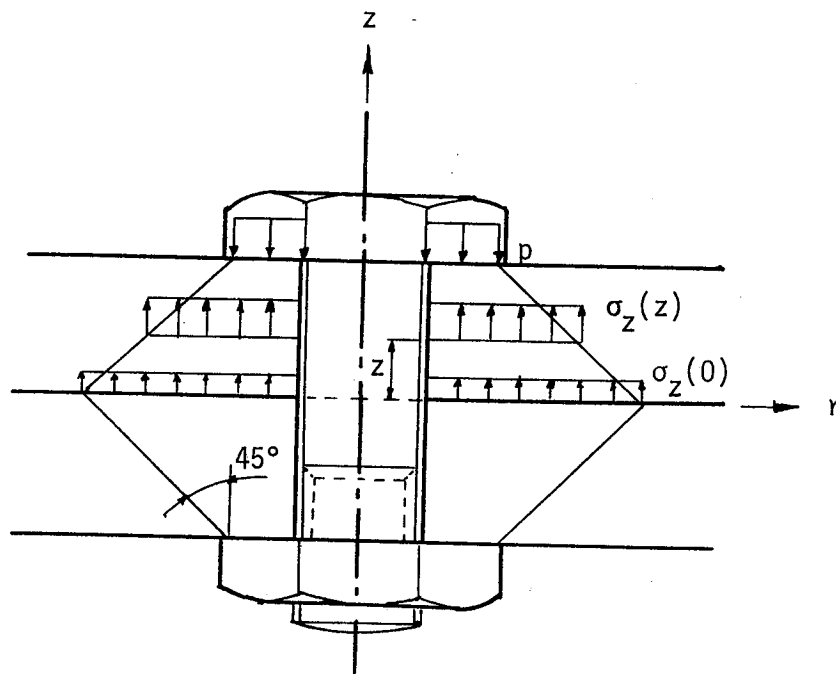


FIG. 2. ROETSCHER'S RULE OF THUMB FOR PRESSURE DISTRIBUTION IN A BOLTED JOINT

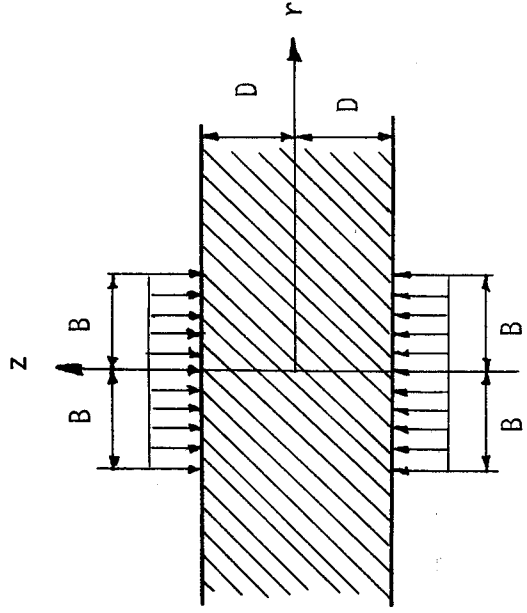


FIG. 3(a)

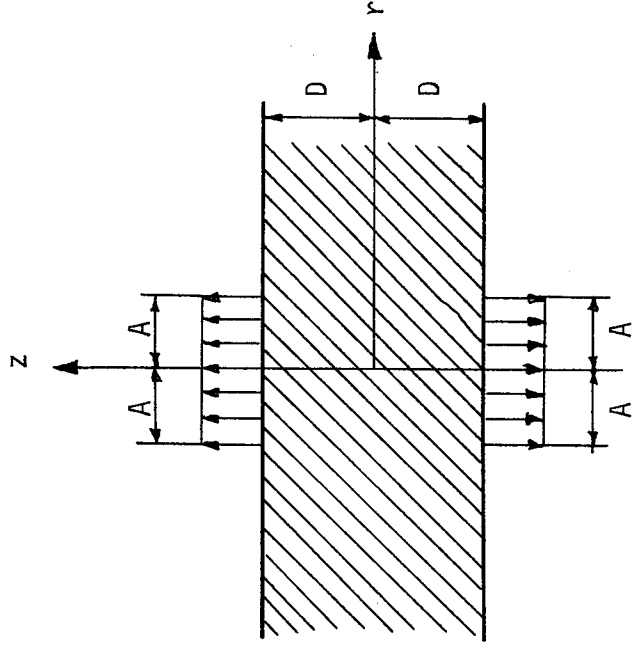


FIG. 3(b)

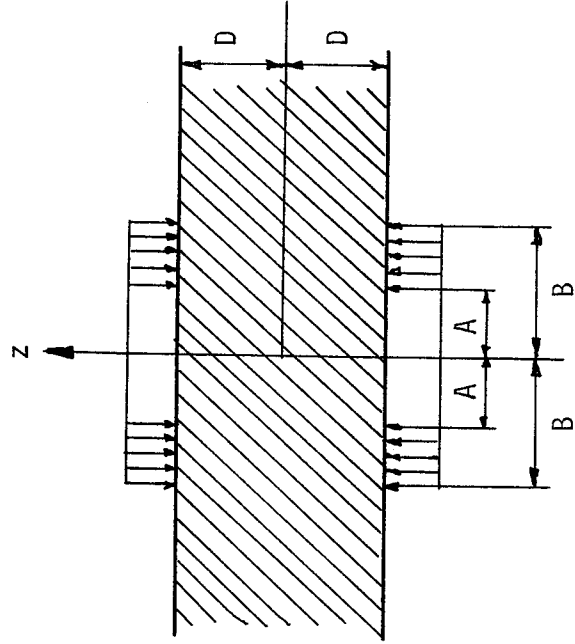


FIG. 3(c)

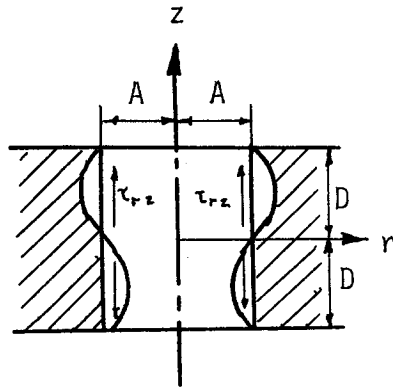


FIG. 3(d)

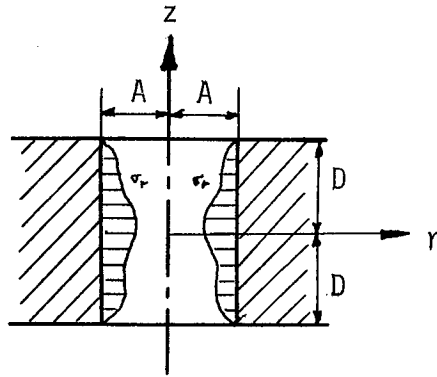


FIG. 3(e)

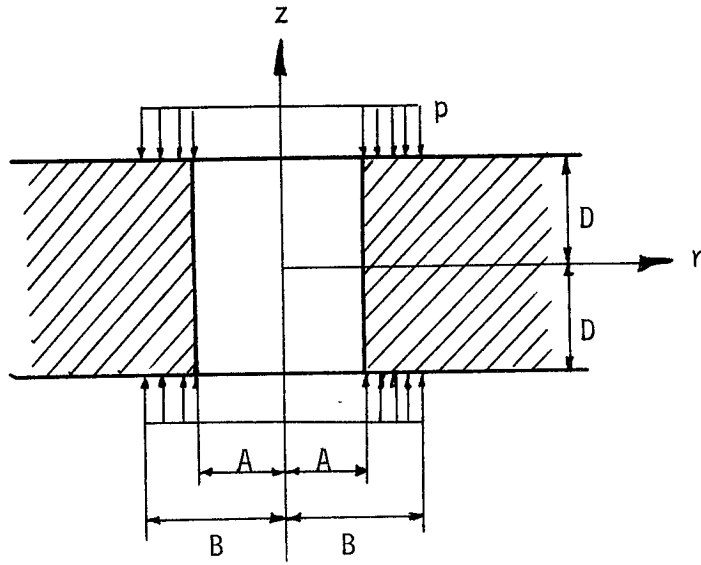
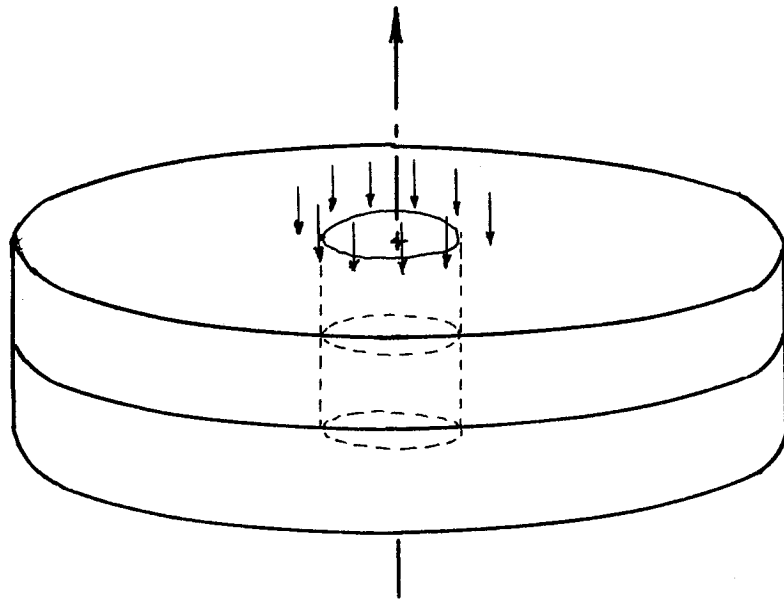
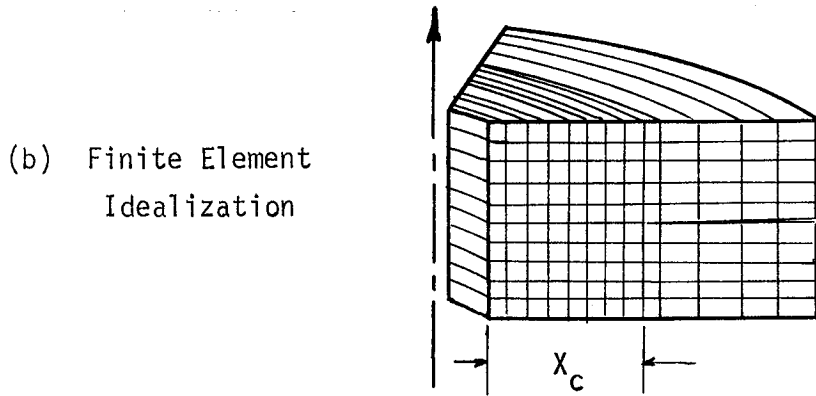


FIG. 3(f)

FIG. 3. FERNLUND'S SEQUENCE OF SUPERPOSITION



(a) Actual Plates

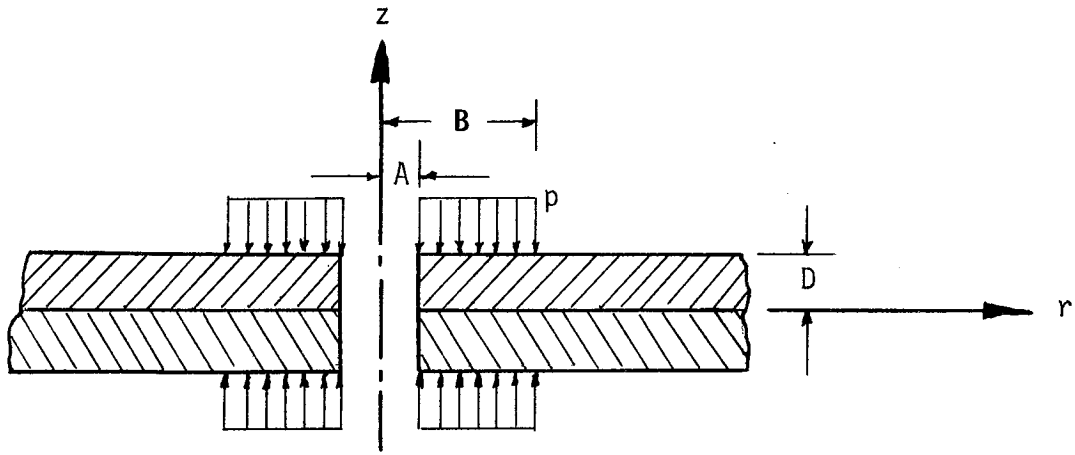


(b) Finite Element Idealization

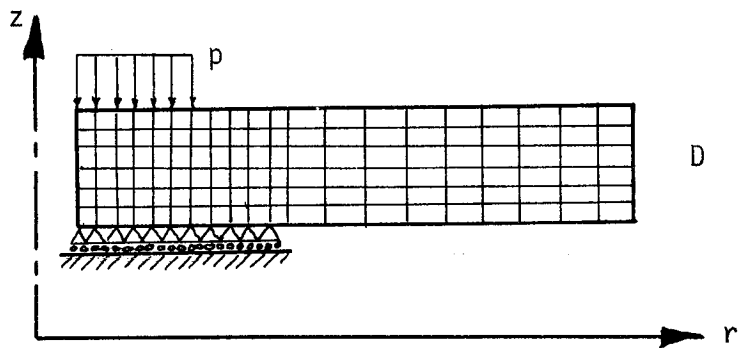


(c) Single Annular Ring Element

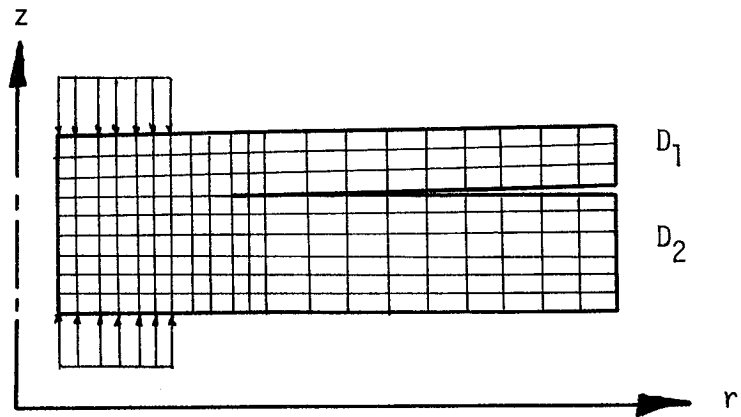
FIG. 4. FINITE ELEMENT IDEALIZATION OF TWO PLATES IN CONTACT



(a) Plates of Equal Thickness Under Load

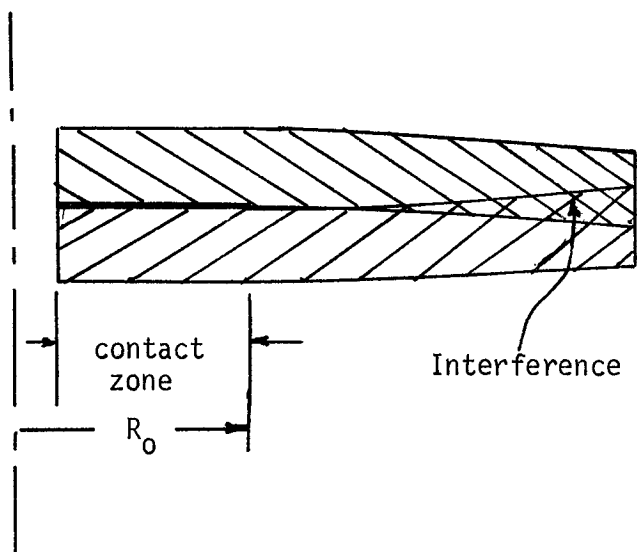


(b) Finite Element Model for Plates of Equal Thickness

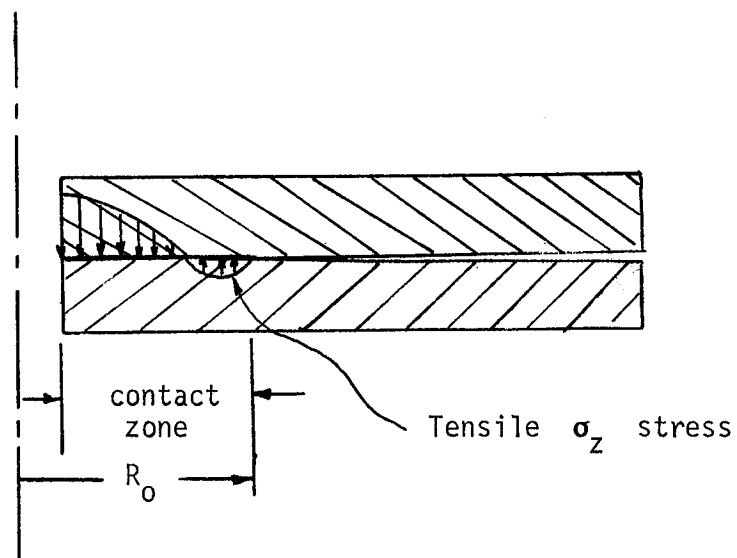


(c) Finite Element Model for Plates of Unequal Thickness

FIG. 5. FINITE ELEMENT MODELS



(a) Plates Intersect, R_0 too small



(b) Contact Zone Sustains Tension, R_0 too large

FIG. 6. EXAMPLES OF UNACCEPTABLE SOLUTIONS

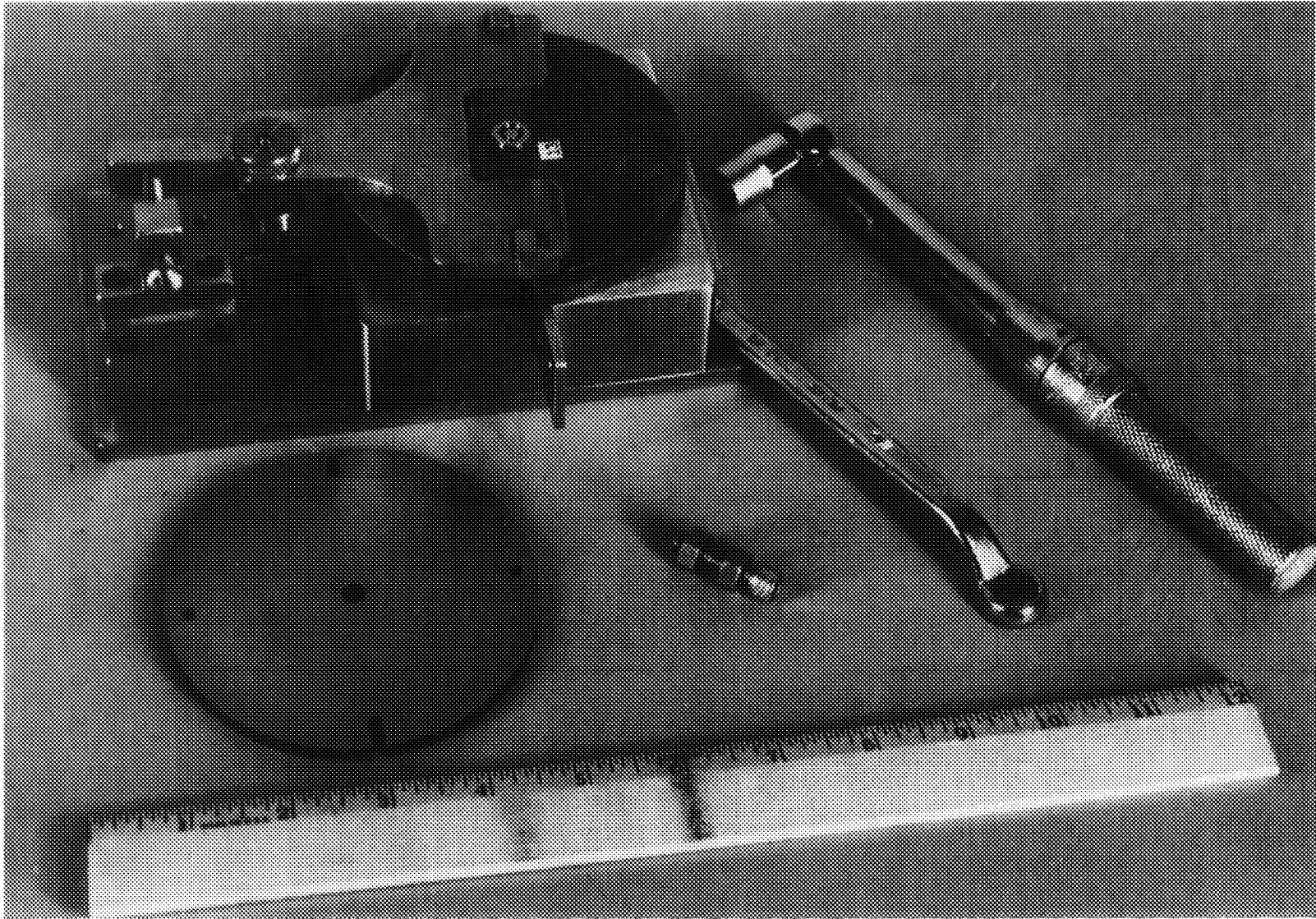


FIG. 7. PLATE SPECIMEN, BOLT AND NUTS, FIXTURE AND TOOLS.

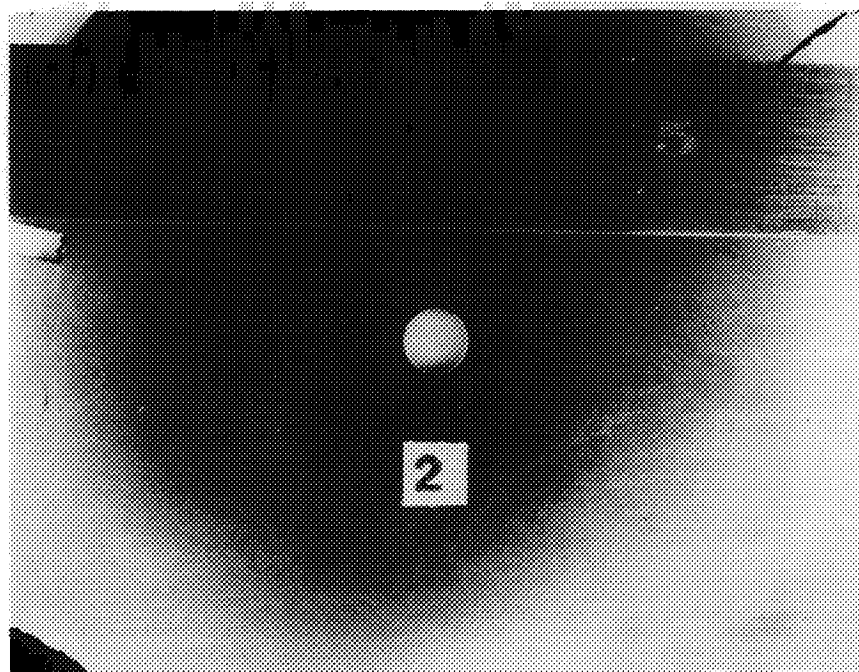
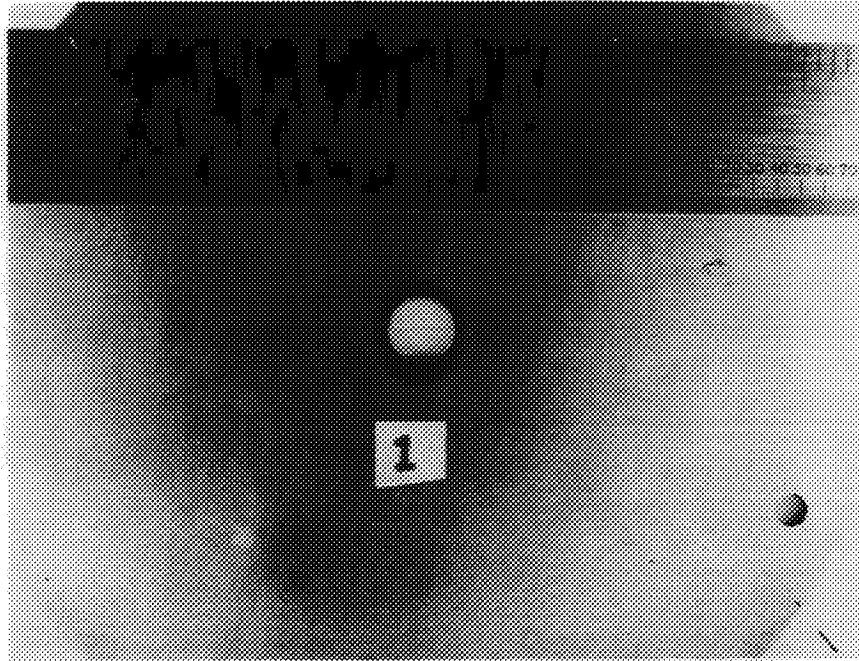


FIG. 8(a). FOOTPRINTS ON MATED PAIR OF 1/16 INCH PLATES.

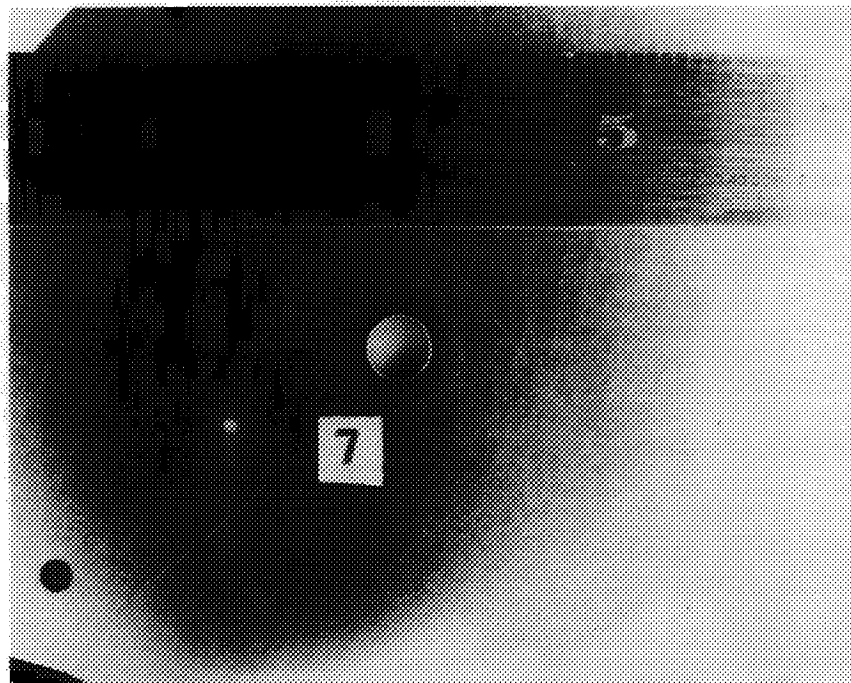
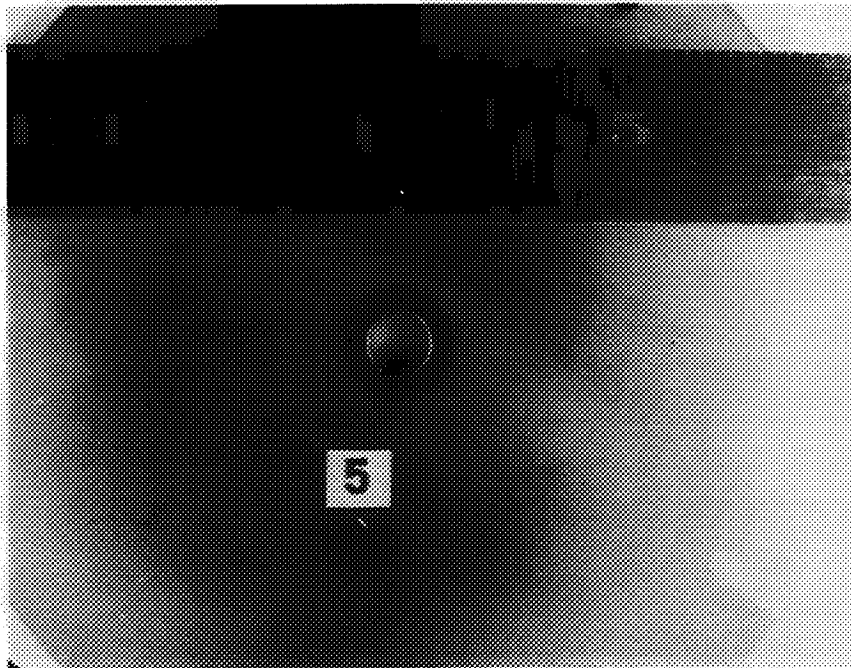


FIG. 8(b). FOOTPRINTS ON MATED PAIR OF 1/8 INCH PLATES.

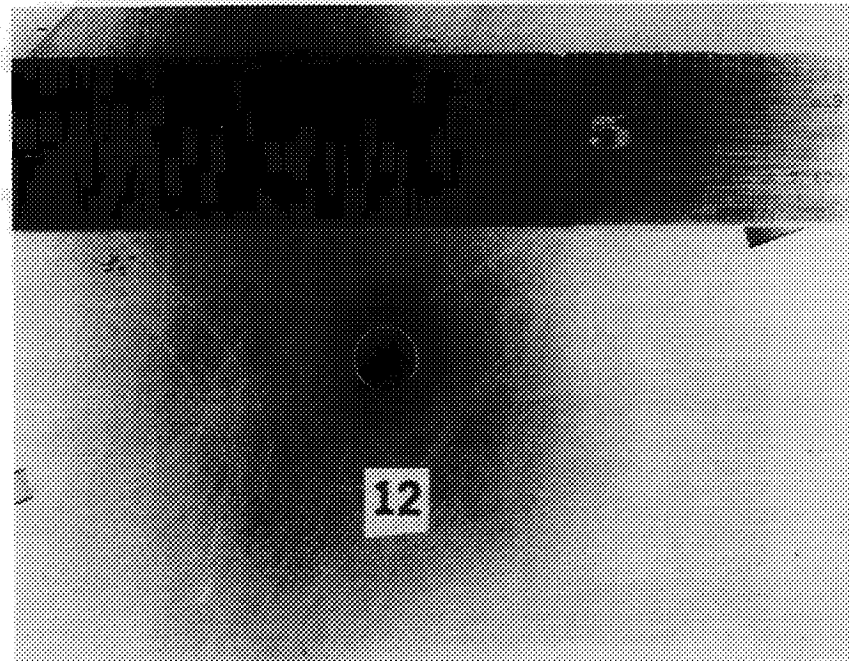
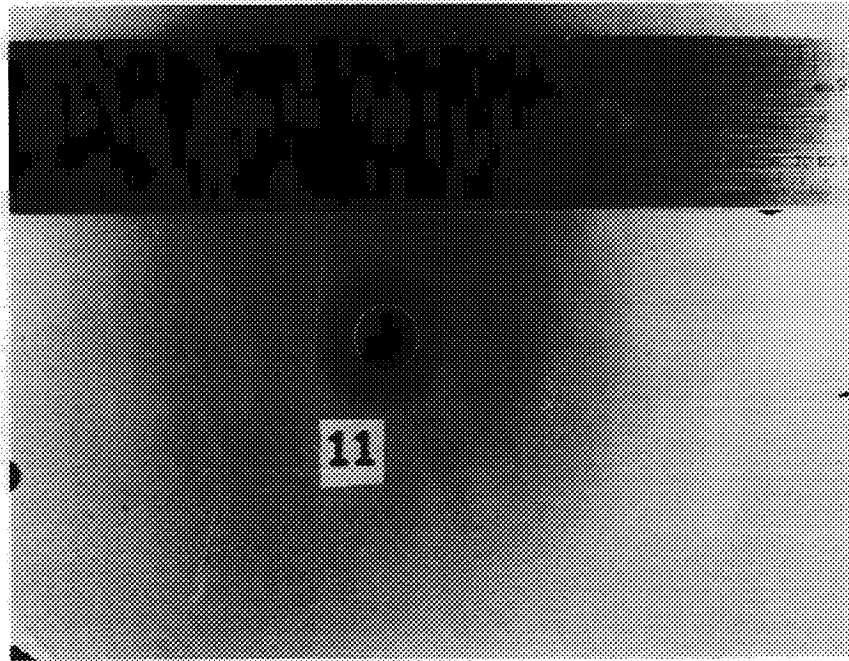


FIG. 8(c). FOOTPRINTS ON MATED PAIR OF 3/16 INCH PLATES.

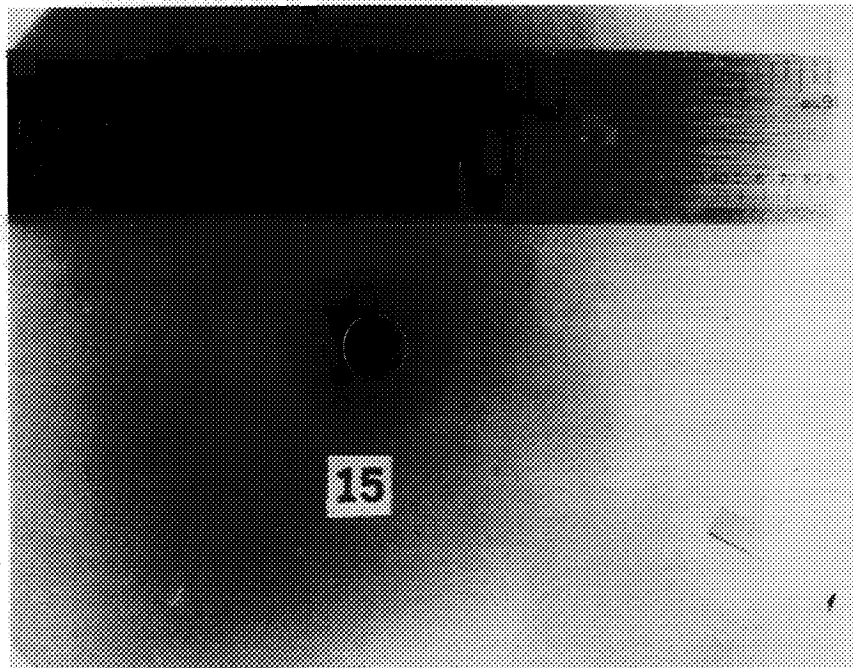
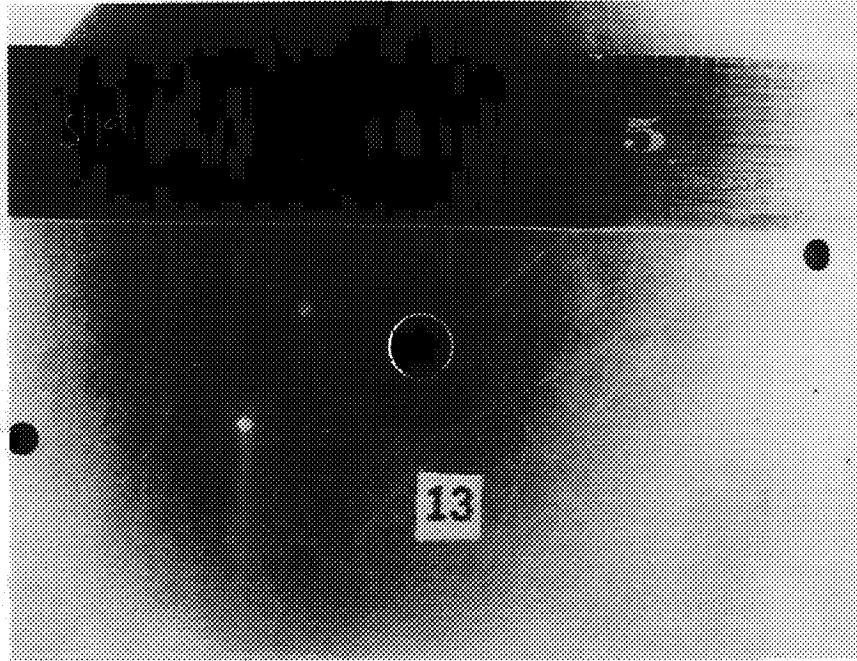


FIG. 8(d). FOOTPRINTS ON MATED PAIR OF 1/4 INCH PLATES.

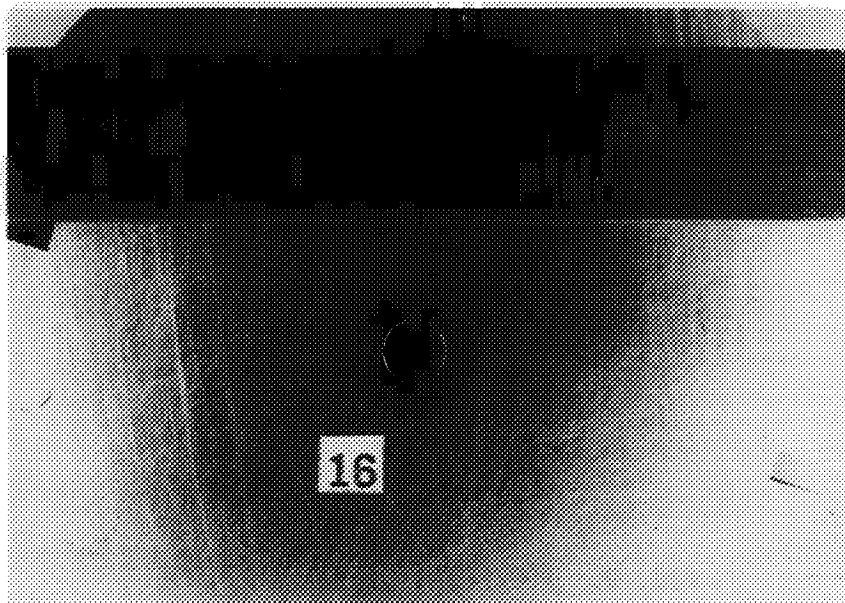
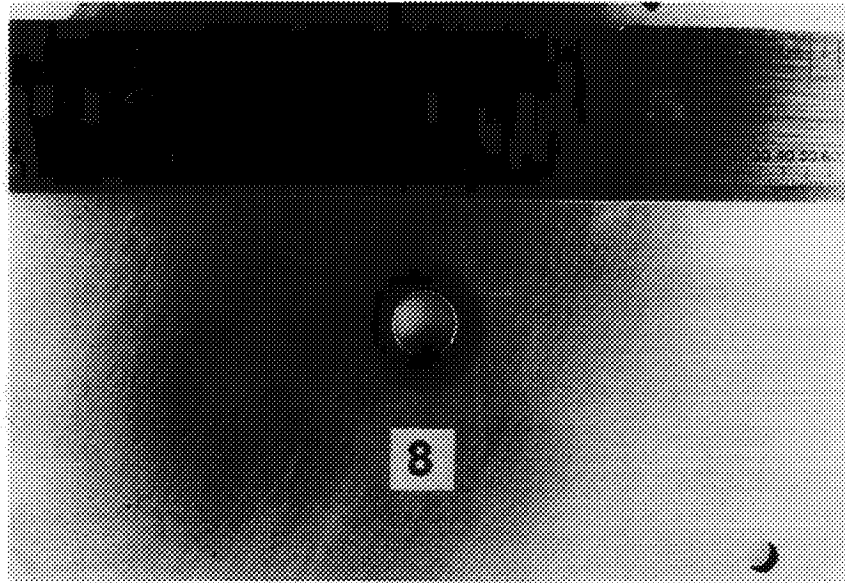


FIG. 8(e). FOOTPRINTS ON MATED PAIR OF 1/8 AND 1/4 INCH PLATES.

FIG. 8. FOOTPRINTS ON THE MATING SURFACES OF 1/16 - 1/16,
1/8 - 1/8, 3/16 - 3/16, 1/4 - 1/4, and 1/8 - 1/4
PAIRS. (A = .128, B = .21)

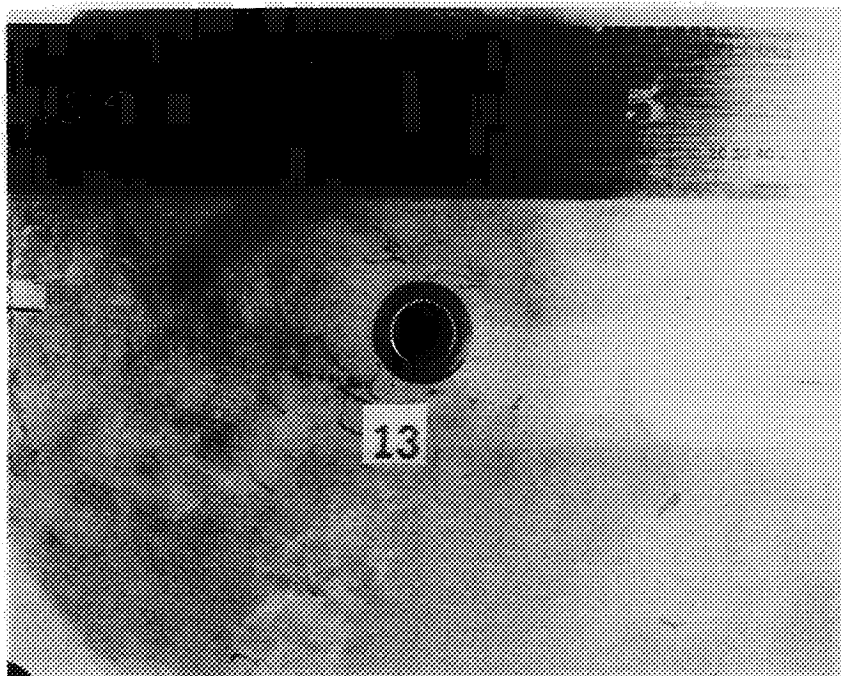


FIG. 9. FOOTPRINT OF NUT ON PLATE.

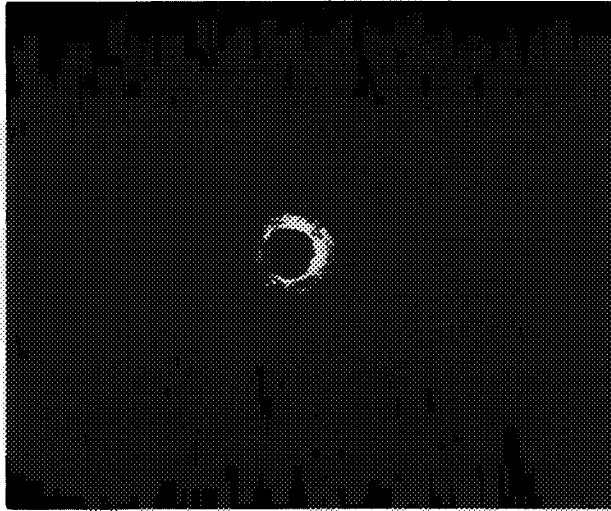


FIG. 10 (a). 1/16 INCH
PAIR

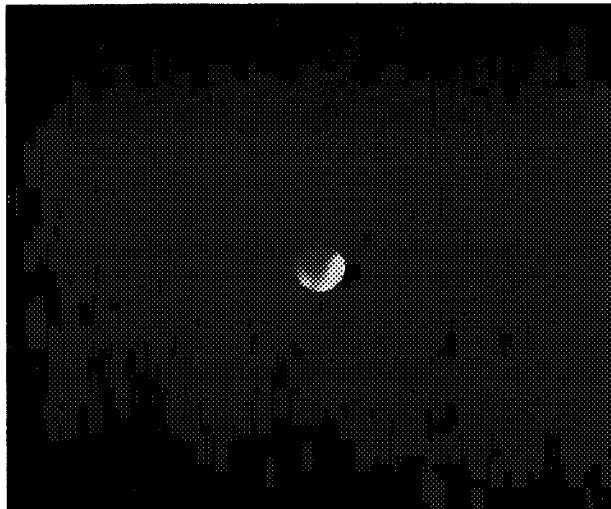


FIG. 10(b). 1/8 INCH
PAIR

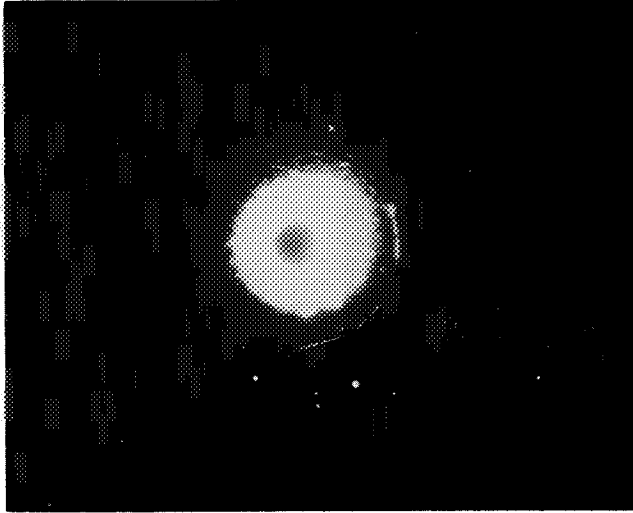


FIG. 10(c). 3/16 INCH
PAIR

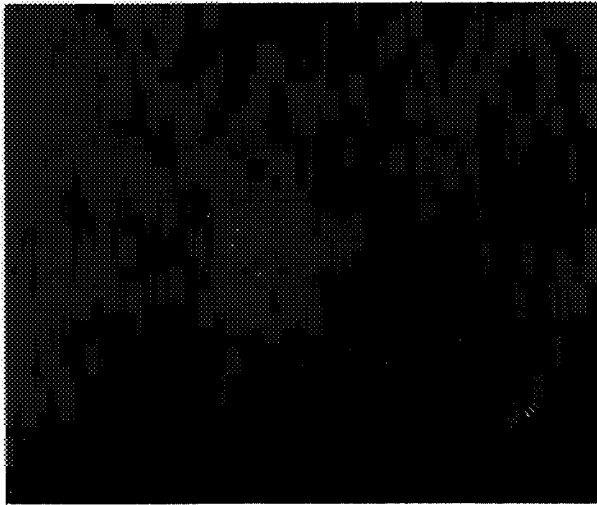


FIG. 10(d). 1/4 INCH
PAIR

FIG. 10. X-RAY PHOTOGRAPHS OF CONTAMINATION TRANSFERRED
FROM RADIOACTIVE PLATE TO MATED PLATE. 1/16, 1/4,
3/16, 1/4 INCH PAIRS. (A = .128 in., B = .21 in.)

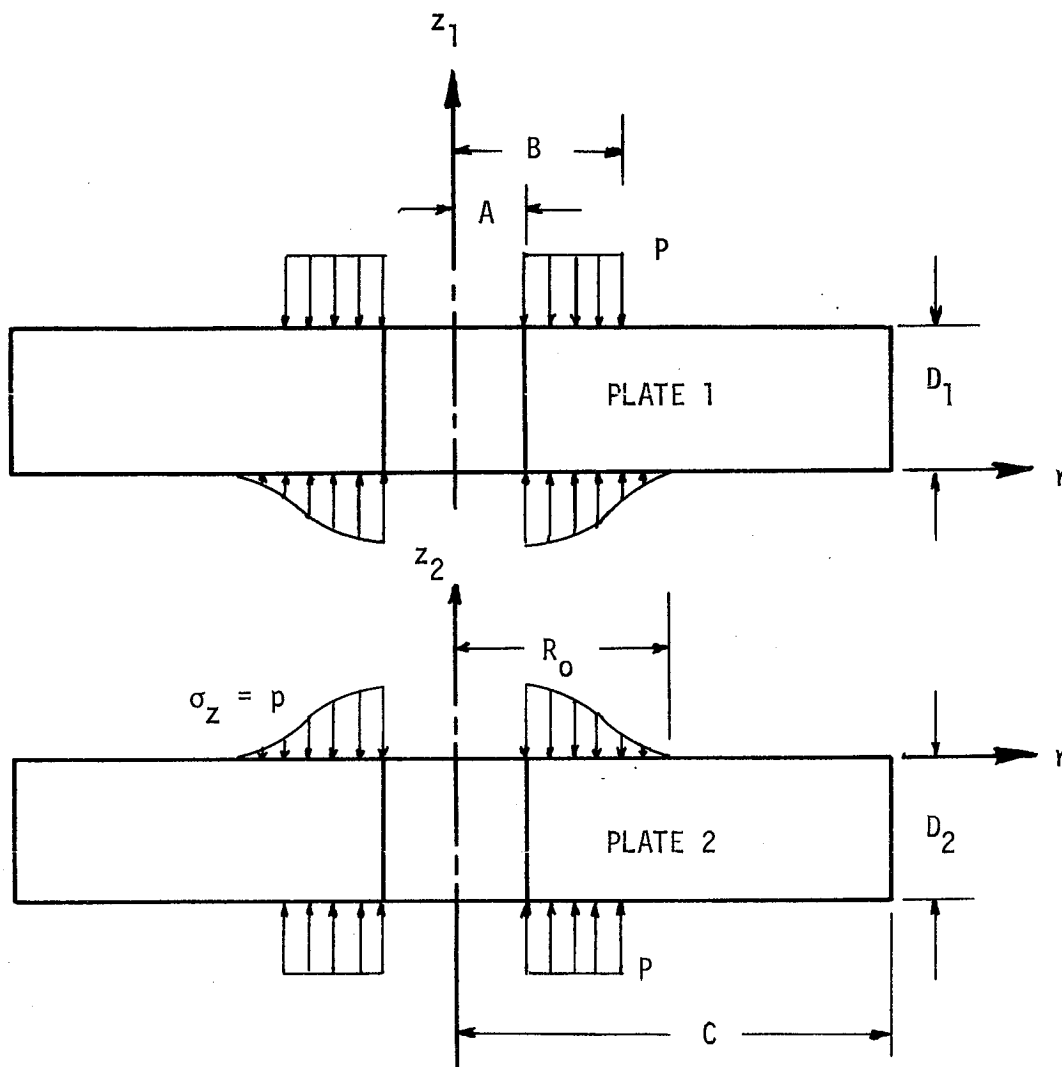


FIG. 11. FREE BODY DIAGRAM FOR TWO PLATES IN CONTACT.

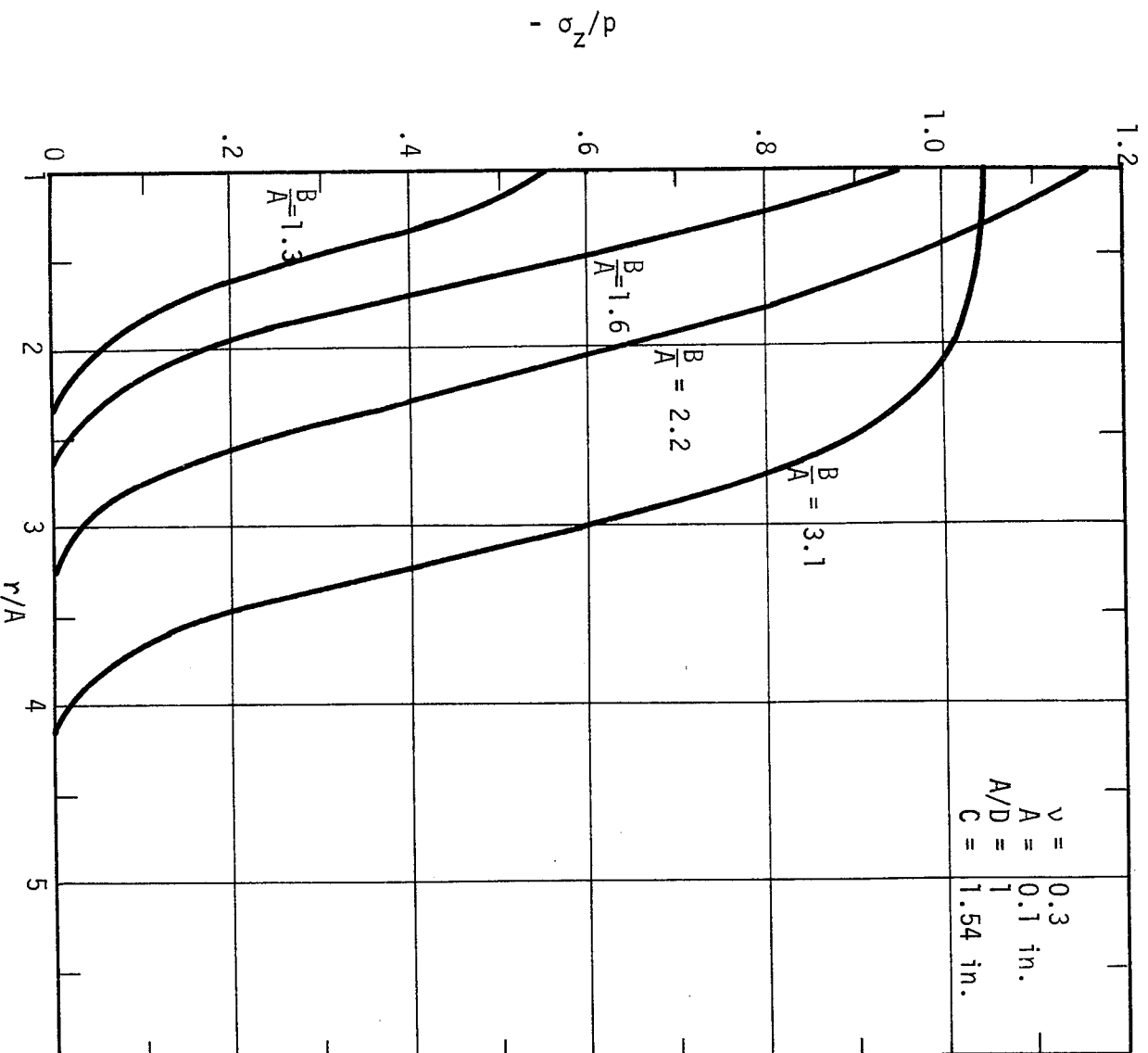


FIG. 12. SINGLE PLATE ANALYSIS-MIDPLANE σ_z STRESS DISTRIBUTION (D = 0.1 in.)

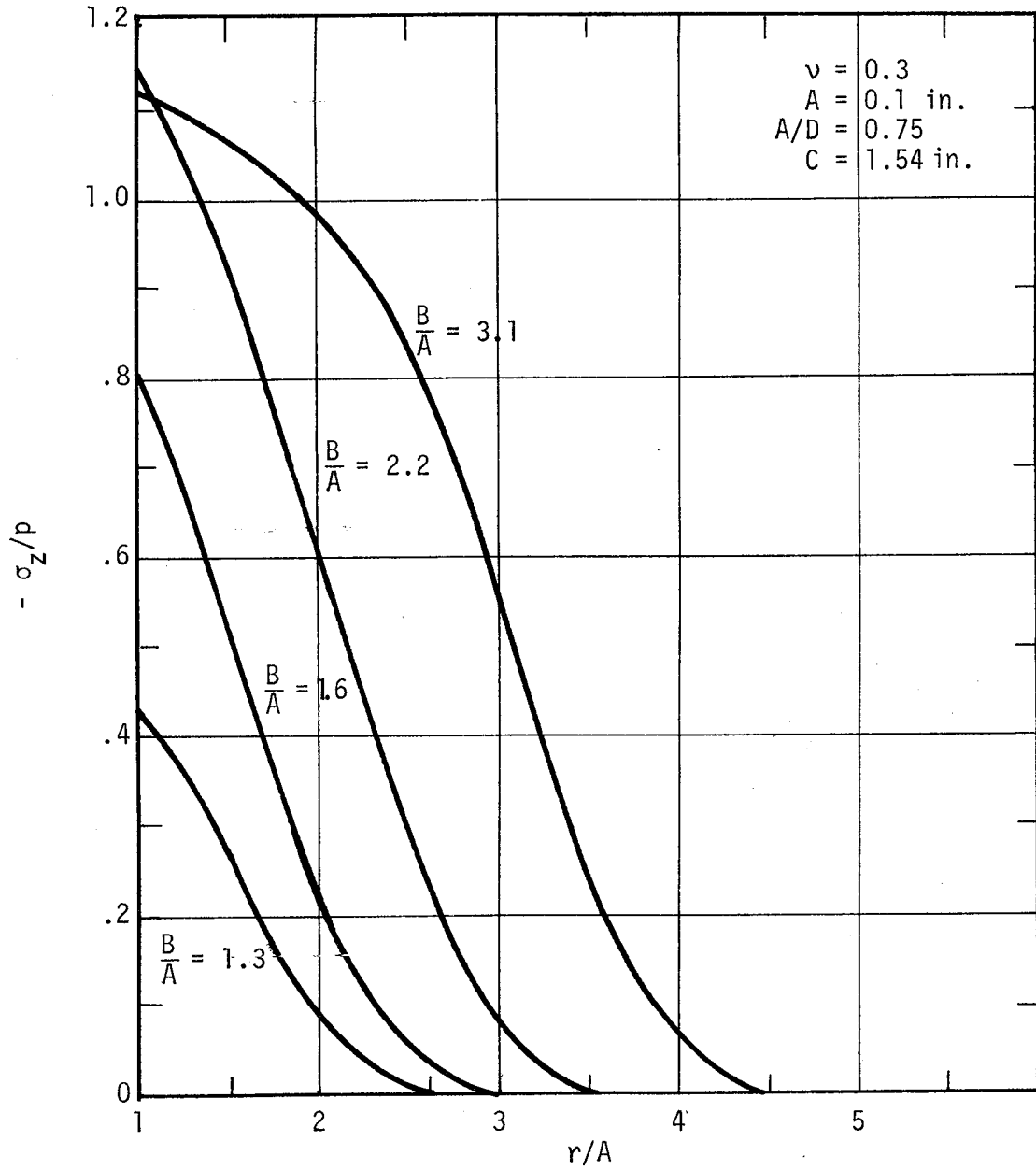


FIG. 13. SINGLE PLATE ANALYSIS-MIDPLANE σ_z STRESS DISTRIBUTION ($D = 0.133 \text{ in.}$)

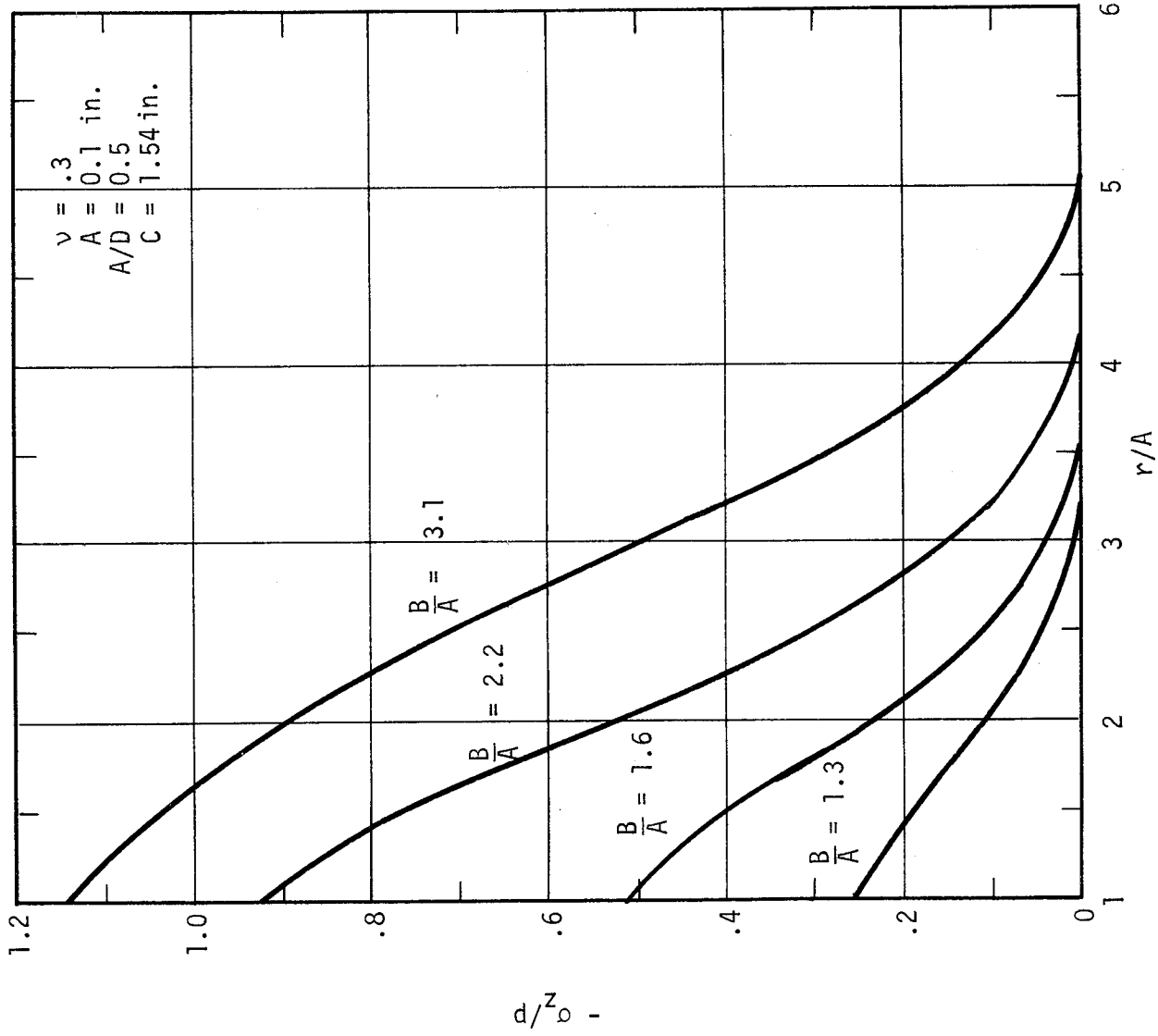


FIG. 14. SINGLE PLATE ANALYSIS-MIDPLANE σ_z STRESS DISTRIBUTION ($D = 0.2 \text{ in.}$)

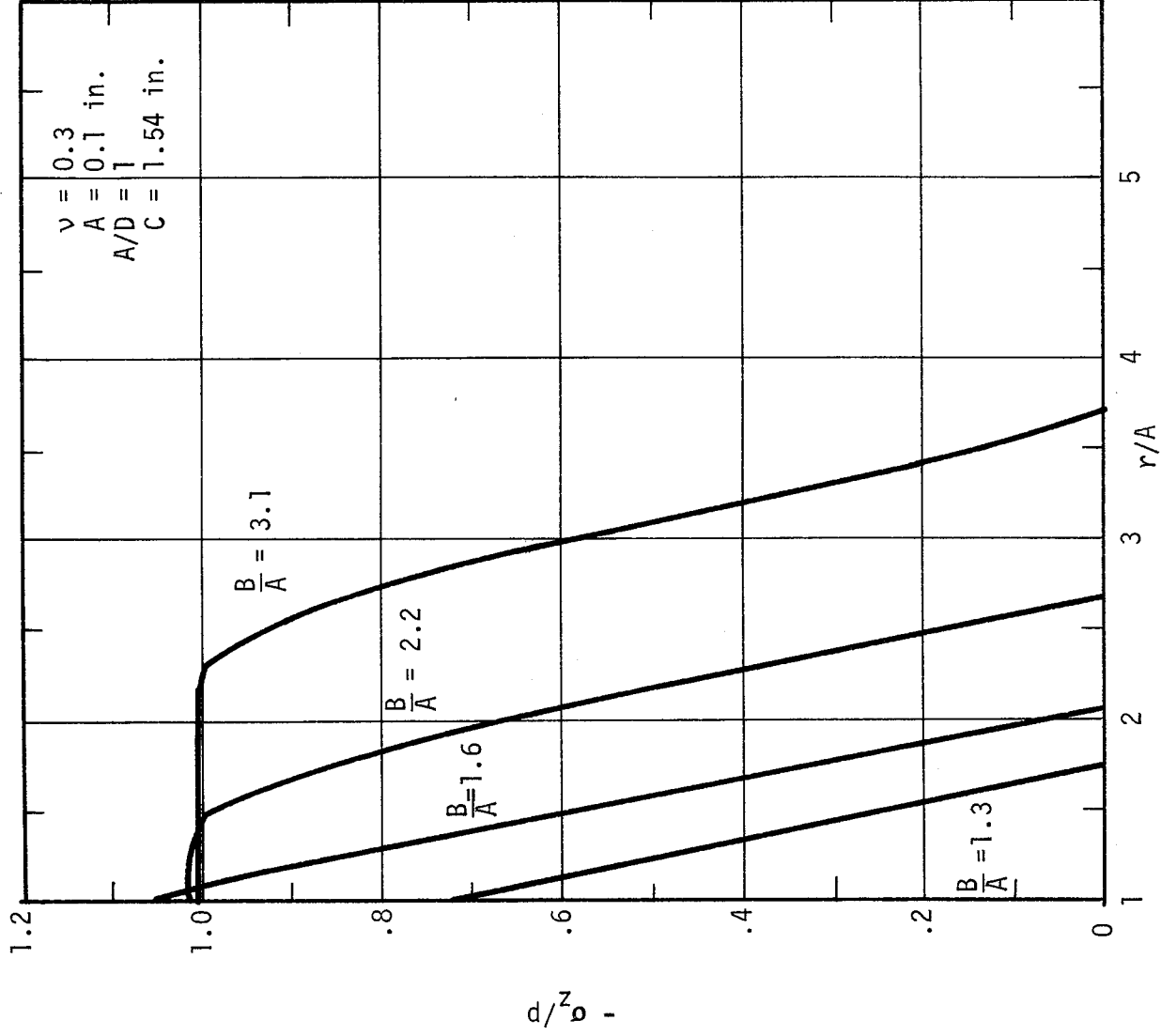


FIG. 15. INTERFACE PRESSURE DISTRIBUTION IN A BOLTED JOINT

($D = 0.1 \text{ in.}$)

3

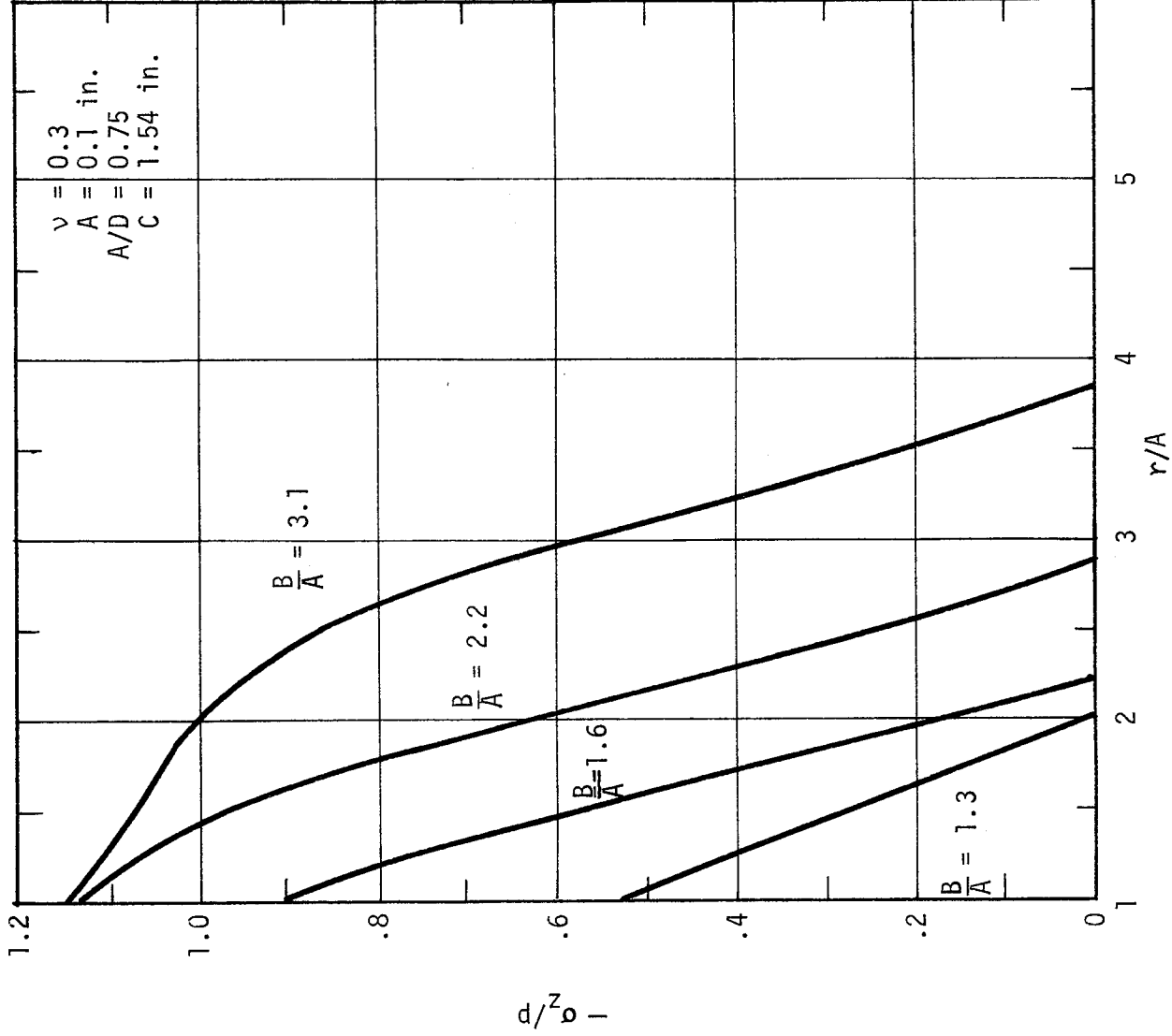


FIG. 16. INTERFACE PRESSURE DISTRIBUTION IN A BOLTED JOINT
($D = .133 \text{ in.}$)

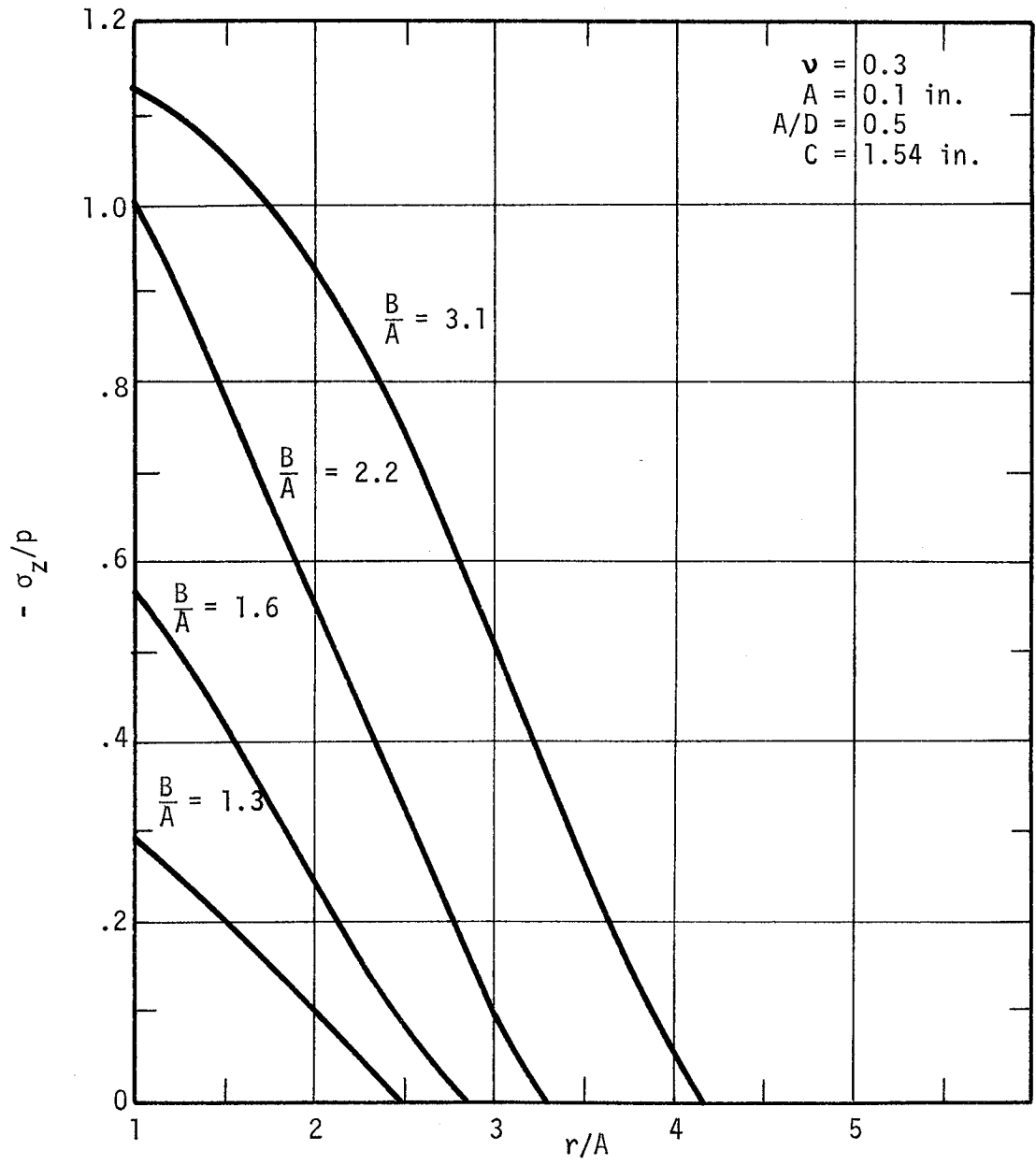


FIG. 17. INTERFACE PRESSURE DISTRIBUTION IN A BOLTED JOINT
(D = 0.2 in.)

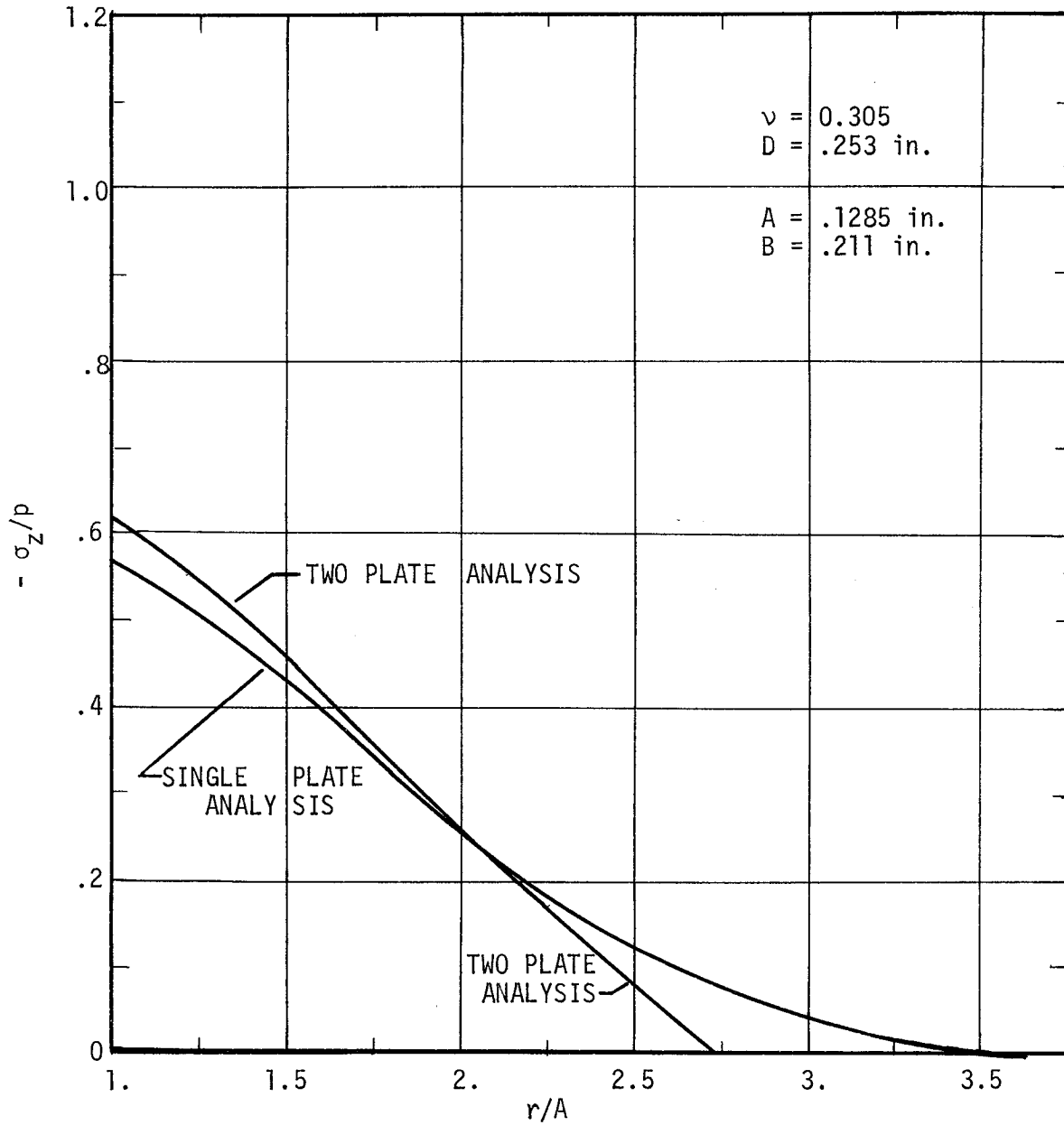


FIG. 18. FINITE ELEMENT ANALYSIS RESULTS FOR 1/4 INCH PLATE PAIR.

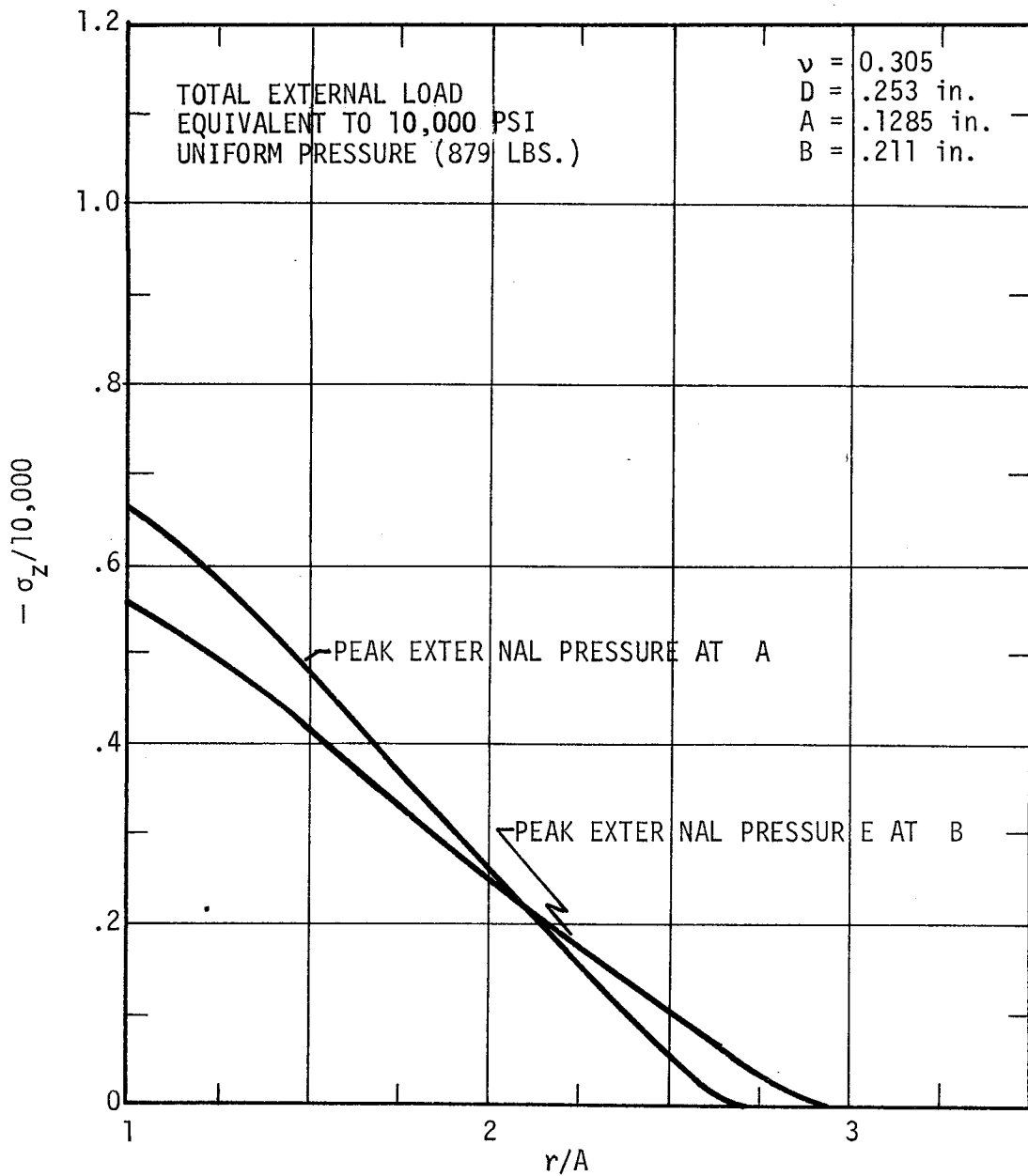


FIG. 19. PRESSURE IN JOINT, TRIANGULAR LOADING

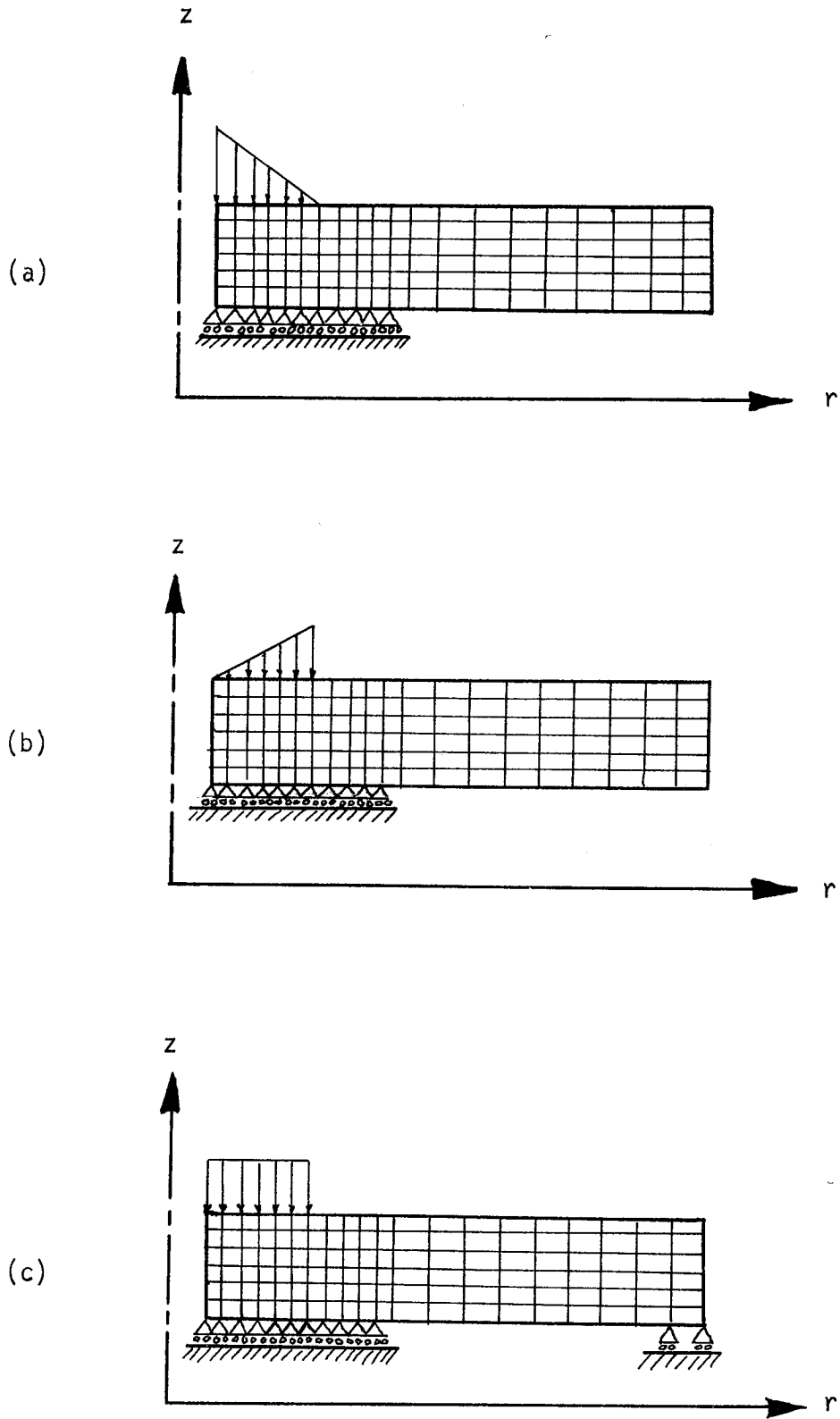


FIG. 20. VARIATIONS OF LOADING AND BOUNDARY CONDITIONS.

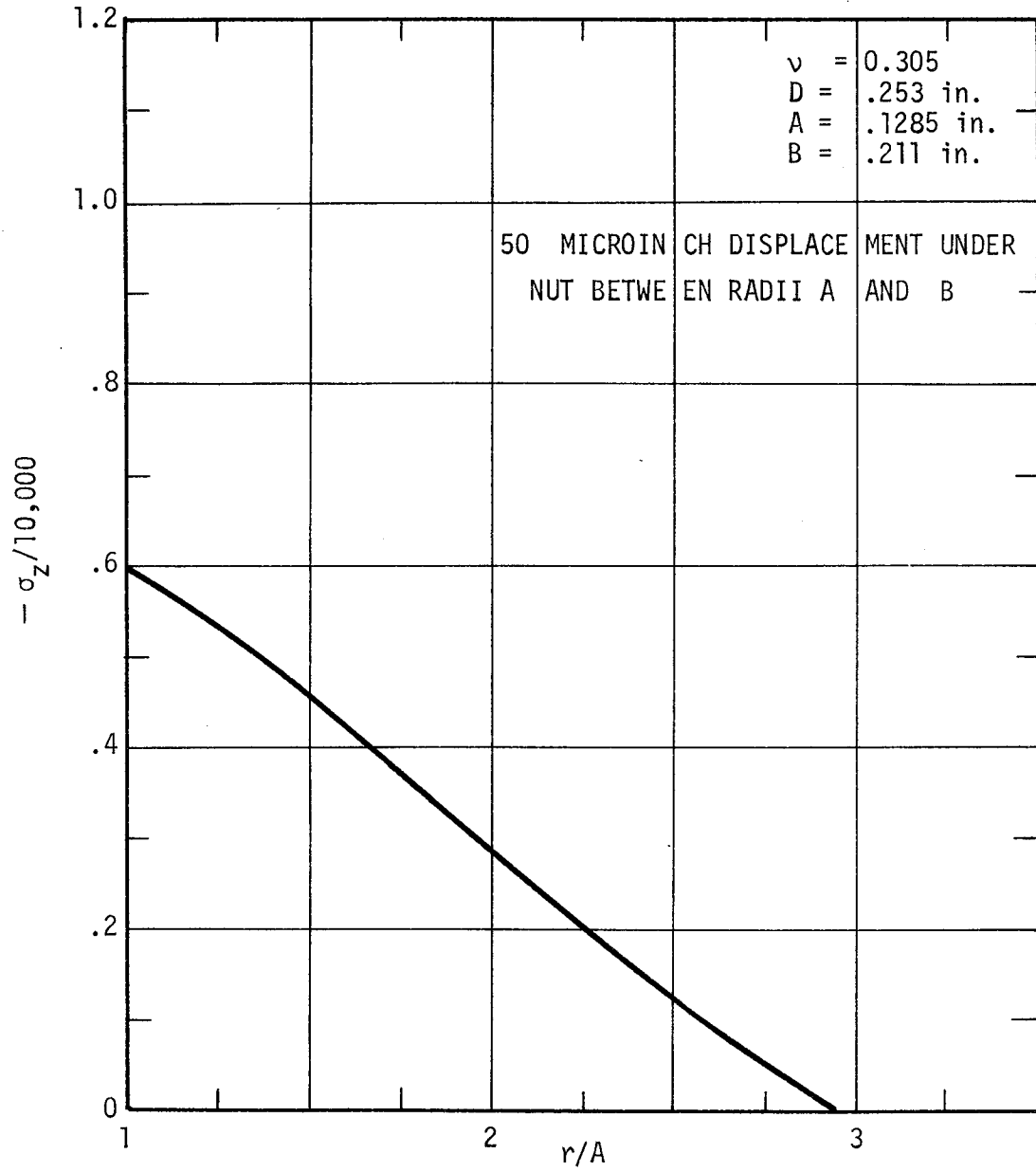


FIG. 21. PRESSURE IN JOINT, UNIFORM DISPLACEMENT UNDER NUT.

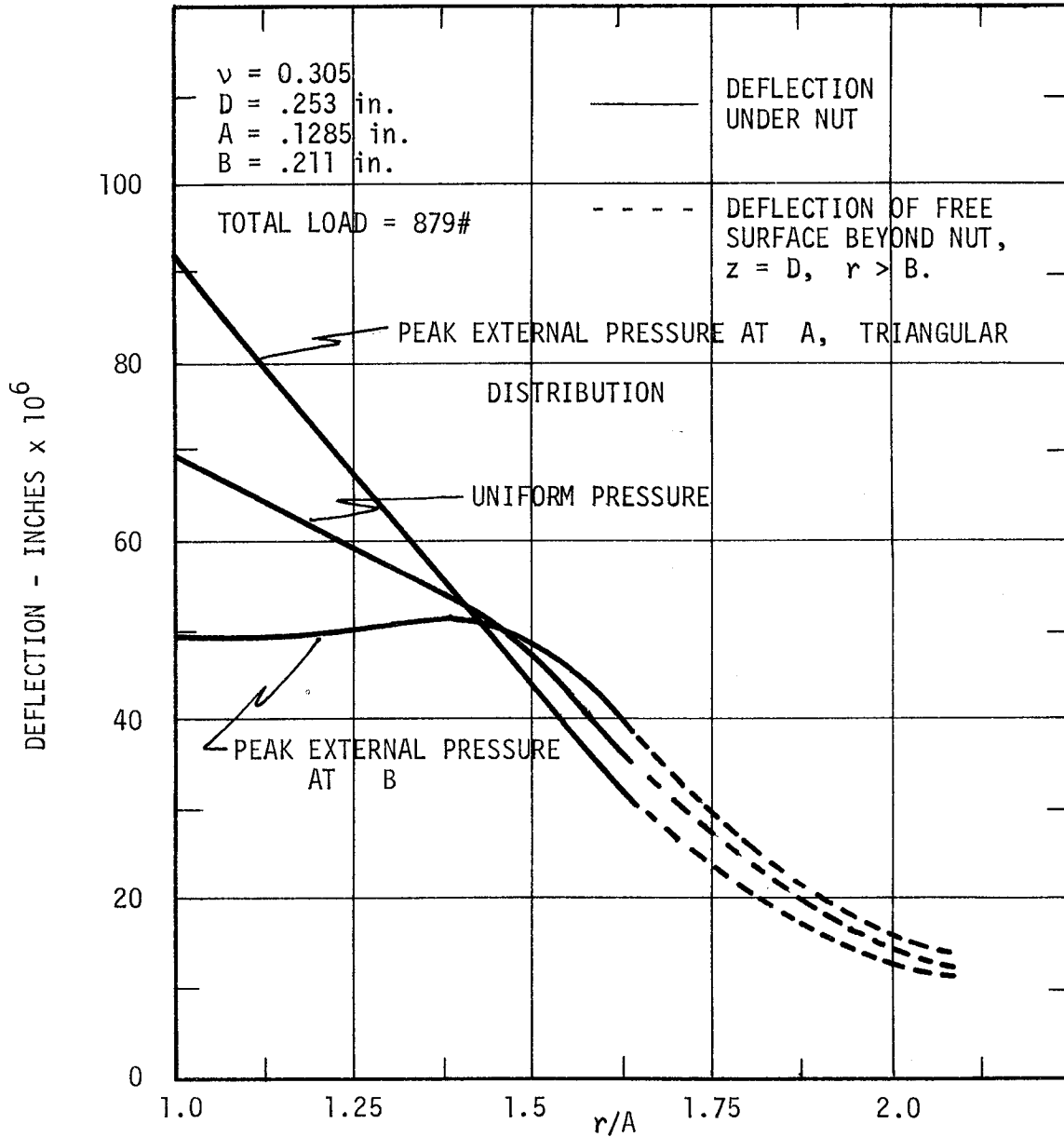


FIG. 22. DEFLECTION OF PLATE UNDER NUT.

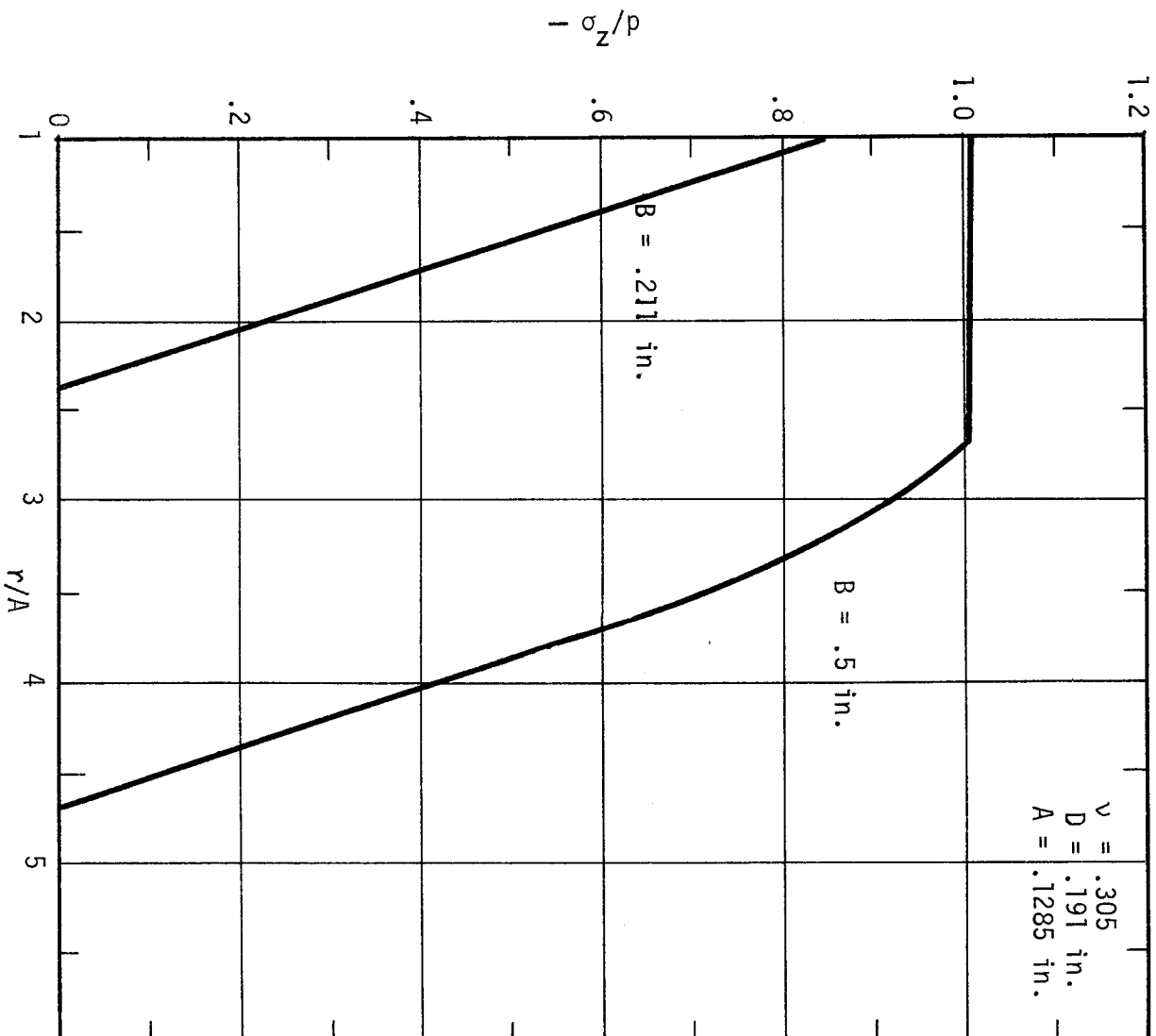


FIG. 23. FINITE ELEMENT ANALYSIS RESULTS FOR 3/16 INCH PLATE PAIR.

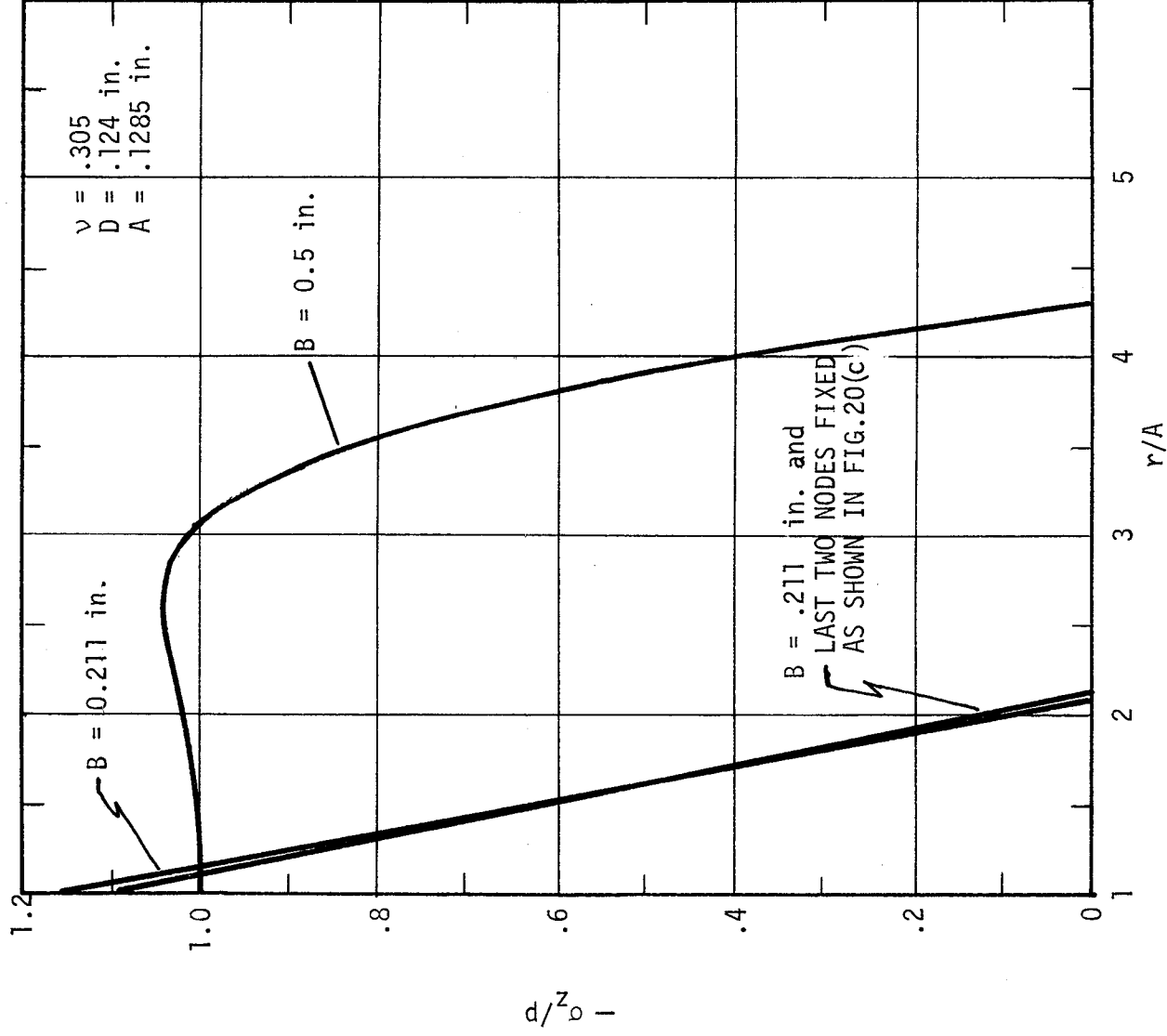


FIG. 24. FINITE ELEMENT ANALYSIS RESULTS FOR 1/8 INCH PLATE PAIR.

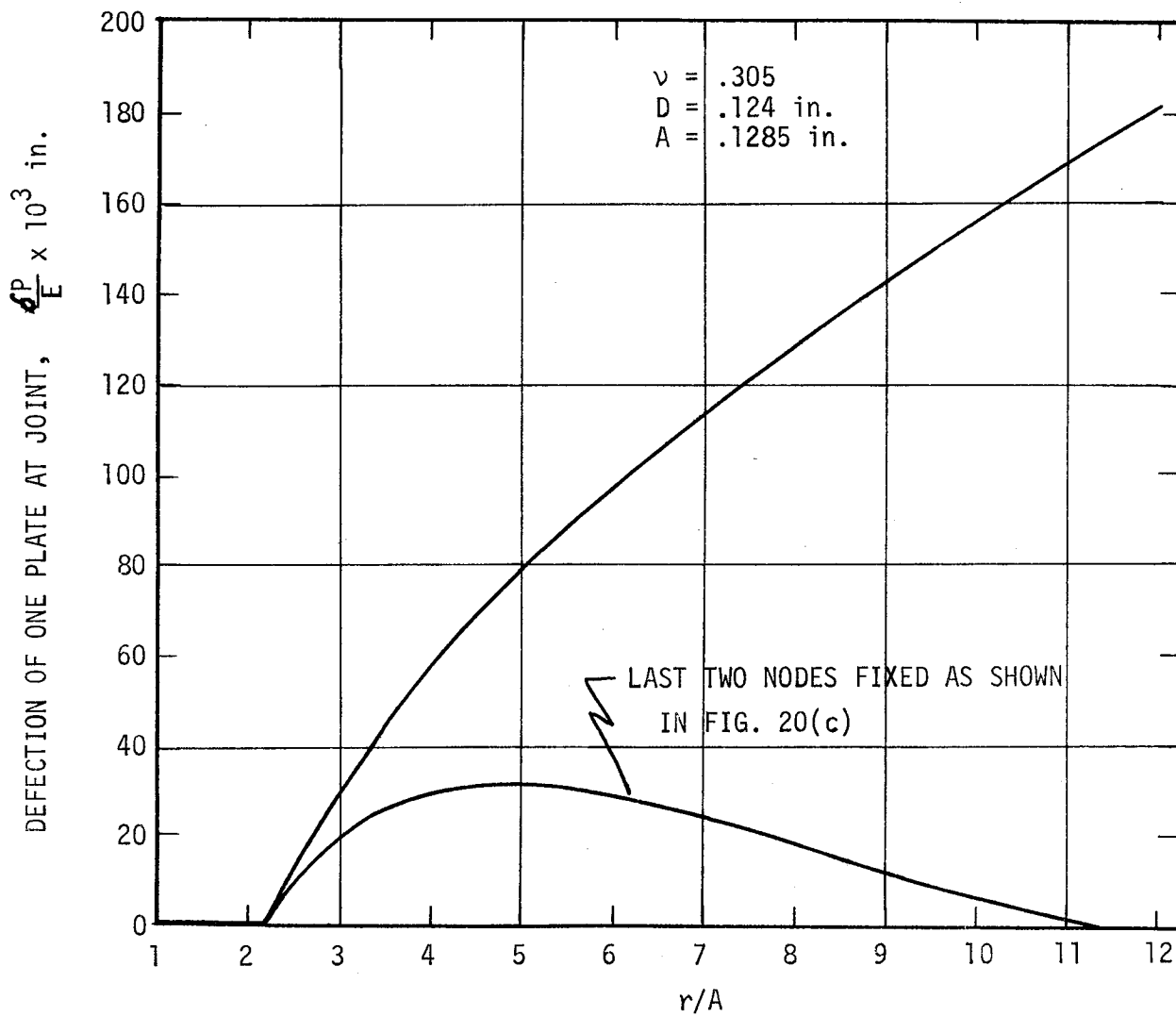


FIG. 25. GAP DEFORMATION FOR FREE AND FIXED EDGES — FINITE ELEMENT ANALYSIS, 1/8 INCH PLATE PAIR.

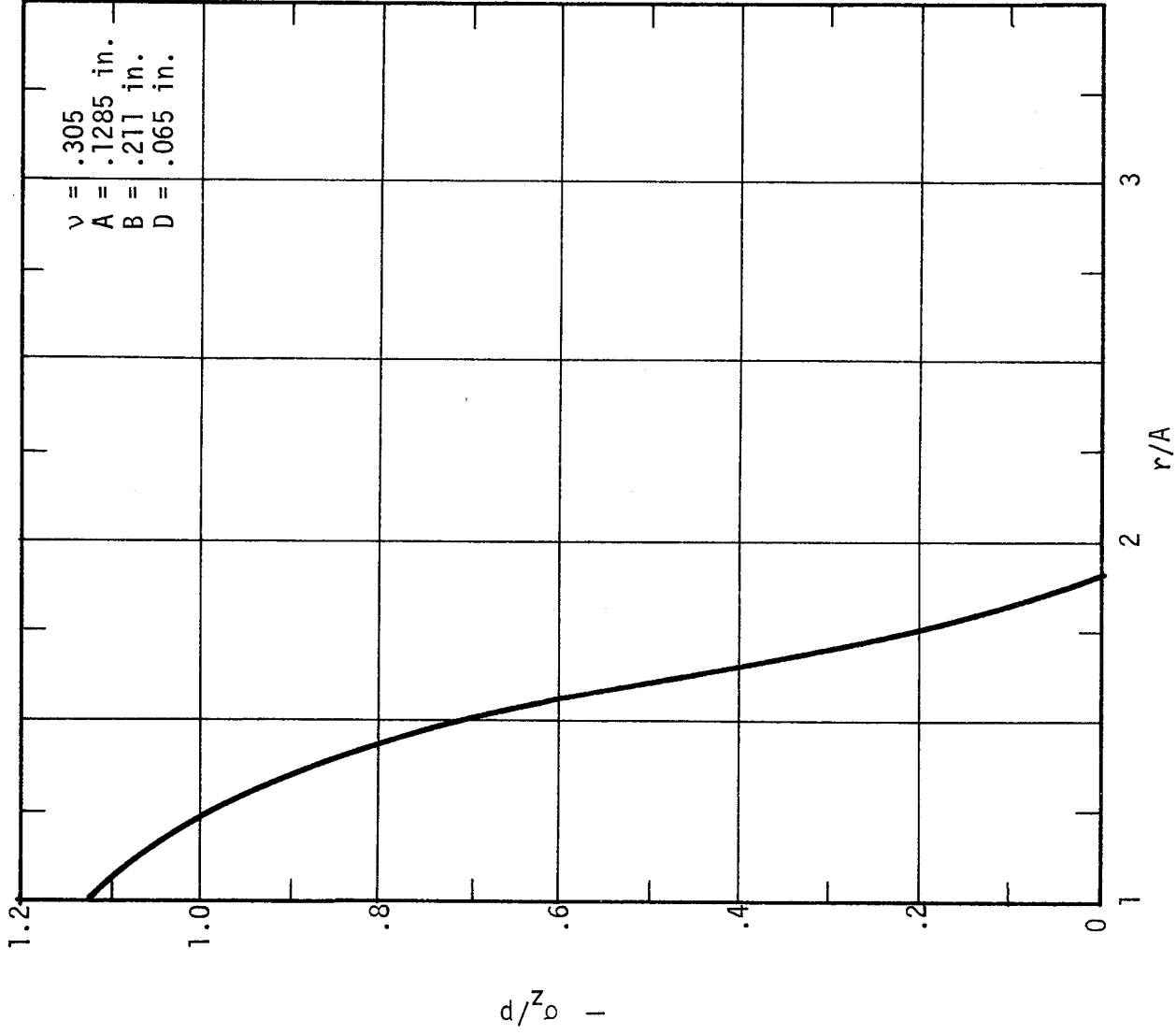


FIG. 26. FINITE ELEMENT ANALYSIS RESULT FOR 1/16 INCH PLATE PAIR.

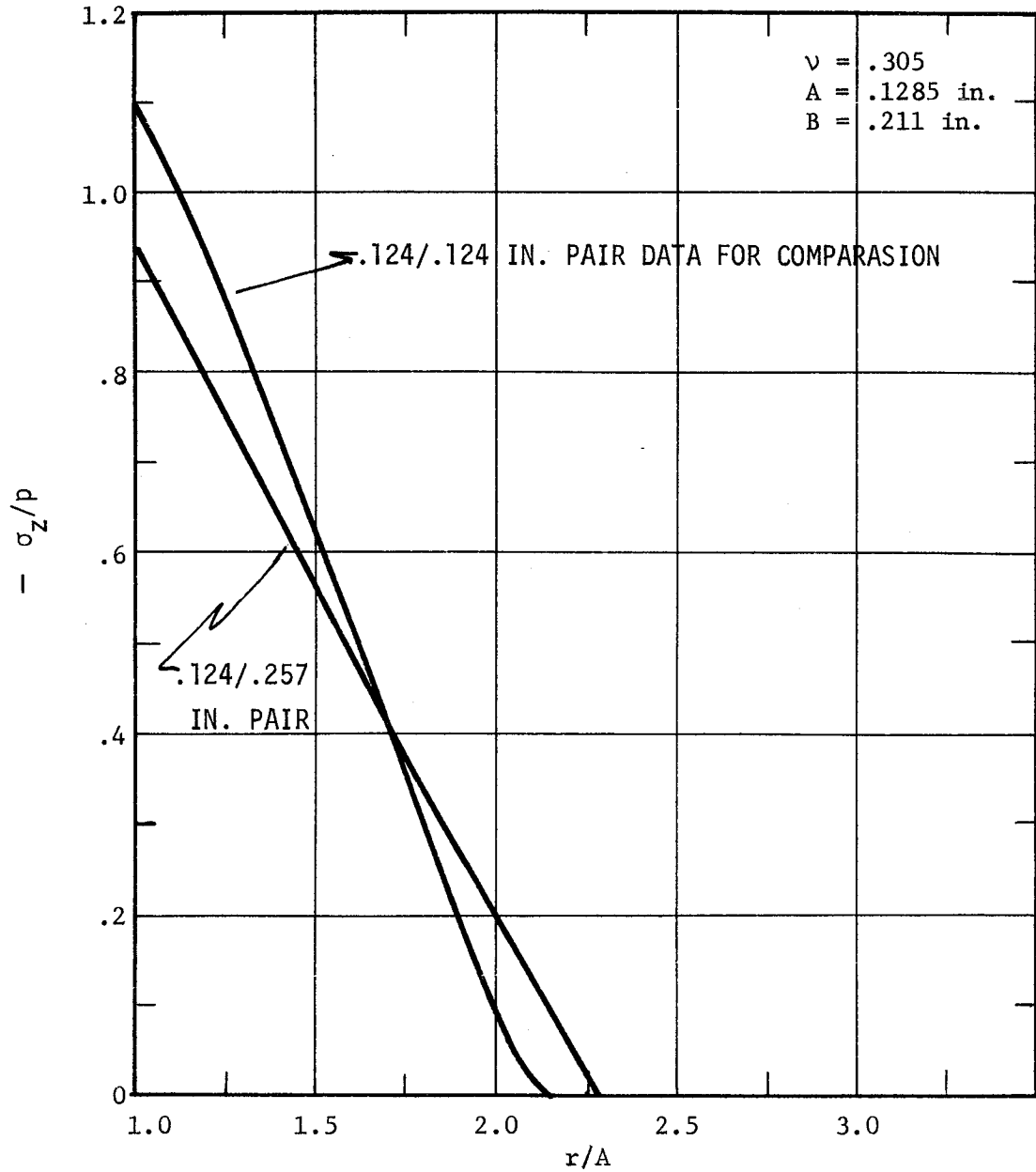


FIG. 27. FINITE ELEMENT ANALYSIS RESULTS FOR 1/8 INCH PLATE MATED WITH 1/4 INCH PLATE.

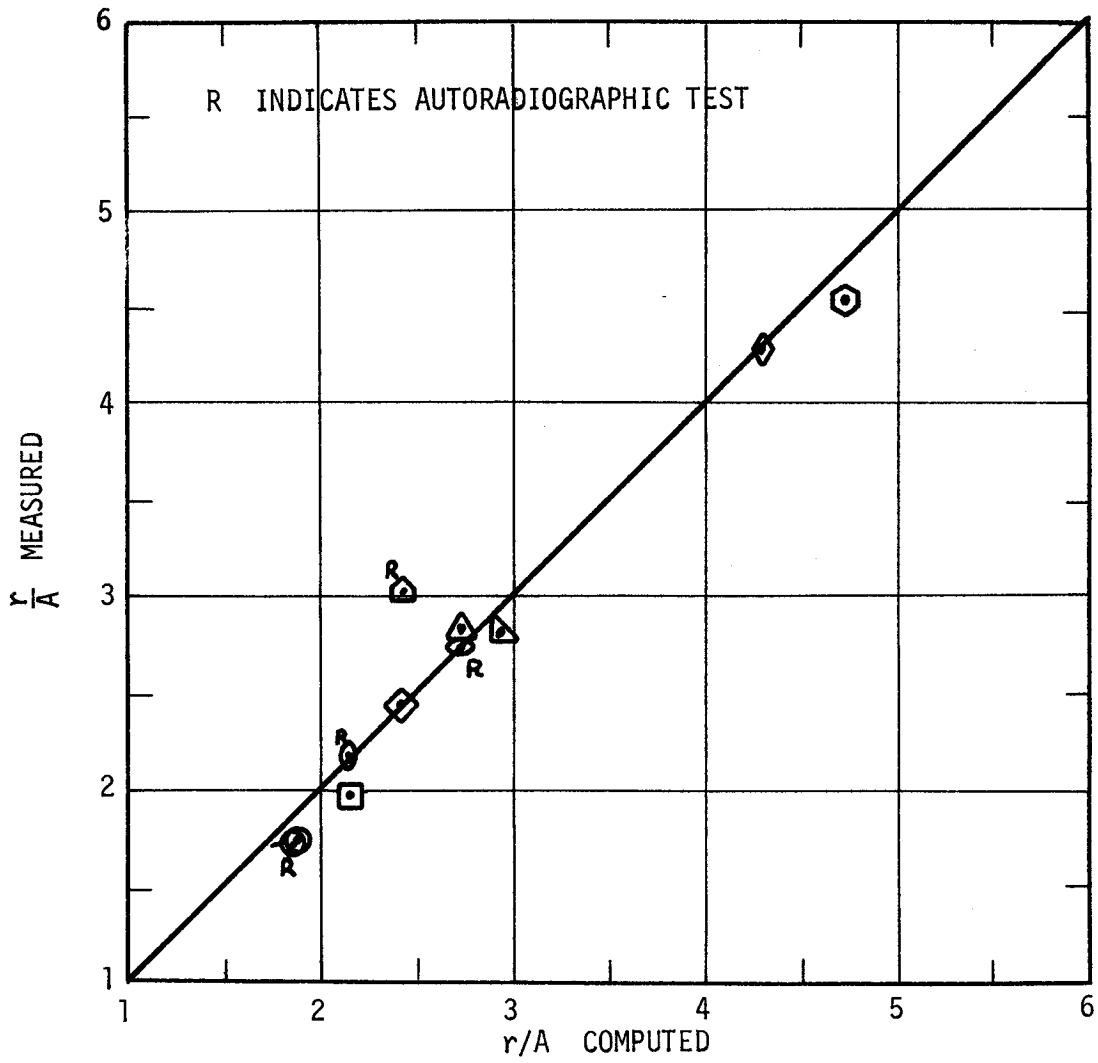


FIG. 28. COMPARISON BETWEEN TESTED AND MEASURED SEPARATION RADII.

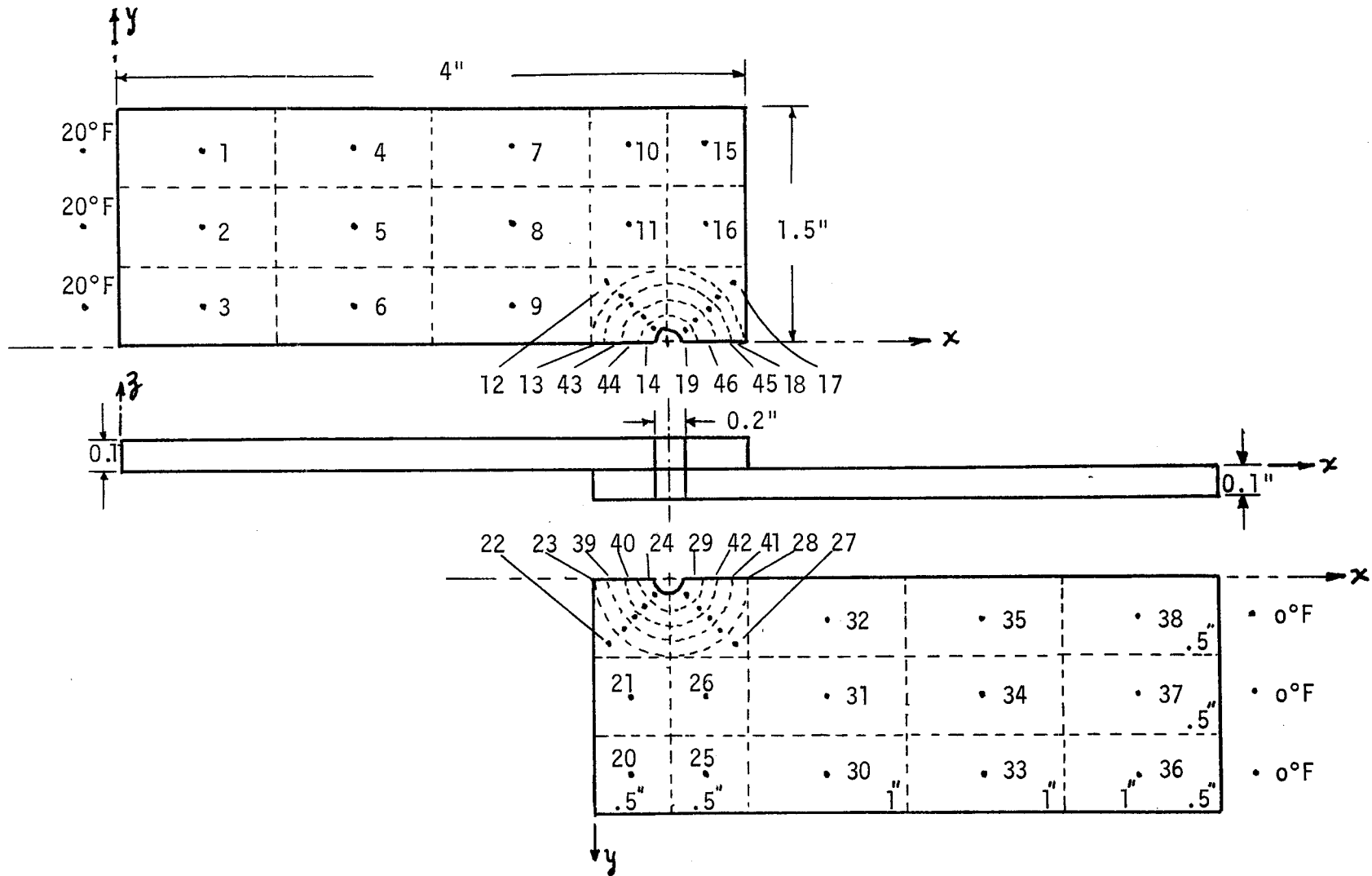


FIG. 29. LOCATION OF NODES — STEADY STATE HEAT TRANSFER ANALYSIS

